Håkon Caspari & Mathias Haugbråten

Back to the Future:
Rebirth of Pure Wind Propelled Ships

Master's thesis in Marine Technology
Supervisor: Stein Ove Erikstad
Co-supervisor: Benjamin Lagemann
June 2023

NTNU
Norwegian University of
Science and Technology

Håkon Caspari & Mathias Haugbråten

Back to the Future:
Rebirth of Pure Wind Propelled Ships

NTNU

Norwegian University of
Science and Technology

Master Thesis in Marine Systems Design

Stud. techn. Håkon Caspari and Mathias Haugbråten

"Back to the Future: Rebirth of Pure Wind Propelled Ships"

Spring 2023

Background

The overall energy demand of the world is only growing, and the need for change is urgent if we are to limit global warming to the 1.5-degree goal set by the Paris Agreement. Global trade is dominated by about 90 000 vessels that are responsible for more than 80% of all cargo transport. In recent years the comeback of wind as a source of propulsion has been discussed to reduce the power generation from fossil fuels. The technologies that utilize wind as a source of power generation are commonly labeled as wind-assisted ship propulsion technologies (WASP technologies).

Overall aim and focus

The overall aim of the project is to provide insight into the consequences on the performance of pure (or a high degree of) wind-assisted propulsion by the use of Flettner rotors.
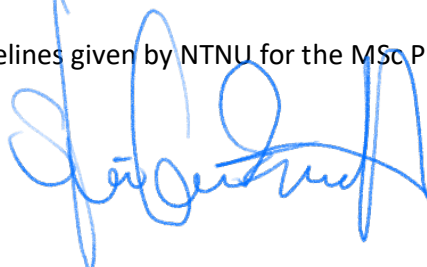
Scope and main activities

1. *Provide a short overview of alternative wind-assisted ship propulsion technologies, their technological readiness level, current status, and important development trends. The main focus should be on Flettner rotor sails.*

2. *Propose a set of key performance indicators (KPIs) that can be used to quantify the performance difference of a pure WASP solution compared to an existing transport system.*

3. *Develop a simulation model that can be used to calculate these KPIs for pure WASP vessels by combining real route and weather data.*

4. *Propose and test improvements that can be made to the pure WASP vessel to strengthen KPI scores.*

5. *Discuss and conclude.*

Modus operandi

At NTNU, Professor Stein Ove Erikstad will be the responsible advisor. Ph.D. student Benjamin Lagemann will be the co-supervisor.

The work shall follow the guidelines given by NTNU for the MSc Project work.

Stein Ove Erikstad
Professor/Responsible Advisor

Abstract

To sufficiently address the goals presented in the Paris Agreement and limit global warming, the maritime sector has to undergo large-scale changes to reduce emissions. The transition from petroleum-based fuels to new solutions is one way that this can be done. There exists currently no simple solution, so a combination of ideas should be evaluated to solve this challenge. One solution is using wind-assisted ship propulsion. The vast amounts of untapped wind energy available on the open sea could present large opportunities for producing power while sailing. With increasing fuel prices and carbon emission taxes, the monetary gains on saved fuel improve, promoting the use of fuel reduction technologies.

This thesis' goal is to establish a set of key performance indicators and develop a simulation model to evaluate the consequences of utilizing a wind-powered ship propulsion system, providing 100 percent of all power from Flettner rotors. The thesis differs from most of the established WASP research by flipping the question of how much power can be saved. The question now reads, "What are the consequences of utilizing Flettner rotors as the only source of propulsion for a vessel?".

The method used in this thesis to answer the main question is split into several parts. First, performing a literature review of studies to establish a foundation for the research topic. Key performance indicators are established to understand how the performance may be measured in an insightful way and to easily compare the pure wind-powered system to conventional systems used today. A simulation model based on a small bulk carrier case vessel is created in Python to evaluate performance on different predetermined routes through the combination of historical wind and AIS data. This model is expanded to include new routes, weather conditions, and technological improvements.

Simulation results show that wind-powered ship propulsion systems perform worse than their conventional counterparts. The simulations also show technological dependency on route planning and underlying weather conditions. Vessel speed is significantly reduced compared to industry standard, whilst schedule reliability may show comparatively better results given lower expected sailing speeds. Return on investments show promising results for the implementation of Flettner rotors due to the increasing fuel prices and high cost of alternative zero-emission fuels.

The main conclusion that may be drawn from this thesis is that solely introducing Flettner rotors into the current maritime transportation system is unfeasible. However, if stakeholder willingness and customer flexibility adapt to the volatile nature of Wind powered ship propulsion, then the technology may be utilized on specific routes, cargoes, and ship types. The base case solution may be improved upon by implementing complementary technologies and techniques to enhance performance on segments of routes that are unfit for the sole use of Flettner rotors. This thesis may serve as a foundation upon which to build and improve future wind-powered ship propulsion solutions. The simulation model established may also be improved upon to increase accuracy and remove simplifications.

Sammendrag

For å møte målene presentert i Parisavtalen og begrense global oppvarming må den maritime sektoren gjennomføre store endinger for å redusere utslipp. Overgangen fra petroleumsbaserte drivstoff til nye løsninger er en måte som dette kan gjøres. Det finnes idag ikke en enkeltstående løsning på problemet og kombinasjonen av forskjellige løsninger burde derfor vurderes. En slik løsning er bruken av vind assistert skipspropulsjon. Den store mengden uutnyttet kraft i havvind har potensialet til å skape store drivstoffbesparelser på fartøy. Med økte drivstoffkostnader of karbonavgifter øker den monetære gevinsten av å implementere teknologier som reduserer eller eliminerer drivstofforbruk.

Målet til denne oppgaven er å etablere et sett med ytelsesindikatorer og utvikle et simuleringsverktøy som kan brukes til å vurdere konsekvensene av å bruke et hundre prosent vinddrevet skip, der fremdrift utelukkende kommer fra Flettnerrotorer. Oppgaven skiller seg fra annen forskning gjort på dette feltet ved å vende om spørsmålet fra hvor mye drivstoff kan spares, til hvor bra kan Flettnerrotorer alene fungere som fremdriftssystem. Hovedspørsmålet i oppgaven blir da som følger. "Hva blir konsekvensene av å utelukkende bruke Flettnerrotorer som fremdriftssystem?".

Metoden brukt i denne oppgaven for å svare på dette spørsmålet kan deles inn i flere deler. Først etableres et litteraturstudie for å legge grunnlaget for videre arbeid. Ytelsesindikatorer blir deretter fastsatt for å forstå hvordan den nye løsningen kan vurderes på en opplysende måte, og for enkelt å sammenlikne ulike løsninger med hverandre. En simuleringsmodell skrevet i Python, basert på et mindre bulkfartøy blir så skapt for å vurdere hvordan løsningen måler seg på ytelsesparametrene. Denne modellen blir i utgangspunktet skrevet på nasjonale ruter og basert på et eksisterende fartøy sitt AIS data, men blir så utvidet til å inkludere arbitrære ruter både nasjonalt og internasjonalt.

Simuleringsresultatene viser at et vinddrevet skip presterer dårligere enn konvensjonelle fartøy. Simuleringene viser også en teknologi som avhenger stort av rutepanlegging og værforhold. Hastigheten skipet seiler i er betydelig redusert i forhold til gjennomsnittet i sektoren, mens påliteligheten gitt en lav forventet hastighet er forholdsvis god. Investeringsavkastningene anses som relativt gode, grunnet økende drivstoffskostnader og dyre alternative nullutslippsløsninger.

Hovedkonklusjonen fra denne oppgaven er at implementeringen av Flettnerrotorer alene ikke er konkurransedyktig i dagens maritime transportnæring. Dersom hovedaktørene er villige til å påta seg ekstra risiko og kundene er fleksible nok til å tilpasse seg et mer volatilt transportmarked vil teknologien potensielt implementeres på spesifikke ruter, laster og skipstyper. Flettnerrotor løsningen alene vil kunne forbedres ved hjelp av komplementerende teknologier og teknikker for å utfylle svakheter iboende i løsningen. Denne oppgaven kan fungere som et grunnlag for videre forbedring av vindassistert skipspropulsjon. Simuleringsmodellen kan forbedres videre og utvikles for å gi et mer komplett og nøyaktig bilde av virkeligheten.

Preface

This master's thesis, subject code TMR4930, is written as the conclusion to the five-year integrated master's programme in Marine Technology at NTNU in Trondheim for the Department of Marine Technology. The thesis is written as a collaboration between MSc. students Håkon Caspari and Mathias Haugbråten. This thesis can be seen as an extension of the work done in TMR4560 - Marine Systems Design, Specialization Project.

We thank Professor Stein Ove Erikstad for his guidance and valuable discussions during the semester. Additionally, we thank Ph.D. Benjamin Lagemann for providing advice and software essential to the project.

Håkon Caspari

Mathias Haugbråten

08.06.2023

08.06.2023

Date

Date

Contents

List of Figures

List of Tables

List of Acronyms

AWA Apparent wind angle.

AWD Apparent wind direction.

BMS Battery management system.

CCS Carbon capture and storage.

CFD Computational fluid dynamics.

CGT Compensated gross tonnage.

DOF Degree of freedom.

ESA European Space Agency.

FR Flettner Rotor.

IOC Intergovernmental Oceanographic Commission of UNESCO.

KPI Key performance indicator.

MUSD Million United Stated Dollars.

ROI Return on investment.

RPM Rounds per minute.

TMS Thermal management system.

TVF Transported volume factor.

TWA True wind angle.

TWS True wind speed.

URANS Unsteady Reynolds-Averaged Navier-Stokes.

WASP Wind assisted ship propulsion.

WPSP Wind powered ship propulsion.

Chapter 1

Introduction

1.1 Motivation

The overall energy demand of the world is only growing, and the need for change is urgent if we are to limit global warming to the 1.5 degrees Celcius goal set by the Paris Agreement (DNV, 2022a). International trade is dominated by about 90 000 vessels responsible for more than 80 percent of all cargo transport. These vessels account for about 3 percent of annual greenhouse gas emissions and must be reduced to ensure a sustainable future in the maritime sector (Oceana, 2022). Emissions from current vessels have the most significant reduction potential by changing or replacing the fuel used with more environmentally friendly fuels. 98.8 percent of all existing vessels utilize conventional fuels while 78.9 percent of planned ships have propulsion systems based on conventional fuels (DNV, 2022b). This illustrates that the maritime sector is changing and that there is a will to make changes to reduce emissions.

There are many options and no simple answer in terms of choosing a solution to achieve a reduction in emissions. Some proposed solutions have been related to LNG, battery/hybrid, LPG, methanol, hydrogen, etc. Common for all these solutions is that they require storage on the vessel and facilities on land. In recent years, the comeback of wind as a source of propulsion has been discussed to reduce the use of fossil fuels for power generation. The technologies that utilize wind as a source of power generation are labeled as wind-assisted ship propulsion (WASP) technologies. WASP is the main focus of this master's thesis and will be presented in detail in section 2.3.1.

Although this topic has been studied in much detail in prior work by other master students, the way this topic has been studied is different in this thesis. While earlier studies have focused on using WASP technology to complement a standard propulsion system to reduce fuel consumption and decrease emissions, this thesis flips the problem. What would the consequences become if a vessel is fully wind-powered, not using wind-assisted propulsion, but a complete wind-powered ship propulsion (WPSP) system? Would the vessel sail at adequate speeds to provide a service that any customer would benefit from? Would the gains of having near-zero emissions and low fuel costs outweigh the increase in sailing time and instability that wind-power is predicted to provide? Will the savings on VOYEX and

emissions defend the CAPEX spending? How much could a vessel that sails only using wind be improved by installing a small secondary power source for specific situations or when wind conditions are especially poor? These are the main topics that will be discussed in this thesis.

1.2 Problem description and overall aim

This thesis aims to provide solid fundamental knowledge about wind-assisted propulsion, and additionally summarize the research and current trends within WASP development. In particular, the focus is on Flettner rotors and to what degree this technology can be utilized as the primary source of propulsion. The applicability of this technology will be evaluated based on a set of KPIs established for the transportation system and tested by creating a simulation model using Python. The simulation model seeks to evaluate how the vessel will perform when sailing several pre determined national routes, based on gathered AIS data combined with real historical weather data. The model may later be expanded to evaluate other national and international routes. The thesis also seeks to find what combinations of technologies may be used with Flettners and what their effect may have on the KPIs. The main research question that the thesis seeks to answer is summarized as follows. *What are the consequences of utilizing Flettner rotors as the only source of propulsion for a vessel?*

Chapter 2

Litterature review

2.1 Previous work

In recent years there has been an increasing amount of papers and research on WASP. This section seeks to identify some of these papers' main trends and findings. After reading, one should see why this thesis differs from previous work, and also gain knowledge about the direction of the specific line of WASP research. In addition, it should provide the reader with knowledge about the fundamentals and the established knowledge that this thesis builds upon. However, the papers mentioned here are in no way a complete list of papers studying WASP. Throughout this chapter and the rest of the thesis, multiple papers will be introduced to support the findings.

The Netherlands Maritime Technology Foundation coordinated a project resulting in the report "New Wind Propulsion Technology: A Literature Review of Recent Adoptions". The paper was delivered in September 2020 to shed light on the potential of WASP within shipping, WASP technology, and the economic and operational impact that WASP technologies may have. This highlights that WASP is still in its early stages, and that the industry needs more research to decide on implementation strategies. One of the main findings from the report is that Flettner rotors, kites, rigid sails, soft sails, and suction wings all can achieve considerable fuel savings. The paper also shows how the solutions perform differently under the same conditions. Therefore, one should choose different technologies based on what routes and weather conditions the vessel will experience. Lastly, the report highlights WASP's broad interest among technology developers, ship owners, operators, classification societies, and others (Chou et al., 2020).

Several papers have examined the aerodynamics and forces that apply when Flettner rotors are used. The paper *Flettner Rotor Concept for Marine Applications: A Systematic Study* gives such insights. De Marco et al. study the use of Flettner rotors for propulsion and how they can be used for the stabilization of vessels in rough seas. The paper presents how one should calculate the thrust from a Flettner rotor. Polar diagrams are created to show the wind directions that result in the highest thrust. In terms of fuel savings, the reported findings range between a 5 to 10 percent reduction in fuel usage (De Marco et al., 2016).

In a research paper published in February 2021, Ibrahim S. Seddiek and Nader s Ammar present a case study where Flettner rotors have been installed on a bulk carrier. In addition, the report presents a power function for the net output power from the Flettner rotor. It is worth noting that this paper and several others do not include the added resistance from drifting. Seddiek et al. conclude that a bulk carrier sailing at a service speed of 13.5 knots can save 22.28 percent of annual fuel consumption by implementing four Flettner rotors. Figure 2.1 shows the configuration of rotors used on the vessel. The levelized cost of energy (LCOE) is also calculated and is found to be $0.05/kWh after eight years of operation. In comparison, the LCOE of hydropower plants produces $0.05/kWh as well (IRENA, 2022), a technology regarded as mature and cheap. The LCOE is found by summating all costs related to the Flettner rotors and dividing it by the total kWh generated by the rotors (I. Seddiek and N. Ammar, 2021).
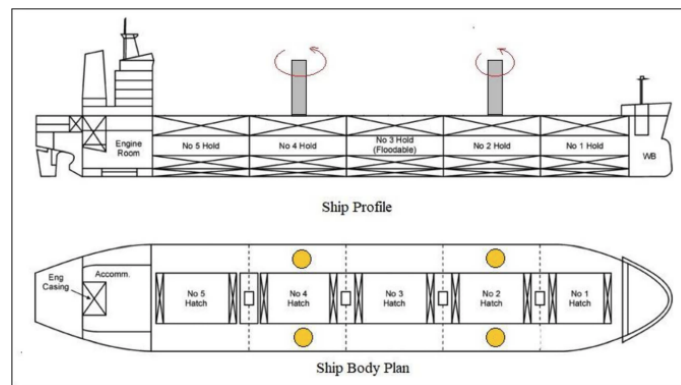
Figure 2.1: Flettner configuration on bulk carrier (I. Seddiek and N. Ammar, 2021)

Seddiek and Ammar neglected the induced resistance due to drift and large rudder angles in their calculations. However, Elger, Bentin, and Vahs have studied this concept further, and found that it is essential for a ship with a wind propulsion system to include this in the propulsion function. They refer to a study by Tillig and Ringsberg where a 1-degree of freedom (DOF) model is compared to a 4-DOF model. The study shows that when not including drift- and rudder-resistance, the reduction in fuel consumption was overestimated by 7 percent, and the propulsion power was overestimated by 40 percent (Elger, Bentin and Vahs, 2020). Elger, Bentin, and Vahs apply many methods to calculate wind-powered vessel's drift angle and added resistance. Concluding remarks include the strengths and weaknesses of the different techniques. In addition, they state recommendations regarding the placement of wind systems on the vessel.

The importance of including the added drift-induced resistance as a result of side forces is supported by the research done by Kramer, Steen, and Savio in the paper *Drift Forces - Wing-sails vs. Flettner Rotors*. They conclude that the Flettner rotor has more added resistance due to drift than non-retractable and retractable sails for the same thrust. The results also suggest that the Flettner rotor in the off position is a significant source of added drift-induced resistance (Kramer, Steen and Savio, 2016).

To make better use of the propulsion from Flettner rotors and other alternative power sources, hull designs could be optimized for lower resistance. Lindstad et al. discuss this in their paper *Decarbonizing bulk shipping combining ship design and alternative power*. The authors conclude that the combination of a slender hull and WASP can cut emissions

by 25 percent and that the reduced fuel bill will cover the expenses of the new design and the WASP system (Lindstad et al., 2022a). Especially interesting is the plots showing the average net propulsion power for different cases, including routing, tiltable Flettner rotors, and different degrees of side forces based on the hull used.

Studies on other WASP technologies are also interesting previous work that lay the foundation for both comparisons and possible combinations with the use of Flettner rotors. Several papers have been written about both kites and different types of sails. Leloup et al. have developed a performance prediction program to assess the possible fuel savings from kites. Both continuous and analytical models are used to solve the parameterization of the kite's motion equations. The authors find that possible fuel saving is 50 percent under Beaufort 7 wind conditions (Leloup et al., 2015). In the paper *Analysis of lift, drag and CX polar graph for a 3D segment rigid sail using CFD analysis*, Atkinson uses CFD to determine the lift and drag characteristics for a rigid sail. By obtaining these characteristics, the propulsion power from rigid sails can be determined. A polar graph is also produced by Atkinson, which presents the wind directions that are optimal for thrust force. The maximum drag force is seen at an angle of attack of 90 degrees (Atkinson, 2018).

In summary, the development and adoptions of WASP technologies are still in their early stages. The recent research mentioned above is mainly focused on how WASP can enable the vessel to achieve some reduction in fuel consumption and act as support to the main machinery. This is one of the areas where this thesis differs from previous studies, as the case without conventional machinery is investigated. As the studies are still in an early stage, simplifications allow for rough estimates. This means that many of the results indicated in these studies could over- or underestimate the actual value significantly. For example, as described by Elger et al. and Kramer et al., the added drift-induced resistance can mean that the propulsion power has been overestimated by as much as 40 percent. By making these simplifications, the differences between the different technologies can be misjudged.

This thesis seeks to build on the previous studies highlighted above and test proposed improvements. The following analysis will differ from much of the earlier research papers by including added resistance from drifting and using WPSP technology. It is of the authors' opinion that this is the direction that the overall WASP research is going. When a solid fundamental and shared understanding of different technologies is established, it is only natural to gradually develop towards a higher percentage of propulsion powered by wind.

2.2   A Historic view on wind-powered vessels

The earliest evidence of boats being used dates back to Egypt and the fourth millennium BCE (Britannica, 2022). Boats were used to transport goods on the Nile, and evolved from using only oars to combining the use of oars and small single-masted square sails. Vessels and sails continued to grow as warships and cargo ships developed in the following millennia. Finally, in about 1400 AD, vessels evolved from single-masted to having multiple masts with a range of sails with different purposes. The multi-mast ships were created to account for varying strength and direction of the wind, and the fact that more masts and specialized sails enable higher speeds (Britannica, 2022).

How effective these wind-powered vessels were, varied according to the configuration of sails, the operational geographic area, and general knowledge of vessel behavior. In the 1800s, some standard terms used by seafarers were "trade winds", "doldrums", and "horse latitudes". The trade winds are the easterly winds blowing near the equator, used by sailing ships to transport items across the ocean. The opposite case of traveling with the trade winds is traveling in the doldrums. Being in the doldrums means being in a wind pattern with little to no wind. Lastly, horse latitudes describe the area between 30° and 35° latitudes. The calm winds combined with hot and dry weather have caused sailors to throw horses and other heavy objects overboard to get through this area.
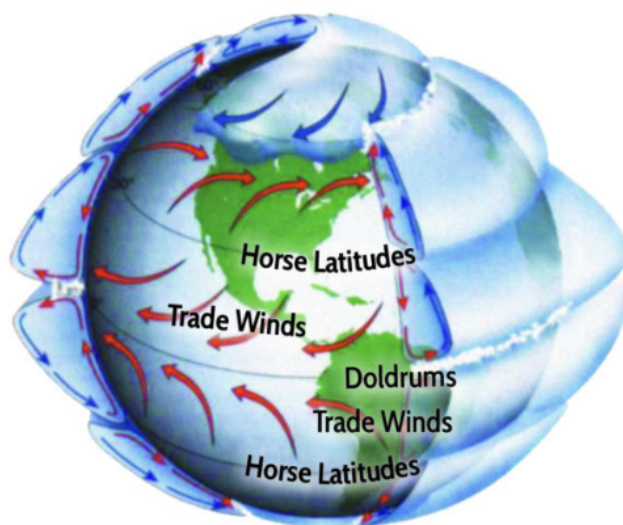
Figure 2.2: Global wind systems (Seahistory, 2022)

The terms presented in figure 2.2 and the development of sail configurations throughout history can give essential lessons that may also be applied in developing solutions today. There will be areas of the world where other renewable solutions are of better use than WASP due to wind conditions described for the doldrums and the horse latitudes. Some routes will experience favorable winds, which for Flettner rotors would be when the vessel is sailing perpendicular to the wind direction. One may see that the challenges of utilizing WASP technology today can be related to several of the difficulties humans have faced for thousands of years.

Although not entirely comparable, it is interesting to compare the sailing speeds achieved by historic vessels with those utilizing WASP. The fastest Roman merchant ships could sail at 6 knots with favorable winds. At the peak of sailing vessels during the 19th century, several high-speed cargo vessels were developed. One of the most famous sailing ships was the Lightning, a clipper ship launched in 1854. Clipper ships were designed to sail at high speeds and carry cargo. The Lightning set several records during her time in service. She sailed 436 miles in a day at an average speed of 18.5 knots, and could sail from New York to Liverpool in 13 days, averaging at 11 knots (Seahistory, 2022). These speeds were, of course, made under favorable wind conditions, and by the end of the 19th century, the clipper ships and other sailing vessels found themselves outperformed by steamships. The era of wind-powered ships ended, and further development was not prioritized. With increased focus on environmental challenges, the shipping industry has once again turned to using wind as a source of propulsion to travel the seas.

2.3 Wind-assisted ship propulsion

2.3.1 WASP technologies

WASP is an umbrella term that covers several old and new technologies. The following section will introduce three of the most prominent ones used today: Flettner rotors, kites, and rigid- and soft sails. The Flettner rotor will be studied further and in greater detail as it is the main focus of this thesis.

Flettner Rotor

The Flettner rotor is a vertically mounted cylinder, as shown in both figure 2.3 and 2.4. It utilizes the Magnus effect, a physical phenomenon where the lift is generated due to a pressure difference between the two halves of the rotor. As an induced wind current attacks the rotating cylinder, it retards the air in one direction and accelerates it in the other (I. Seddiek and N. Ammar, 2021). The rotor thrust can be calculated by a summation of lift and drag in the ship's direction.
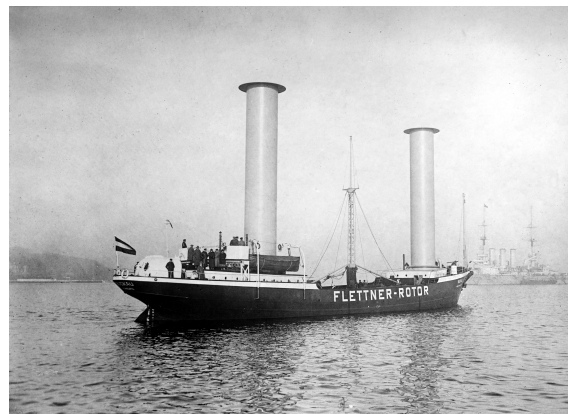
Figure 2.3: First installation of Flettner rotors on the Buckau (Traut et al., 2022)

Flettner rotors are among the most utilized WASP technologies, as seen in table 2.1. The technology has been the subject of multiple research papers in the last few years. However, the concept of a Flettner rotor is not a recent creation. Anton Flettner developed the rotor in the early 1900s (Traut et al., 2014). After creating the concept, he installed rotors on the vessels Buckau (figure 2.3) and the Barbara. As a result, the intended fuel savings were achieved, but the capital cost of the Flettner rotors could not compete with the relatively cheap fuel prices at the time. Today, the price of fuel has increased along with advancements in material science and an increase in focus on lowering emissions. For this reason, Flettner rotors have returned to various vessels worldwide. Recent studies show fuel savings in the 10 to 50 percent range, depending on the amount of Flettner rotors, vessel dimensions, sailing route, etc. (Chou et al., 2020).
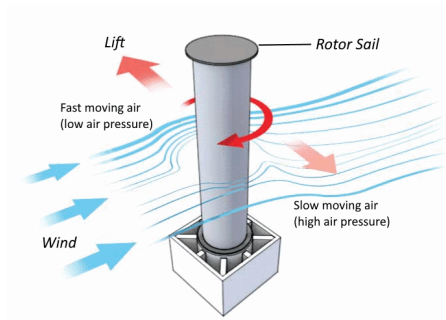
Figure 2.4: Illustration of the Magnus effect (Patowary, 2022)

Kites

A kite rig is a WASP system that utilizes favorable high-altitude wind speeds above the ocean to propel the vessel forward. Kites may be hundreds of square meters large (Airseas, 2022), and provide enough lift to propel smaller vessels by themselves. Typically the kite system is installed in the ship's bow with a fully automated system for deployment and retrieval of the kite. Therefore, the system does not require much deck space and is a good fit for container vessels and other vessels that carry cargo on deck.

An example of how such a kite might look is illustrated in figure 2.5. Airseas designed such a system with characteristics described above. This kite system is paired with a digital twin that ensures that the vessel travels at the optimal route for using the kite as well. On average, this system by Airseas is expected to deliver a 20 percent reduction in fuel consumption. Other competing systems have claimed savings of up to 40 percent, these findings are not studied further.

Figure 2.5: Seawing created by Airseas (Airseas, 2022)

Sails

Several types of sails are considered for WASP. Two of the main types are rigid sails/wing-sails and soft sails. Rigid sails are foils that can be adjusted to optimize aerodynamic forces.

As a result, rigid sails have shown more significant lift coefficients than soft sails (Khan, 2021). Rigid sails are in many ways similar to airplane wings. They tend to consist of two to three parallel sections connected through hinges.

There are mainly two types of soft sails considered for larger vessels. These are the Dynarig and traditional soft sails with modern materials and automated systems. Wilhelm Prölß originally developed the Dynarig, consisting of free-standing, rotating masts with rigid horizontal yards. The soft sails are rolled up inside these yards when furled. When in operation, the Dynarig forms a complete sail from top to bottom of the mast. Dykstra Naval Architect designed the modern Dynarig, which today is mainly used on yachts (Chou et al., 2020).

Traditional soft sails consist of modern textiles as well as automated reefing and furling systems. These systems can be cheaper and lighter than the rigid sail solutions, but the soft sail solutions have not been used much for auxiliary propulsion (DNV, 2020). Furthermore, soft sail solutions typically require more crew training and maintenance than other sails.

(a) Dynarig by Dykstra Naval Architects   (b) Soft sail

Figure 2.6: Soft sail solutions (Chou et al., 2020)

2.3.2   Comparison of WASP technologies

The different WASP technologies introduced above all have their strengths and weaknesses. This has been discussed in several research papers. For example, (Chou et al., 2020) compare Flettner rotors, kites, and Dynarigs in their article "New Wind Propulsion Technology - A Literature Review of Recent Adoptions". The Flettner rotor contributes significantly more to fuel savings than the Dynarig and the towing kite. This results from the Flettner rotor generating power from a broader range of wind directions. Kites are shown to be more volatile in terms of their power output than Dynarigs and Flettner rotors. However, kites have the advantage of catching stronger winds at high altitudes, having a lower impact on roll heeling moment, and requiring less deck space (Chou et al., 2020).

Figure 2.7 below compares a Flettner rotor with rigid wing sails and the Dynarig system. The plot shows that the Flettner rotor performs better downwind (TWA=180°). Dynarig performs well in upwind conditions (TWA=45°), providing higher power savings than the other technologies. Since both the Dynarig and the Flettner rotor are non-retractable, it is observed that the air resistance is influential at pure upwind (TWA=0°). The Flettner rotors may, in some cases, be folded down in more modern models. The rigid wing sails

all perform similarly at pure downwind (TWA=180°). At TWA=90°, the rigid wing sail with a slotted flap performs superior to the other solutions.

The comparison above is for a case with a sailing speed of V_s = 12.5 knots and TWS = 10 m/s. The results in figure 2.7 will not be the same for all cases of V_s and (TWS). For example, the Flettner rotor will not perform well for higher TWS. This is due to the fact that it has a maximum (RPM) (160 in this study) that limits the rotor's spin. The maximum RPM of the Flettner rotor causes it to perform worse than other WASP technologies at high TWS. In short, the Flettner cannot achieve the same high-velocity ratio and lift coefficient as the other WASP solutions mentioned above for exceptionally high winds. However, the Dynarig and rigid wing sails will have their limitations concerning ship stability and structural limits.
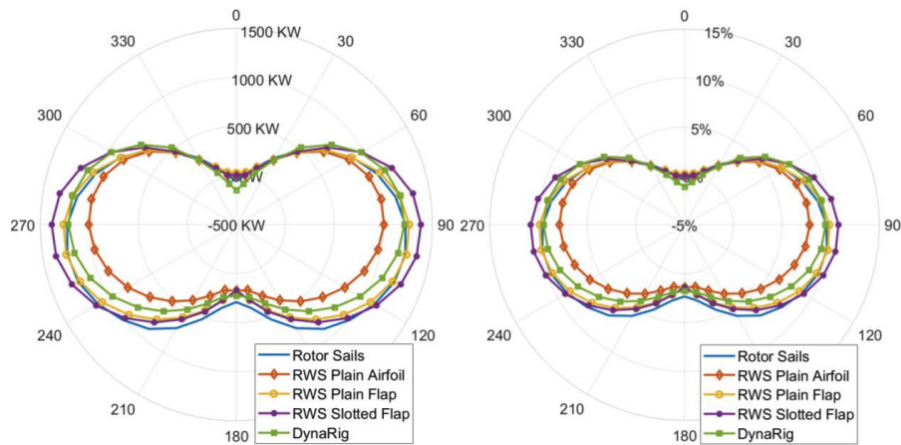
Figure 2.7: Polar diagram comparison of power savings in kW (left) and percentage of engine power (right) (Reche-Vilanova, Dr. Heikki and Dr. Harry, 2021)

2.3.3 Technological readiness

As of 2020, 21 large vessels are operating with wind-propulsion systems. According to the International Windship Association, 25 vessels were installed in 2022, and a further 23 have been planned and will be created in 2023 (Allwright, 2023). As more systems are being utilized, technological readiness and capital costs decrease.

The suction wing has also gained interest and usage by general cargo vessels. Figure 2.8 shows two suction wings installed on the general cargo vessel Ankie. The technology has not been tested and developed as much as the Flettner rotor and the towing kites. In 2020, only two operational vessels had suction wings installed, but according to the International Windship Association, several installations are planned. The suction wings installed on Ankie are currently 10 meters tall, but will be extended to 16 meters in the near future as the technology is developed further.

Table 2.1: Recent adoptions (Chou et al., 2020)

Ship name	Ship type	DWT
Flettner rotor		
E-Ship	General Cargo/Ro-Lo	10 020
Estraden	Ro-Ro	9700
Viking Grace	Passenger	6107
Fehn Pollux	General Cargo	4250
Maersk Pelican	Tanker	109 647
Afros	Bulk Carrier	64 000
Copenhagen	Ferry	5088
Annika Braren	General Cargo	5100
SC Connector	Ro-Ro	8843
Kite		
Micheal A	General Cargo	4884
BBC Skysails	General Cargo	9832
Theseus	General Cargo	3667
Aghia Marina	Bulk Carrier	28 522
Theseus	General Cargo	3667
Aghia Marina	Bulk Carrier	28 522
Suction wing		
Ankie	General Cargo	3600
Frisian Sea	General Cargo	6477

Overall, the Flettner rotor and the kites are the WASP technologies with the most maturity and technological readiness for commercial adaptations. However, one may see an increased development for several other technologies and expect the diversity of installed WASP technologies to grow in the coming years.

Figure 2.8: Suction wing installed on general cargo vessel Ankie (Chou et al., 2020)

2.3.4 Flettner rotor configurations

The different WASP technologies presented will all have several possible configurations depending on factors such as ship type and size of the WASP equipment. Since this thesis is focused on Flettner Rotors (FRs), this section will present some possible configurations of FRs and the related issues that need to be addressed.

When installing FRs on a vessel, one must consider the deck space it will utilize. Ship types such as container and cargo vessels will find it challenging to give up deck space to FRs, as it would mean they could carry less cargo. As a result of this, they are likely limited to configurations where the FRs are placed either in the bow or the stern.

Bulk ships have far more flexibility in terms of FR configurations. Since cargo is stored under the deck, the cargo hatches are the only areas to avoid. Figure 2.9 presents a couple of solutions that may solve this. Oldendorff Carriers have chosen a configuration where the FRs are placed midships between the cargo hatches, while many vessels commonly choose a symmetrical configuration with rotors on both sides. Such a configuration is shown in figure 2.9b.

(a) FR configured amidships (Oldendorff, 2021)

(b) FR on both sides of the deck, with the possibility of being moved on rails (Anemoi, 2020)
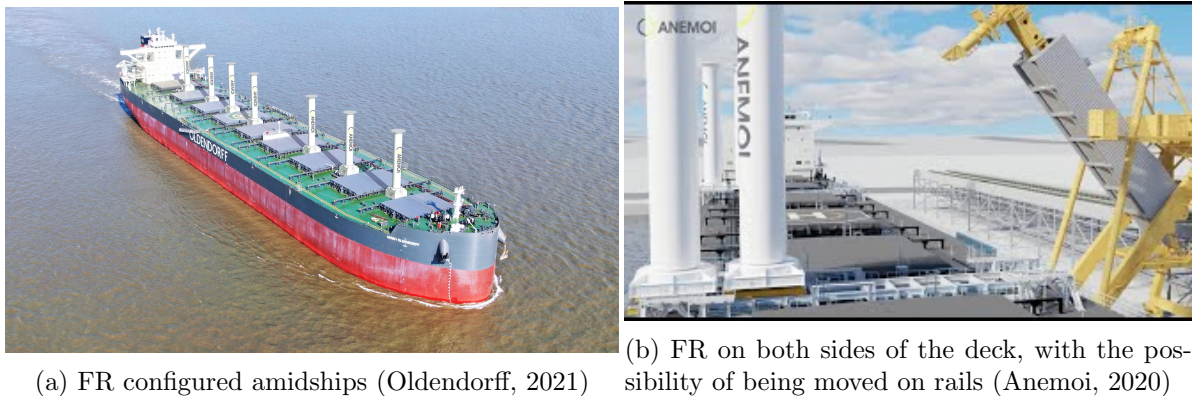
Figure 2.9: FR configurations on bulk vessels

In addition to claiming deck space, the rotors obstruct cargo handling in port due to their height. Therefore, FRs are designed to fold down or move by rails, as illustrated in figure 2.9b. The ship in figure 2.9a is also configured so that all rotors can be tilted down. This is sometimes also needed when ships are passing under bridges. These features are another advantage of the FR and give a competitive edge compared to solutions such as sails.

A typical configuration for vessels fitted with smaller rotors is to place fixed FRs on one side of the vessel. These are less expensive, and placing them all on one side does not hinder cranes during port operations (Riski, 2021). The dimensions of the FR vary with model and company. For example, Norsepower is one of the producers that have delivered rotors to ships currently in operation. Their rotors range from a rotor with dimensions 18x3 (height [m] and diameter [m]) to rotors with a size of 35x5 (Norsepower, 2022).

Due to the relatively large size of current models, both Norsepower and competitors such as Anemoi are working towards releasing even smaller rotors. This is supposed to enable a broader range of vessels to install the FR. The producer Anemoi has stated that it

will release 21x3.5 and 24x3.5 models in the near future (Anemoi, 2023). Efforts are also made to collaborate in combining different WASP technologies. In a recent press release, world-leading sustainable wood bioenergy producer Enviva and marine transport group MOL Drybulk said they will deploy a WASP vessel in 2024 (Buitendijk, 2022). The vessel will combine FRs from Anemoi and a rigid sail developed by MOL. Such combinations can efficiently exploit the advantages of the different WASP technologies. This will be discussed further in section 5.5.4.

2.4   Flettner rotor as a propulsion system

In this section, the fundamentals needed to understand the way a Flettner rotor provides propulsion are explained. One may study the sources in this section for a more in-depth explanation.

2.4.1   Magnus effect and forces from Flettner

The forces generated by the Magnus effect depend on the pressure differences experienced on each side of a rotating rounded object, like a ball or cylinder, exposed to a fluid. This force is called the Magnus force, as it was first observed and scientifically explained by Gustaf Magnus in 1851 (Ahlborn, 1930). The lift force created comes from the change in the speed of airflow around the cylinder, and is explained through the Kutta-Joukowski theorem as follows:

$$L' = \rho_\infty \cdot V_\infty \cdot \Gamma \tag{2.1}$$

The lift per unit span L' over a cylinder of infinite length, in a two-dimensional flow, is given by the product of the fluid density, the fluid velocity, and the circulation Γ of the cylinder. Γ is again provided by the line integral of a closed contour C of the product of the rotational speed and the cosine of the angle of the incoming airflow θ.

$$\Gamma = \oint_C V \cdot cos(\theta) ds \tag{2.2}$$

The resultant function shows that one may increase the force generated from the Flettner by increasing its size and rotational speed. Access to stronger metal alloys and more efficient engines to turn the rotors has allowed the Flettner rotors today to have a much higher output than those used on the Barbara or the Buckau. Correct positioning of the Flettner in relation to the wind, ensuring that the flow of air working on the cylinder is perpendicular to the direction in which the force is to work, will also increase the amount of propulsive force generated. "Produced force" is decomposed into "propulsive force" and "perpendicular force" by the direction it acts in relation to the vessel heading. Produced force is the total force created by the Flettners, while the propulsive force is the force created in the direction of travel. The perpendicular force is the force created perpendicularly to the direction of travel. The image below, from the publication of F. Ahlborn in 1930, shows how such a cylinder may observe the increased pressure difference and how the rotational speed is proportional to lift.
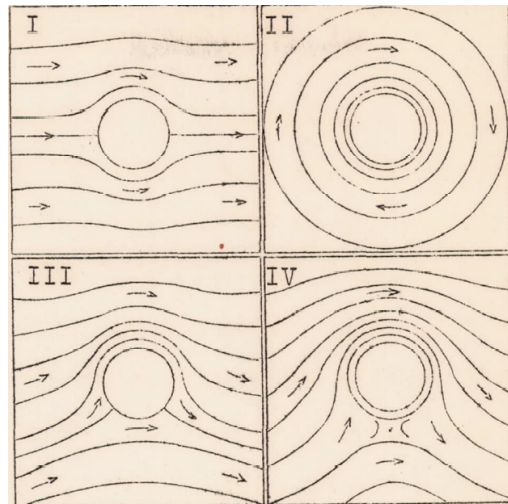
Figure 2.10: Effect of rotation on pressure differences in inviscid flow (Ahlborn, 1930)

In the image above, "I" shows a non-rotating cylinder seen from above exposed first to a potential flow while not rotating. No force is generated. The second image, "II" shows a cylinder rotating in a non-moving fluid, causing the fluid to rotate with the cylinder. Due to the no-slip condition of fluid mechanics, the fluid rotates with the cylinder, but no propulsive force is generated. "III" shows the cylinder rotating with a low $V_{rotational}$ in a moving fluid flow, and "IV" finally shows a cylinder rotating with a higher speed. As one sees, the higher the rotation rate, the more unhindered the fluid passing over the upper part of the cylinder becomes, while the fluid passing over the bottom part is hindered and slowed down. The optimal rotational speed of the cylinder is given by the spin ratio, which is defined in subsection 3.1.5 later. The Bernoulli principle, first proposed by Daniel Bernoulli in 1738, long before it influenced Magnus's introduction of the Magnus effect, states that an increase in fluid speed causes a complementary decrease in pressure (Qin and Duan, 2017). This principle is given in its most common form:

$$\frac{v^2}{2} + g \cdot z + \frac{p}{\rho} = constant \tag{2.3}$$

An increase in velocity must be countered by a decrease in pressure, which finally creates the force that the Flettner rotor capitalizes on. With a reduction in pressure, the cylinder that makes up the "Flettner sail" is pulled or sucked towards the area of lower pressure. Similarly, like how an airfoil pulls an airplane upwards, the vertically mounted FR pulls the vessel forward.

The assumptions made by the Kutta-Jukowski theorem include a cylinder of infinite length in a two-dimensional flow. In practice, the rotors are finite in length with observed boundary layer effects at the ends. Therefore, the actual forces acting on the inner parts of the cylinder may be regarded as close to those found theoretically, while the forces from the ends may produce lower forces. Through several studies, end plates have been fixed to the rotors. These end plates have helped imitate the flow that an infinite cylinder without boundary layer effects over the end would observe. This closes the gap between theoretical and practical solutions and reduces the losses observed.

Consequently, the two-dimensional flow criteria may be observed around most of the cylinder, just not precisely at the edges. Many studies have observed how these parameters affect the output, but theoretical consensus and practical experiments, such as the early use on the Buckau, point to a reality that closely matches scientifically challenged theory. Therefore, even after simplification, the results closely match experimental findings.

2.4.2 Drifting angle and added resistance

The force created by the Magnus effect is the driving force behind a Flettner rotor. The propulsive force component provides thrust that the vessel uses to sail with. The perpendicular force component gives rise to a drifting phenomenon all sailing vessels observe. This perpendicular force causes the vessel to sail slightly angled, leading to an added resistance called drifting resistance. This resistance may be calculated based on the drift angle introduced and calculated below for the case vessel used in this thesis' simulations. Drift resistance is a significant cause of resistance for any sailing vessel. Thus, for a simulation to be accurate, this resistance must be calculated and added to the resistance observed by a vessel sailing with conventional machinery.

Added resistance due to drift angle

The drift angle β of a vessel is given as the angle between the center line of the ship and the tangent of the path that the ship travels (Rawson and Tupper, 2001), see figure 2.11 below.
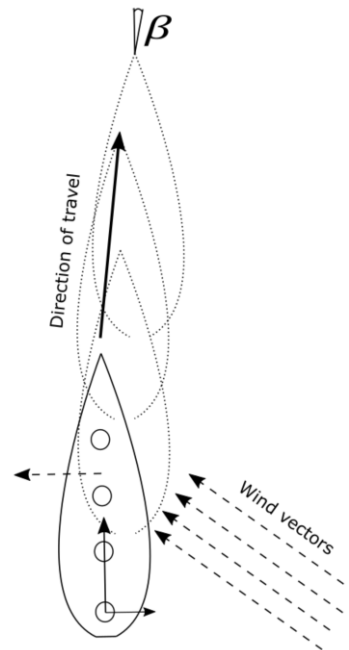
Figure 2.11: Drift angle of vessel

The image above shows that the drift angle occurs due to two opposing forces. The

Flettner rotors generate the first force. This force component of the Flettners works perpendicularly to the direction of travel. This force equals zero when the wind's Apparent Wind Angle (AWA) is 90 degrees and at a maximum when the AWA equals 0 or 180 degrees, corresponding to clean tail or headwinds. The wind resistance of the vessel and sails gives the other side force. This force works in the opposing direction of the Flettner perpendicular component, but is usually smaller than the force provided by the rotors (Kramer, Steen and Savio, 2016). When the angle of the wind is precisely 90 degrees to the direction of travel, then the drift angle will only be given by the friction forces of the wind against the rotors and any wind resistance added by the body of the ship itself. When the wind direction is strictly with or against the direction of travel (0 or 180 degrees), the drift angle due to wind will only come from the rotor perpendicular force output. However, whenever the apparent wind direction (AWD) is anything other than $n \cdot 90, n \epsilon \mathbb{N}$ degrees, the drift angle will be given by the relation between Flettner and wind forces as well as the opposing righting drift forces created by the rudder and hull.

The drifting angle gives rise to several effects that lead to overestimating fuel savings or effectual power output generated by the rotors (Lindstad et al., 2022b). Lindstad et al. (2022b) state that this overestimation of the propulsion system may be as high as 40 percent. Therefore, finding the drift angle that the vessel observes is critical to evaluating the power output lost due to increased drag from the vessel drifting. When the vessel starts moving sideways, the hull and the rudder moving through the water at an angle will create an opposing lift force to stabilize the perpendicular movement.

The mathematical equilibrium that must always be satisfied to find the drifting angle that the vessel will experience is given below. This equilibrium is provided by the perpendicular forces acting from the Flettner rotors operating against the righting forces from the vessel drifting and the wind resistance working on the vessel. Currently, wind forces are negated, and focus is placed on the righting force from the drift angle.

$$F_{perpendicular} = F_{driftangle} \tag{2.4}$$

The perpendicular force, $F_{perpendicular}$, may be written as shown below in equation 2.5.

$$F_{perpendicular} = Flettner\ output \cdot cos(AWA) \tag{2.5}$$

The force from the drift angle, $F_{driftangle}$, may be found by using formula 2.6 below from (Kramer, Steen and Savio, 2016). It gives the lift force created by the vessel's hull as a function of the hull coefficient of lift, C_l. Furthermore, ρ is the density of the seawater, and L, T, and U are vessel length, draught, and velocity, respectively.

$$F_{driftangle} = C_l \cdot 0.5 \cdot \rho \cdot L \cdot T \cdot U^2 \tag{2.6}$$

Only C_l is a non-constant and is studied in the following section.

Coefficient of lift from drift

(Tillig and Ringsberg, 2019) provides a numerical method for finding the coefficient of lift. A specific angle will be reached when the WPSP system's side force and the keel's hydrodynamic lift are equal. Since this angle is dependent on the lift coefficient, one may solve the equation from Lindstad et al. (2022b) below and obtain the coefficient of lift.

$$c_L = Y_\beta \beta + Y_r r + Y_{\beta\beta}\beta|\beta| + Y_{rr}r|r| + (Y_{\beta\beta r}\beta + Y_{\beta rr}r)\beta_r \tag{2.7}$$

Several methods have been evaluated to find this drift angle of a slender body model, and they have been summarized and evaluated in (Elger, Bentin and Vahs, 2020). The methods use either real values found from existing vessels using the technology or, as done in this thesis, model tests to quantify the added resistance from given angles set by physically changing the orientation of a test vessel. For example, in equation 2.7 above, the normalized yaw angular speed "r" is equal to 0, and thus the function reduces to the following:

$$c_L = Y_\beta \cdot \beta + Y_{\beta\beta} \cdot \beta \cdot |\beta| \tag{2.8}$$

Now, both Y_β and $Y_{\beta\beta}$ are given as a function of vessel's dimensions (Kijima et al., 1990). Imputing the comparison vessel's dimensions may therefore be done.

$$Y_\beta = \frac{1}{2}\pi\kappa + 1.4C_b B/L \tag{2.9}$$

$$Y_{\beta\beta} = 2.5d(1 - C_B)/B + 0.5 \tag{2.10}$$

$$\kappa = 2d/L \tag{2.11}$$

Most values of the comparison vessel are stated in table 3.1. However, the block coefficient C_b is not available. The block coefficient is a function of the volume displaced underwater compared to a block of the same vessel's breadth, length, and depth. If the comparison vessel is fully laden, its weight is given by its lightweight summed with its dead weight. The deadweight of 5850 metric tonnes and lightweight of 3006 metric tonnes may be found using the vessel's IMO number. That data is used in the calculation of a block coefficient. Due to the fact that these numbers are estimates, the block coefficient may also be calculated in other ways, giving an approximation that may be better suited. Using knowledge from multiple approximations may provide a more precise result than only using one formula. Therefore, three methods are shown below, and their average is used further. First, the standard estimation given all necessary data; second, the Schneekluths formula; and third, a simplified formula discussed in *Probability and Mechanics of Ship Collision and Grounding* (2019).

$$F_n = \frac{V}{\sqrt{gL}} \tag{2.12}$$

$$C_b = \frac{\nabla}{L \cdot B \cdot D} \tag{2.13}$$

$$C_b = 1.07 - 1.68 \cdot F_n \tag{2.14}$$

$$C_b = \frac{0.14}{F_n} \tag{2.15}$$

The results of these three estimate of the block coefficient are given below, and their average is computed last.

$$F_n = \frac{7.7}{\sqrt{9.81 \cdot 101.26}} = 0.2443$$
$$C_b = \frac{8856}{101.26 \cdot 18.7 \cdot 10.15} = 0.4608$$
$$C_b = 1.07 - 1.68 \cdot 0.2443 = 0.6596$$
$$C_b = \frac{0.14}{0.2443} = 0.573$$

The average block coefficient estimation is then given as follows:

$$C_b = 0.5645$$

Finally, the value for Y_β and $Y_{\beta\beta}$ may be calculated as below:

$$Y_\beta = \frac{1}{2} \cdot \pi \cdot 2 \cdot \frac{10.15}{101.26} + 1.4 \cdot 0.5645 \frac{18.7}{101.26}$$
$$Y_\beta = 0.4609$$
$$Y_{\beta\beta} = 2.5 \cdot 10.15 \cdot \frac{1 - 0.5645}{18.7} + 0.5$$
$$Y_{\beta\beta} = 1.091$$

With Y_β and $Y_{\beta\beta}$ known, one may rewrite 2.7 as:

$$c_L = 0.461\beta + 1.091\beta|\beta| \tag{2.16}$$

Tillig and Ringsberg (2019) gives an alternative method of obtaining the C_L from beta compared to the technique gone into depth with above. The method Tillig and Ringsberg

(2019) uses gives a different equation for solving C_l as a function of beta. The result, as shown below, is of a similar form, but is of a higher degree. For further comparison, one may study Tillig and Ringsberg (2019,p.115).

$$\frac{X_H}{Y_H} = 0.0004 \cdot \beta^4 - 0.009 \cdot \beta^3 + 0.0754 \cdot \beta - 0.0015 \tag{2.17}$$

$$X_H = 0.0004 \cdot \beta^4 - 0.009 \cdot \beta^3 + 0.0754 \cdot \beta - 0.0015 \cdot Y_H \tag{2.18}$$

$$X_H = 0.0004 \cdot \beta^4 - 0.009 \cdot \beta^3 + 0.0754 \cdot \beta - 0.0015 \cdot C_L \cdot (\rho/2) \cdot T \cdot L_{pp} \cdot v_s^2 \tag{2.19}$$

The total resistance using the new formula is then given by multiplying the hydrodynamic resistance with a multiplier (C_L) as found using the method above. The total resistance may alternatively be used by using summating the hydrodynamic resistance with the added resistance X_H.

To show the difference this makes to the C_L regarding the drift angle, one may observe the table below, where C_L has been calculated for all angles between 0 and 9 degrees. The first row shows the calculations of Tillig and Ringsberg (2019), and the second one shows the formula found in this thesis. One may notice that the drift angle is barely noticeable using the formula by Tillig and Ringsberg (2019). Even with a very high drift angle, the method used by Tillig and Ringsberg (2019) generates barely any side forces. For this reason, this thesis utilizes the other formula for calculating C_L.

Drift Angle	0	1	2	3	4	5	6	7	8	9
C_L $\cdot 10^-3$	0.0	7e-02	0.12	0.15	0.18	0.20	0.21	0.22	0.23	0.24
C_L $\cdot 10^-3$	0.0	1.55	5.29	11.2	19.3	29.6	42.0	56.7	73.5	92.5

Drift resistance

Now that a function for the coefficient of lift for the vessel given the drift angle is found, one may utilize the function of lift force on the vessel to see what angle the vessel will drift at to provide sufficient opposing force at any given time. One may find this drift angle and use it to find the added resistance from drift using a 1-dimensional linear regression formula over Skogman's prediction for added resistance, as seen in the graph below (Elger, Bentin and Vahs, 2020).

Figure 2.12 shows a plot of drift angle against the x-fold resistance. The methods used are Skogman's method, Wagner's method, and a model test. The model test is performed to validate the results from the other methods. Skogman's method builds on the work done by Inoue et al. (1981) in "A practical calculation method of ship maneuvering motion". The development by Skogman enabled the output of the drift angle β. Wagner's method is developed by performing two model tests and results from other model tests. As seen in figure 2.12, Skogman's method aligns well with the model test. The technique from

Wagner has aligned with the model tests for vessels with similar dimensions to those used to derive the coefficients in the method. The Wagner method overestimates the resistance for larger drift angles for arbitrary vessels.
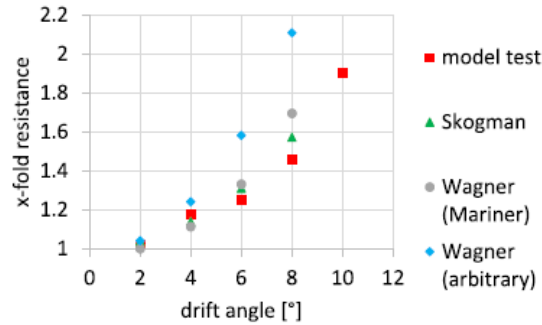
Figure 2.12: X-fold resistance of vessel

This means that the vessel will encounter an x-fold amount of hydrodynamic resistance compared to what was first assumed. As a result, the vessel needs to produce more power than calculated when drift is ignored. The propulsion demand is given in the Python script at all points, and the percentage of the required output that the Flettners can produce is also included. This is done by iteratively finding which angle of drift creates what x-fold resistance factor. When the hydrodynamic resistance, multiplied by this factor, is large enough to be equal to or larger than the perpendicular force, equality is reached, and a solution is found to equation 2.4. In this manner, the drift angle needed to counteract drifting is found, which again may be used to find what speed the vessel will sail at. This iterative process is implemented in the code, and is used to find the new speed given both the heading and the prior speed that the vessel was sailing at. A closer study of the code may be found in section 3.1.1.

2.5   Simulation

In this section, we will introduce what a simulation is and how it may be used as a tool for understanding the performance of a WPSP vessel. A simulation can be defined in many ways. The Cambridge Dictionary defines it as "a model of a real activity, created for training purposes or to solve a problem" (Cambridge Dictionary, 2023). A more technical definition is given by MIT, which defines a simulation as "the process of exercising a model for a particular instantiation of the system and specific set of inputs in order to predict the system response" (Weck and Willcox, 2004). Simulations can be used for all kinds of systems where there are inputs and responses. Examples of possible cases range from grocery stores to airplanes. The possibilities of simulations are limitless, and almost everything can be simulated.

The use of simulation has several benefits. It allows for a safe and controlled environment where systems can be experimented with under all possible conditions. This is done without the risks and costs of conducting the same experiments in real life. For the case of using Flettner rotors, it would be expensive to install four full-size rotors on a vessel and conduct measurements on a wide range of routes. If one wants to test the system under extreme weather conditions or other critical situations, such as collisions, it is far safer and less expensive to observe the system response in the simulation.

In addition to being safer and less expensive, simulations can be repeated and run both day and night without the need for constant supervision. Good simulation models also allow you to "see into the future" by simulating several years of operation within minutes. This means that future problems can be detected in the simulation and corrected before it becomes a problem for the real system. Consequently, simulation also allows for establishing good maintenance routines and operational patterns of the system.

There can be downsides to simulation. The simulation results rely on the accuracy of the model and input in the simulation. If parts of the parameters within the simulation are inaccurate to the real conditions, the consequence is that results are different in simulation than what the true system will output. If decisions are made purely on simulations, one should be aware of the possibility that the results in real life may be different.

Another large factor that influences the results and variance obtained from a simulation is the assumptions and many choices that go into it. The simulation is only as good as the code, the assumptions and the choices behind it. One such choice that must be made is the level of accuracy one needs the simulation to provide. This accuracy is influenced by the granularity of the underlying data or the data fidelity. For example, for a simulation system that simulates the position of a car at any time, using a measurement of every hour will result in a solution that deviates widely from reality. This is due to the fact that, over the course of an hour, the car will have made many turns or stops impacting the trend one is studying. Measuring every millisecond will lead to much higher precision, but also 3 600 000 times more calculations. The more calculations or iterations one needs to take to complete a simulation, the more time it will take to finish, and the more of an influence the assumptions and simplifications will have on the result. Therefore, a balance between time consumption, simulation fidelity, and accuracy must be found. There is no mathematical law or rule for this, and the fidelity must change regarding what is simulated, for instance a car or a ship, and what level of accuracy one might need. A discussion of the data

fidelity for this simulation is presented later in chapter 5 Discussion.

A simulation is in summary a much used and well suited method for testing the feasibility of large scale systems like a FR configuration on a vessel. Although it has several benefits, and may provide highly accurate results when used and implemented correctly, one should be aware of both its drawbacks and potential weaknesses. However, when used correctly, a simulation may save both time and mony and provide usefull insight and knowledge into a system and its functionality.

2.6 Automatic Identification System

The Automatic Identification System (AIS) is a system used by ships and other vessels to automatically transmit information about their ship type, navigational status, location, speed, and heading to other nearby vessels and to either land-based stations or satellites. This information is typically used for navigation and collision avoidance, as well as for tracking the movement of ships for security and logistical purposes. AIS data is the information transmitted by vessels using the AIS system. It is typically collected and processed by receiving stations on shore to create a real-time map of vessel traffic in a given area. Organizations such as port authorities and maritime agencies can also use this data to monitor and manage shipping activity (Kystverket, 2022).

AIS was developed to avoid accidents and enhance safety in the maritime industry. It was developed in the 1990s and became mandatory for most vessels early in the 2000s. The International Convention for the Safety of Life at Sea requires AIS on all ships above 300 gross tonnes. However, it is worth noting that AIS data does not cover 100 percent of ship traffic. Numerous factors can influence AIS and its quality. These factors include technical failures, installation errors, data link/network problems, manipulation of signals, data noise, data coverage, and others (Kim and Smestad, 2021).

As satellite and base stations do not have full coverage worldwide, certain areas will have challenges transmitting AIS data. The result is that some sets of AIS data will contain gaps. For example, Norway has about 50 receiving stations along the coast that can collect information out to around 60 nautical miles. Section 2.7.1 contains an AIS analysis of a vessel traveling along the Norwegian coast. As shown in figure 2.13, this vessel's AIS coverage seems complete.

Overall, AIS data plays a vital role in the global maritime industry, providing critical information for navigation, safety, surveillance, and other purposes. The availability and use of AIS data will likely become increasingly important in the years ahead, due to both a growing commercial fleet with more activity and larger ships. It will be essential to continue increasing coverage and reduce malfunctions.

2.7 Case introduction

To evaluate the use of Flettner rotors as the only propulsion of a vessel, it is necessary to choose a case vessel for comparison. The case vessel enables comparisons between real operational data and the output from the simulations. Table 2.2 presents the main particulars for the chosen vessel. The vessel conducts operations between ports ranging from Stavanger to Sandnessjøen. These will be the first routes the vessel will travel in the simulations.

Table 2.2: Vessel data

Vessel type	general dry cargo
Deadweight	5850 tons
Net tonnage	1904 tons
Length over all	101.26m
Breadth	18.7m
Draught	10.15m
Speed	14.8 knots

2.7.1 AIS analysis of case vessel

An AIS analysis is performed to gain precise knowledge about the operational pattern of the case vessel. This data can then be fed into the simulation models to simulate operations under the same conditions as the case vessel. The Python packages "Pandas" and "Plotly.express" are used to analyze the AIS data and provide illustrative plots. For example, figure 2.13 plots the vessel's movements and clearly shows how it moves along the Norwegian coast and in sheltered water. In addition, the status is displayed as either "Under way using the engine", "Moored", or "Not under command". These labels enable easy identification of the different operation phases, and can explain changes in vessel speed and course.
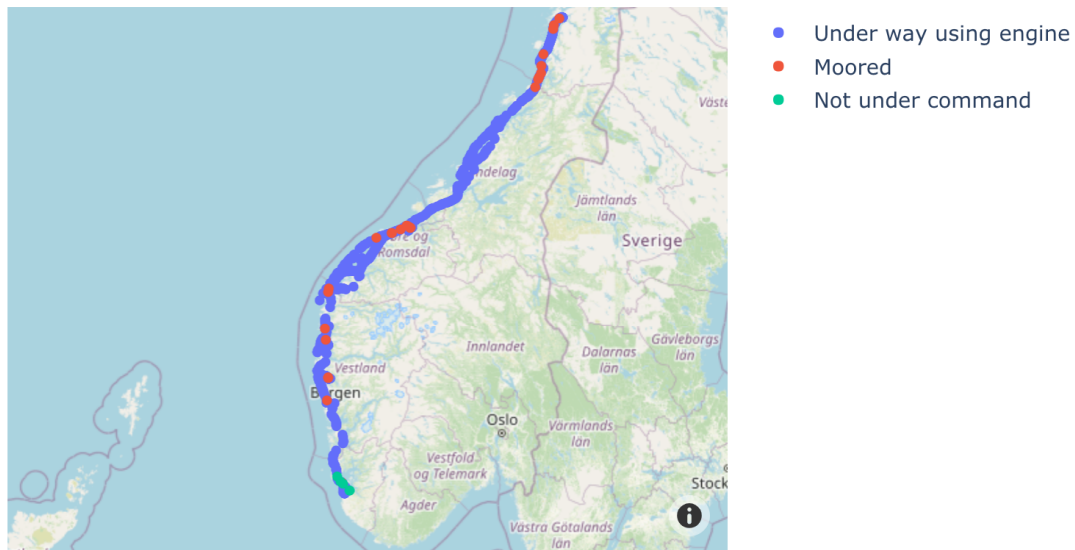
Figure 2.13: Operational route from AIS data

The comparison vessel has no WASP technologies installed, and therefore travels close to the coast where the weather is better than at open sea. Plot 2.14 provides the speed distribution of the vessel with wave height as color coding. As the plot shows, the vessel rarely experiences waves above 1-2 meters, and as expected, the bad weather is mainly between November and February. These conditions are both positive and negative for a WPSP vessel. On one side, smaller waves mean the vessel experiences less resistance and can travel faster. On the other hand, low waves would indicate less wind, but also less resistance. Therefore, planning a route with optimal wind and wave conditions would be necessary for a WASP vessel. Although route planning is studied further in this thesis, wave conditions have been neglected to avoid overly complicating the simulation and the rest of the thesis. Both authors understand that this will impact the accuracy of the results, and encourage the implementation of wave forces in later studies.
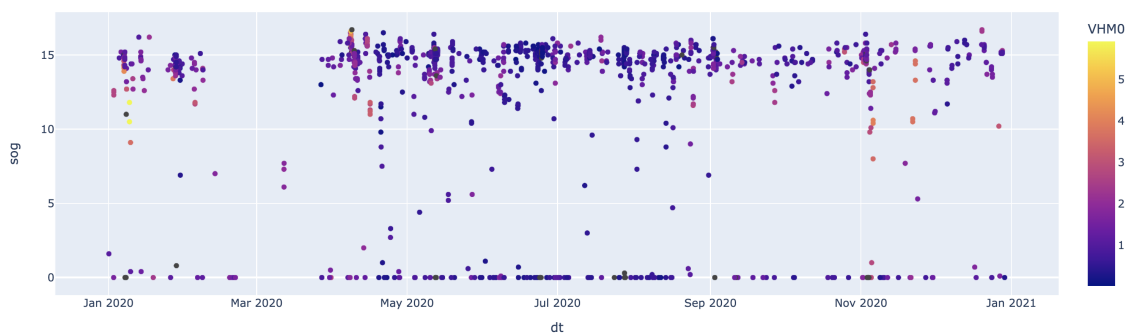
Figure 2.14: Significant wave height with vessel speed

The AIS data shows that the vessel keeps a speed of about 14.8 knots for most of its operation. This allows for predictable and scheduled operations for all stakeholders, thus increasing vessel reliability. A histogram is presented in figure 2.15 and highlights the

operational profile. The performance of the WPSP vessel in terms of consistency in speed will therefore be interesting in evaluating how it performs as part of a logistics chain. It may need a lower service speed to perform consistently and predictably.
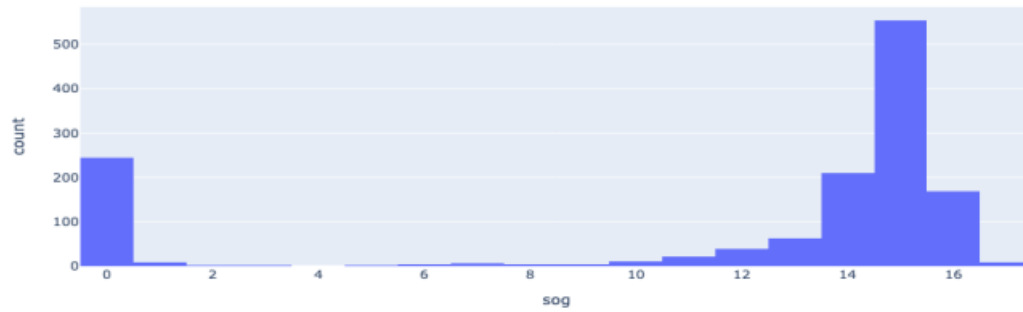
Figure 2.15: Speed distribution of AIS vessel

2.8   Key Performance Indicators

KPI introduction

A Key Performance Indicator (KPI) is any given measurable attribute of a product or, in this case, a vessel that provides insight into the product's long-term performance (Twin, 2023). KPIs will work as a basis for comparing existing solutions with conventional machinery and the WPSP solution.

The goal of any market-based company, from here on denoted as "actor", is to be successful in their given segment or area of focus. How one measures this success varies from actor to actor and from market to market (Hofstede, 2004). To provide value for the stakeholders or beneficiaries, the actor must provide something of value to a consumer or customer. The degree to which the actor can provide this value may then be considered the degree of success of the actor. How does one then create a successful actor or operation? In its purest form, the actor must provide a more desirable service than those of its opposing actors. Providing the same service will not give any advantage, and the actor will likely not succeed. With a limited amount of resources available, the role of the actor must therefore be to allocate the resources available to it in such a way that it provides consistently, or at least more often than not, better results than the actor's competitors (Ohmae, 1982). KPIs are introduced to evaluate which focus areas should be prioritized when allocating resources. The goal is that resources are allocated in such a way that they maximize company utility per invested resource.

What are the goals of the vessel being simulated, and which key performance indicators should be evaluated to assess its degree of performance and success? Arguably, the more important KPIs for any vessel are related to safety for the crew and the vessel itself. In modern shipping, a safe vessel will be prioritized over an unsafe one, even in cases where profit margins are highly favorable for the hazardous alternative. Therefore, safety as a KPI is one of the first indicators a company will look at when chartering a vessel. Safety and other KPIs such as stability, loading speed, crew facilities, or any other KPI not related to the actual transport operation will, however, not be an area of focus for this thesis. While the importance of different parameters and their influence on a vessel is acknowledged, the main goal of this thesis is to evaluate the consequences of transporting goods and materials using WASP technologies. Therefore, the KPIs chosen are vessel speed, schedule reliability, and return on investment (ROI).

2.8.1   KPI 1: Vessel speed

Arguably, one of the most critical and challenging aspects of any WPSP vessel is its sailing speed capabilities. Traditional bulk vessels in the size category that the simulation vessel falls into, around 6000 dwt., sail mainly in the range of 10-15 knots. However, a sailing vessel of 6000 dwt may not necessarily need to maintain this speed. Therefore, finding the speeds that the vessel could maintain on different routes is an important measure to evaluate, and has been a central goal for the program developed. To solve this problem and find the simulation's results, the achieved sailing speed was recorded for each point along each route. This process was repeated through 17520 iterations of the code for all

routes. The results are presented in chapter 4 Results, and discussed later in chapter 5 Discussion.

2.8.2 KPI 2: Schedule reliability

The second KPI to be evaluated is schedule reliability. Schedule reliability is defined as the percentage of times the vessel can sail a specified route at a predetermined speed. This KPI is important as it provides customers with knowledge of waiting time. At what speed or time may a customer be close to certain that their goods will arrive without delay, or at least close to the industry average? According to the Sea-Intelligence GLP report issue 132, the reliability of global vessel transport varied in 2022 from around 27 to around 48 percent on scheduled arrivals. The average time these vessels were late was given for several years in the same report, and is shown in the figures below (TLME News Service, 2022). Sailing delays are therefore not only common, but more common to occur than to not occur. Thus, an on-par performance of a WPSP would be to have a reliability of around 35 to 40 percent for international routes. For national routes, specific reliability data for vessels was challenging to find. However, assuming lower delay due to shorter routes could be reasonable, a reliability score of between 45 and 60 percent could be considered valid. The results of this KPI are again presented in the results chapter 4 Results and discussed later in chapter 5 Discussion.
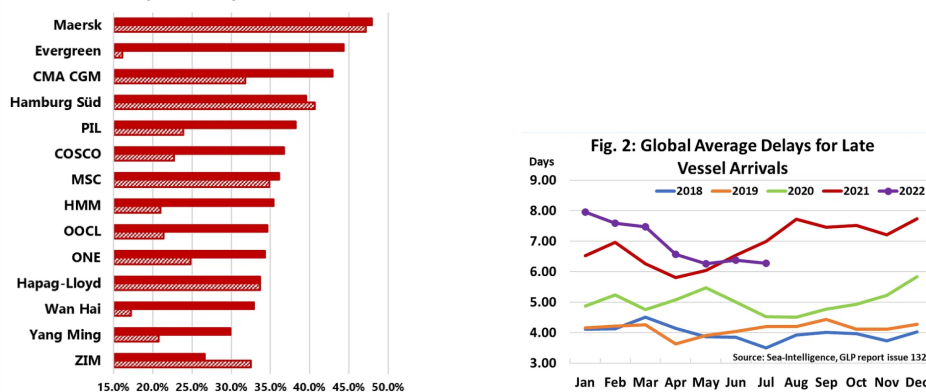
(a) Reliability of global vessel transport 2022 - 2021, (TLME News Service, 2022)

(b) Global average delays for late vessel arrivals (TLME News Service, 2022)

Figure 2.16: Vessel reliability

2.8.3 KPI 3: Return on investment

The final KPI discussed in this thesis is the return on investment, or (ROI), of a bulk carrier like the one in the simulation. The costs concerning CAPEX, OPEX, and VOYEX will be discussed and compared to that of a conventionally fueled ship. How does the price of a newbuild compare to that of a retrofit for this segment? Which combinations of technologies are viable? How are the costs shared between investors, and what problems arise from this? Is there a way to surpass this challenge?

Chapter 3

Method

3.1 Performance prediction model

This section will discuss how the code for the simulation program has been created. The program simulates a vessel sailing using only FRs over defined routes. The program aims to evaluate a theoretical vessel performance with respect to the KPIs outlined in section 2.8. In short, the program does this by combining force calculations with weather and positional data. All parameters regarding vessel particulars are given in the table below, and the weather data is collected from the Copernicus Marine Database. Early in this project, the program was tested on a route where an existing comparison vessel sailed by using this vessel's AIS data as a route foundation. The route may be seen in figure 2.13 in section 2.7.1. Later, multiple international routes were created based on possible sailing paths, and the simulation was tested on these data sets to provide a broader data foundation. Below, a table of the vessel used for the simulation, 3.1, is repeated for convenience. These particulars, taken from datasheets from the comparison vessel, are used to facilitate comparison and reflection on the resulting performance of the simulations.

Table 3.1: Vessel data

Vessel type	general dry cargo
Deadweight	5850 tons
Lightweight	3006 tons
Weight Displacement	8856 tons
Net tonnage	1904 tons
Length over all	101.26m
Breadth	18.7m
Draught	10.15m
Speed	14.8 knots

The program has been created using Python, an open-source programming language using a function-based programming technique. Compared to the original script written in the Marine systems design specialization project, the new method resembles an actual

simulation. Given the available data, it repeats all calculations as often as possible. As the weather data is only updated once every hour, and the location for this data is only available with a granularity of $0.125 \cdot 0.125$ degrees, the simulation will be coarse. However, this granularity is sufficient for showing trends arising from the data and the feasibility of the technology in question. In addition, this version of the simulation also utilizes the vessel heading relative to the wind. Combining these three changes leads to a more realistic simulation than the older version.

3.1.1 Code description

The weather data is collected once every hour over two years. Therefore, one may observe how a vessel that leaves port on 01/07/2020 at 00:00:00 can perform, and compare this to a vessel that sails precisely one hour later. One may run the simulation repeatedly for each consecutive hour that one has weather data for. As a result, a historical trend will arise, giving answers to exactly how much output the Flettner rotors will provide the vessel with over two years. Below is a flowchart of the code and how it functions.
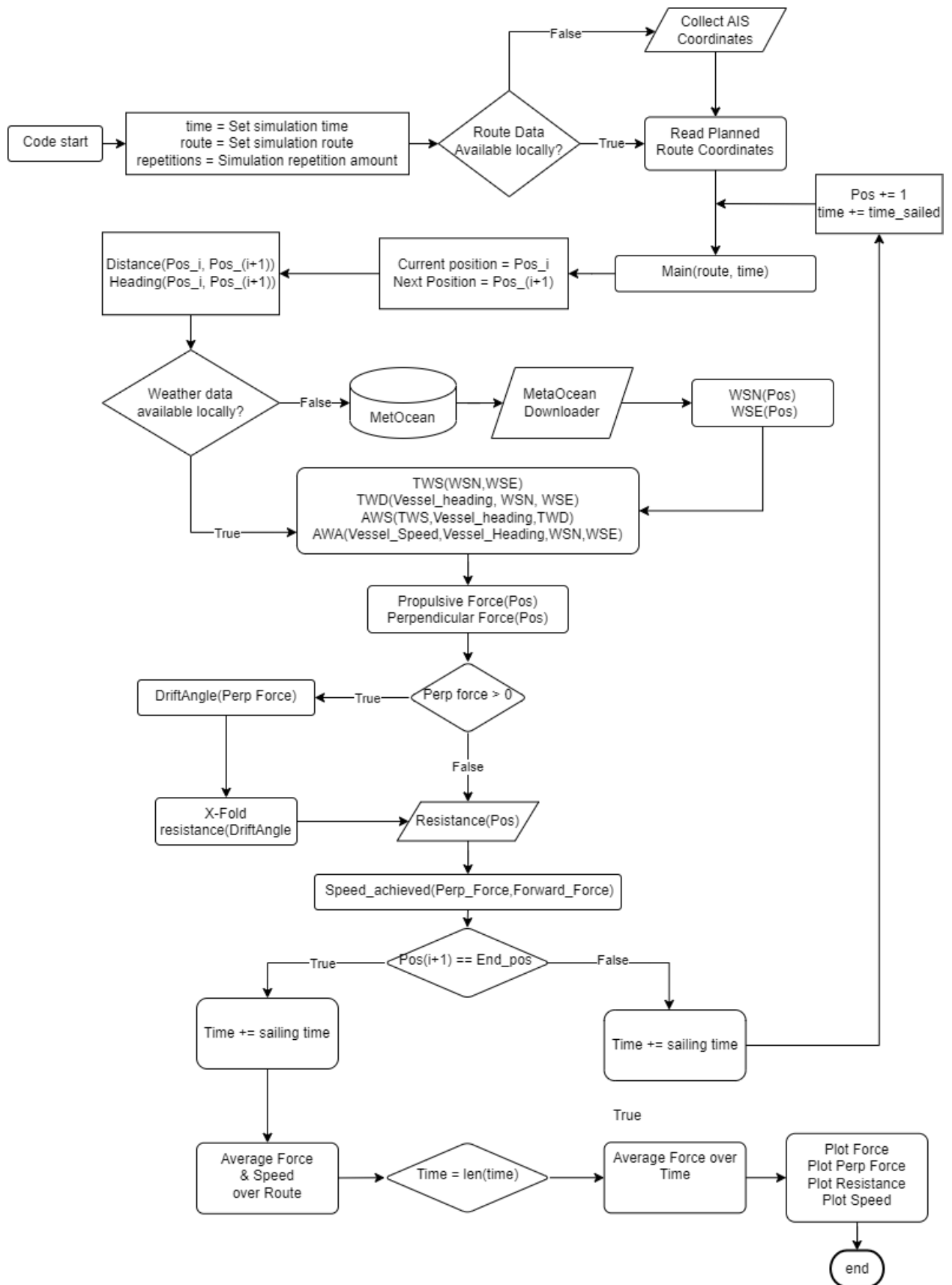
Figure 3.1: WASP Flow Chart

In the flow chart above, the system begins by setting some parameters from which the simulation may proceed. First, a start time for the voyage is set, a route is selected, and the amount of simulation repetitions is set. Here, 17520 repetitions would give one repetition for each hour over two years; more repetitions will not alter results. Fewer repetitions may provide similar results, but with less run time, a proposition that is discussed later in chapter 5. The map shown below shows the True Wind Speed, TWS in the north sea. Higher speeds have a dark red color, while low speeds are shown in blue.
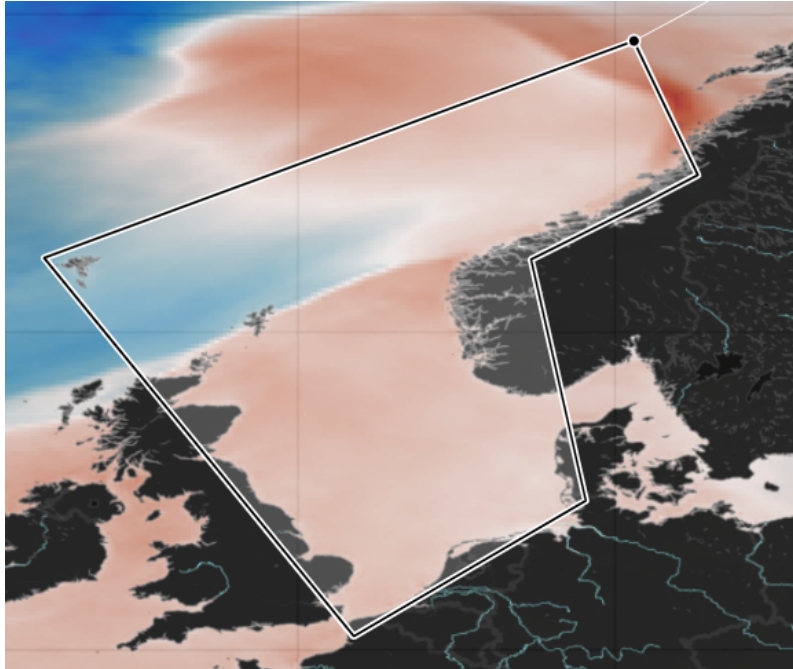
Figure 3.2: Weather map

Some inputs that should be noted: First, the parameters set for time are between the dates that weather data is available. Second, the route is predetermined to be heading over water, but not necessarily checked as a feasible route for the vessel regarding depth, obstacles, or any other sailing-specific considerations. As this simulation is created to be used on planned routes taken by existing vessels, having a route that is at least feasible is assumed to be sufficient. Applying the program to specific routes may be done in the future. Using historical weather and not trying to predict possible future weather is done simply to make sure that the weather patterns that the vessel observes are realistic. Using historically recorded weather ensures that the system is tested on feasible weather situations.

3.1.2 Experimented routes

Figure 3.3: Map of experimented routes

In the map in figure 3.3 above, one sees the approximate route paths that the vessel sails during different simulations. Note that the map only shows what ports and routes are sailed, while a separate Python script generates the actual routes on which the simulations are based. The set of routes has been expanded from national short-distance routes to include international routes. Shorter national routes were used at the start of this project due to the availability of comparison vessel data for these routes. The new routes and destination ports are chosen to provide a wider variety of wind profiles that a vessel could encounter while sailing. This also compares the feasibility of using WASP technology in short sea shipping versus longer voyages. For example, when sailing close to the coast of Norway, where the wind is predominantly in northerly and southerly directions and less powerful than the wind observed when sailing from Ålesund to the Faroe Islands, sailing speeds calculated by the simulation will be lower than for routes where the wind is predominantly heading in a perpendicular direction to the direction traveled. The prevalent winds observed on all routes have been collected and analyzed. Results are seen in section 4.4. To further evaluate the feasibility of a vessel sailing these routes, all routes are sailed in both directions.

After the route has been established and the parameters for the simulation are decided, the function called "main function" starts for each iteration. This function begins by calculating the distance and direction between one set of coordinates and the next. It then checks whether weather data is available locally, or if this must be downloaded from the MetOcean database. Here, the new method diverges from the one created in the pre-master thesis as the weather data at the right place and time is utilized, not an average. This markedly decreases the time the simulation needs to calculate a result, as weather data is only found for the specific location it is needed, and not for the entire route for

each repetition. After the weather data has been found for the specific coordinate that the simulation is now evaluating, the code calculates, in consecutive order, the TWS; true wind direction (TWD); apparent wind speed (AWS); and apparent wind angle (AWA), utilizing the speed with which the vessel enters the new coordinate, which in the first iteration is set to 4 knots, and for the remaining iterations is set to the speed sailed in the prior iteration. From these wind speeds and headings calculations, a propulsive and perpendicular force is calculated using equations presented by Traut et al.(2014). From the perpendicular force found, a drift angle β is calculated using the method formulated by Elger, Bentin and Vahs (2020). This drift angle is used to find a constant for multiplied resistance due to drifting. Next, a resistance force calculation is created to see how much resistance is created at speeds ranging from 0 to 20 knots. To find the speed that the vessel can then maintain using the propulsive force from the Flettners, the equation below is solved:

$$Force\ Propulsion = Resistance\ (Speed) \cdot Multiplication\ factor(Beta) \tag{3.1}$$

The result provides the speed achieved by the vessel at each coordinate. The calculations outlined through this "main function" are repeated for each journey step throughout the route. Each iteration shifts the time from when the weather data is collected with the time the vessel uses to sail from one location to the next. Thus, due to fairer weather conditions, a vessel sailing on 01/07/2021 may use less time to sail the entire route than a vessel that leaves port an hour earlier. In reality, if a later vessel "catches up to" the vessel in front of it, then these will sail at an equal speed for the rest of the route as they will experience the same wind conditions. Now that the speeds of the vessels are only updated in specific steps, the simulation may deviate from results that one can expect to observe in reality. Realistically, a scenario where two identical ships set sail with an hour's separation to travel the same route with the same load is close to an impossibility. The simulation runs for the predetermined amount of repetitions before a dictionary is returned with the sailing speeds of each iteration and results from each calculation. This data may then be plotted in a histogram showing the total time the vessel travels at different speeds. Such a plot is presented below and will be discussed more in chapter 4 Results.
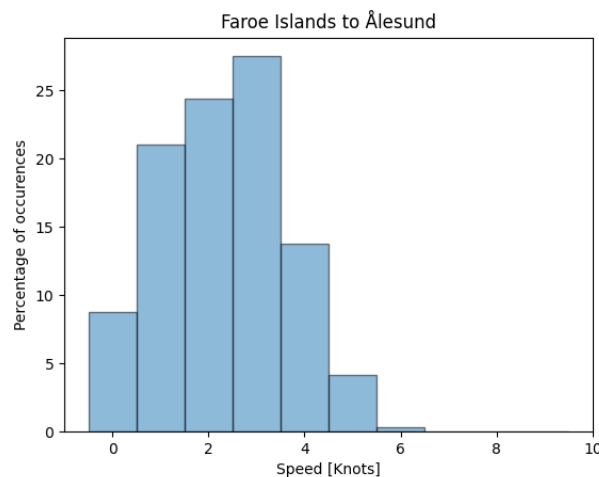
Figure 3.4: Histogram of sailing speeds

3.1.3   Route generation

In this section, the process of generating and refining routes for the code is presented. The method is made so that a new user may create a route and run simulations on it. In figure 3.3, a map showing most of the routes that are used as a foundation for the results and discussions in this thesis is provided.

The routes have been generated using code in Python. First, the coordinates of ports have been specified, then intermediate points have been selected if a direct route is not possible due to visible land obstructions. Sailing from the Faroe Islands to Esbjerg is an example of such a route. Here, an intermediate point is manually added to navigate around the Shetland Islands. The route segment is split into a series of stretches that are a maximum of 7 kilometers long, as this is less than the granularity of the weather data. This was done to ensure that whenever the vessel entered an area with newly calculated weather data, the weather conditions the simulation uses would change. The stepwise method for generating routes is shown below.

1. Create a folder in which to save a route file.

2. Input a start and end point for the route.

3. Input one or more midpoints for feasible sailing.

4. Calculate the distance between the start and the endpoints.

5. Split the distance into sufficient segments so no stretch is more than 7 kilometers long.

6. Add intermediate points between the beginning and end points of these segments.

7. Save the route as a series of coordinates in a .csv file.

8. Mapped coordinates are shown in a browser.

The code for this may be seen in the "route_handling" function in the code appendix I. The steps result in the images that are shown below.

(a) Route generation step 1

(b) Route generation step 2

(c) Route generation step 3
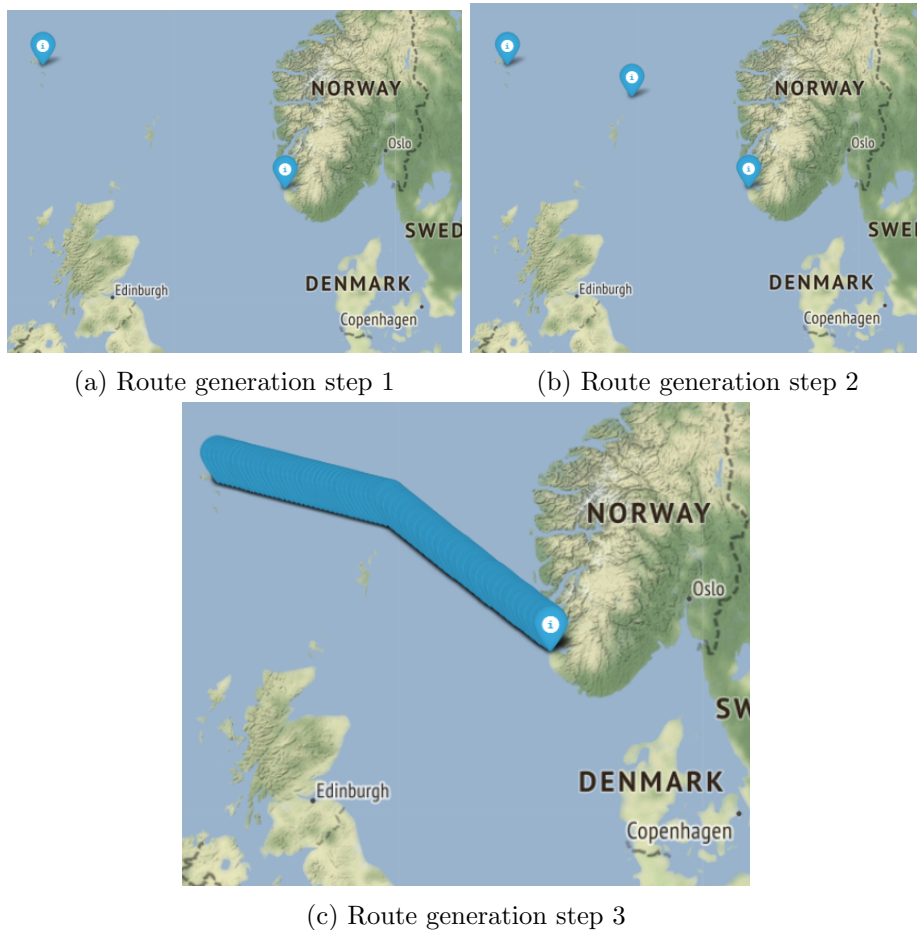
Figure 3.5: Route generation

The reason that the routes shown in 3.3 above are chosen are due to several reasons. There are three different sailing routes that warrant testing for the Flettner configuration. National and international routes for short or longer-ranged shipping and sailing routes with differently dominating weather patterns. National shipping routes were first chosen as specific AIS data for a comparison vessel was available. This allowed for a benchmark with which one could evaluate the simulations with real data regarding specific KPIs. Next, international routes were considered as data from national routes showed low wind speeds and, thus, poor performance. Comparing the sailing speeds achieved on route Trondheim-Ålesund (figure A.14a) with Faroe Islands-Ålesund (figure A.11), one sees this difference in results quite clearly. The average windspeed for each location is 7.08 versus 9.37.

3.1.4 Route discretization

A choice has been made in creating this simulation between discretizing the voyage routes into time steps or distance steps. Both types of discretization may have their strengths and weaknesses. In this thesis, a discretization by distance is used. This is due to the fact that the distance traveled will be planned ahead of time, and thus the calculations regarding time spent may be easier to reevaluate later. If a time discretization were to

be utilized, then the number of calculations that would have to be done or the degree of precision that the simulation would run over, would change with each repetition, since the time spent sailing varies significantly with the amount of wind over the route. By using intervals of a fixed distance, one can foresee how many splits the route will have. Therefore, future evaluation of the results is expected to be more accessible. Furthermore, by dividing the routes into equally distanced segments, one may study specific routes over many simulations, and evaluate which areas one may seek to avoid due to poor wind conditions. This may, in turn, be used to create a new route creation system later.

3.1.5 Values of C_D and C_L

As the values for the drag and lift coefficients are of great importance to the lift provided by the Flettners, a more thorough explanation for their provided values is given here. The values chosen for the drag and lift coefficient are the same as the ones found in (Traut et al., 2014). In this source, $C_D = 0.2$ and $C_L = 12.5$ are given in line with De Marco et al. (2016). There are three main ways to calculate these formulas. The first uses data from specific Flettners showing their total lift and drag force when subjected to different winds. The second is a numerical method using ratios and predetermined coefficients based on geometrical and functional factors. The last method uses a numerical method to solve the Reynolds equation for the effect of fluids on the surface of the rotor. These methods are described below, starting with empirical values found from testing. C_D and C_L may be calculated from the following formulas using the Lift force, or drag force, observed in experiments of specific FRs (De Marco et al., 2016):

$$C_L = \frac{Lift\ force}{0.5\rho A U^2} \tag{3.2}$$

$$C_D = \frac{Drag\ force}{0.5\rho A U^2} \tag{3.3}$$

This method, however, is hard to use when access to experimental tests for the given rotors is limited or nonexistent. In the early design phases of a vessel, a designer would greatly benefit from being able to evaluate how different Flettner sizes would suit their specific design choice. Choosing specific sizes tailored to the vessel's needs is critical when designing a vessel. Numerical methods and computational fluid dynamics, (CFD) analyses may bypass this problem and calculate an FR's lift and drag coefficients without experimental results. Both Seddiek and Ammar (2021) and De Marco el al. (2016) use the following formula to calculate the coefficients numerically.

$$C_L = \sum_{i=1}^{4} \sum_{j=1}^{4} \sum_{k=1}^{3} a_{ijk} SR^i AR^j (\frac{d_e}{d})^k \tag{3.4}$$

$$C_D = \sum_{i=1}^{4} \sum_{j=1}^{4} \sum_{k=1}^{3} b_{ijk} SR^i AR^j (\frac{d_e}{d})^k \tag{3.5}$$

In these equations, SR is the spin ratio, see 3.6 below; AR is the aspect ratio, see 3.7 further below; and a_{ijk} and b_{ijk} are "coefficients related to the geometrical and functional operations of the Flettner rotors" (I. S. Seddiek and N. R. Ammar, 2021), and may be found using numerical results from Badalmenti and Prince (2008). Finally, $\frac{d_e}{d}$ is the diameter ratio between the end plates and the diameter of the rotor's main body. The validity of these ratios is stated to be between $1.0 <= SR <= 3.0$, $2.0 <= AR <= 8.0$, and $1.0 <= d_e/d <= 3.0$.

$$SR = \frac{\Omega \cdot d}{2 \cdot U} \tag{3.6}$$

Where Ω is the angular velocity in radians per second, seen in figure 3.6, d is the diameter, and U is the wind velocity. In short, the spin ratio compares the rotation of the rotor with the speed of the encountered wind. These values will change for all conditions concerning the FR's wind and rotational speeds.

The Aspect ratio relates the height to the diameter of the rotor, is therefore constant, and thus given as the following:

$$AR = \frac{H}{d} = \frac{35}{5} = 7 \tag{3.7}$$

Both these equations are collected from De Marco et al. (2016). The ratio $\frac{de}{d}$ should, in theory, be easy to find, but attempted correspondence with Norsepower has been unsuccessful in obtaining correct measurements. For simplicity, a ratio of 2 has therefore been used, based on a rough visual observation seen in pictures from the Norsepower technical brochure 2022 for example. Through these coefficients and the numerical studies found in Badalmenti and Prince (2008), values for C_D and C_L have been found.

A third way to find drag and lift coefficients is by using CFD, to calculate numerical solutions to the Reynolds equation. These solutions describe fluid flow, for this purpose, air, around the Flettners, thus giving insight into the drag and lift generated. This method is utilized in Craft et al. (2012). They use a technique where "a 3D, unsteady, primitive-variable discretization of the Reynolds equations using a multi-block, non-orthogonal, collocated grid that extends in the axial direction of the cylinder either 1 or 3 diameters" is utilized. More simply, this means using a 3D model of the space, in the x, y, and z plane typically, to account for flow variations in all directions. "Unsteady" relates to a simulation that considers changes in the flow over time, and a primitive variable discretization simplifies the solutions by decomposing the problem into its most simple variable solutions. In fluid dynamics, the primitive variables are pressure, temperature, and velocity in 3D space. A multi-block, non-orthogonal, collocated grid means that the area over which the calculations take place is split into a grid of non-perpendicular lines where these primitive variables are located simultaneously for all grid squares. Other specifics describing boundary conditions, simplifications, and more are described in the paper by Craft et al. (2012). The results used in this thesis build upon the solution found using a 3-D Unsteady Reynolds-Averaged Navier-Stokes, (URANS) model. This model is "able to reproduce the vortex shedding behind a backward-facing step" (Fadai-Ghotbi, Manceau and Borée, 2008), giving accurate results for the FR. As the backward-facing

step method is a widely used flow separation model used in aerodynamic flows (Fadai-Ghotbi, Manceau and Borée, 2008), like the ones seen in airfoils, wings, and FRs, then the method is considered well-suited. A simplification, which leads to reduced processing power needed, with only a negligible loss of accuracy, is accepted in the thesis. The H/d "domain length ratio" of the surface computed over is fixed to 1, as using both a H/d ratio of 1 and 3 yields more or less the same results. As a result, De marco et al. (2016) fixes the H/d ratio to 1 for all computations of C_D and C_L. Finally, the results from this thesis, using the method and simplifications described above, and a spin ratio of 5, gives a C_d of 0.2 and a C_L of 12.
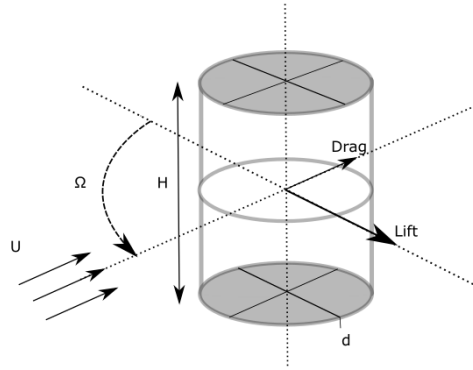
Figure 3.6: Flettner Rotor

Using the FR from Norsepower, which, according to the brochure, has a maximum RPM of 180, or 3 radians per second, a spin ratio of 5 may be achieved for wind speeds up to 9.42 m/s, after solving equation 3.6 for U. A higher wind speed than 9.42 m/s will thus give a smaller spin-ratio, resulting again in a lower lift coefficient.

$$5 = (3 \cdot 2 \cdot \pi [\frac{1}{s}] \cdot 5[m])/(2 \cdot U[m/s]) \rightarrow U = 3\pi \qquad (3.8)$$

In graph 3.7 below, the change in the lift coefficient with the spin ratio is shown. One should observe that at a spin ratio reduction from 5 to 3, the reduction in C_L is about 20 percent. In this thesis's case, if winds exceed 9.42 m/s, the resulting C_L should also be reduced. It should be noted that the graph below is given for a Flettner with an AR of 6. However, due to the fact that all of the mentioned code and assumptions being based on an FR with an AR of 7, this slight discrepancy will be ignored, and the results are assumed equal.
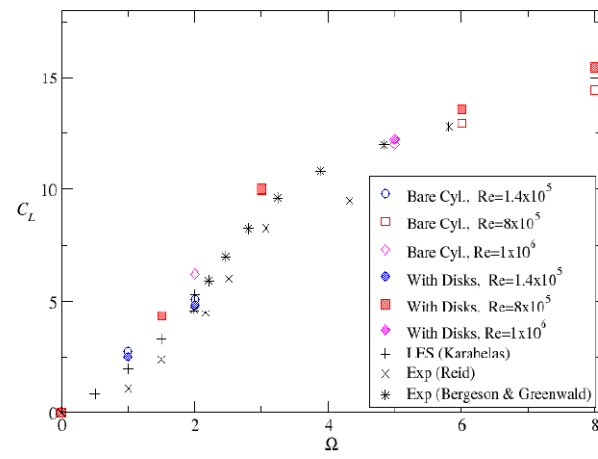
Figure 3.7: Lift coefficient (C_L) from (Craft et al., 2012)

Chapter 4

Results

The following chapter will present the results from the performance prediction simulations. The simulation results will be compared to the case vessel using the KPIs presented in section 2.8. The KPIs are "sailing speed", "reliability", and "return on investment". At the end of this chapter, a review of wind conditions observed over the different routes is presented. The results will be introduced here before a thorough discussion is performed in chapter 5 Discussion.

4.1   KPI 1: Vessel speed

The results of all sailing speeds throughout the simulations are presented as histograms in appendix III. Speeds vary between 0 and 6 knots for the retrofit vessel with only FRs, with most routes having the most occurrences in the 2-3 knots range. This means that compared to a standard speed profile as presented in figure 2.15, the WPSP vessel, at best, offers a 50 percent reduction in speed. Most of the time, the result is about 20 percent of the average performance. The routes have been simulated in both directions. The table below shows the average speed for all routes studied, provided as an overview.

Table 4.1: Average speed sailed over studied routes

Route	Average speed sailed	Average speed sailed on return
National routes	[knots]	[knots]
Trondheim - Ålesund	2.33	2.33
Ålesund - Florø	2.56	2.56
Florø - Bergen	2.58	2.59
Bergen - Stavanger	2.43	2.54
International routes		
Aberdeen - Faroe Islands	2.49	2.49
Amsterdam - Newcastle	2.43	2.40
Denmark - Amsterdam	2.45	2.43
Faraoe Islands - Ålesund	2.76	2.53
Newcastle - Aberdeen	2.29	2.29
Ålesund - Danmark	2.27	2.64

One of the routes with particularly good results is the one between the Faroe Islands and Ålesund. The resulting histograms can be seen in figure 4.1 below. Unlike the other routes, a peak is seen for speeds between 3-4 knots. In addition, about 20 percent of occurrences are between 4-6 knots. The results can be seen in connection with the rose plot shown in figure 4.2. Winds are frequently experienced from optimal directions and with good strength leading to favorable results. The plot shows the speed compared to those seen when sailing between Bergen and Stavanger, one of the poorer-performing routes.
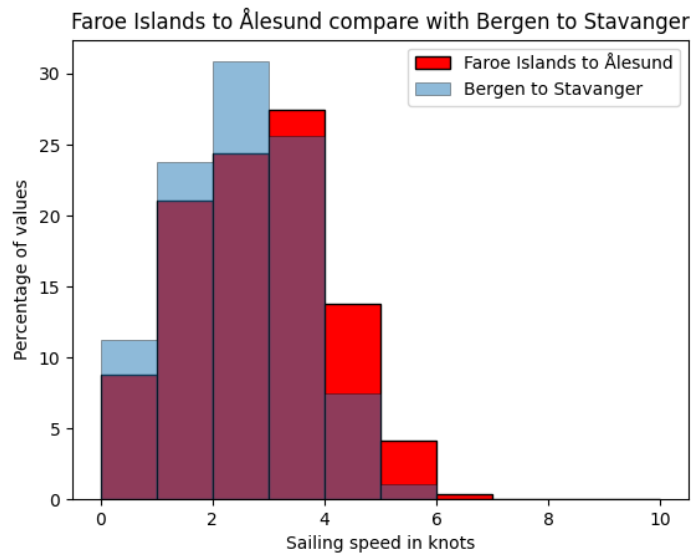
Figure 4.1: Sailing speed on routes Faroe Islands to Ålesund vs. Bergen to Stavanger

(a) Faroe Islands to Ålesund (b) Bergen to Stavanger
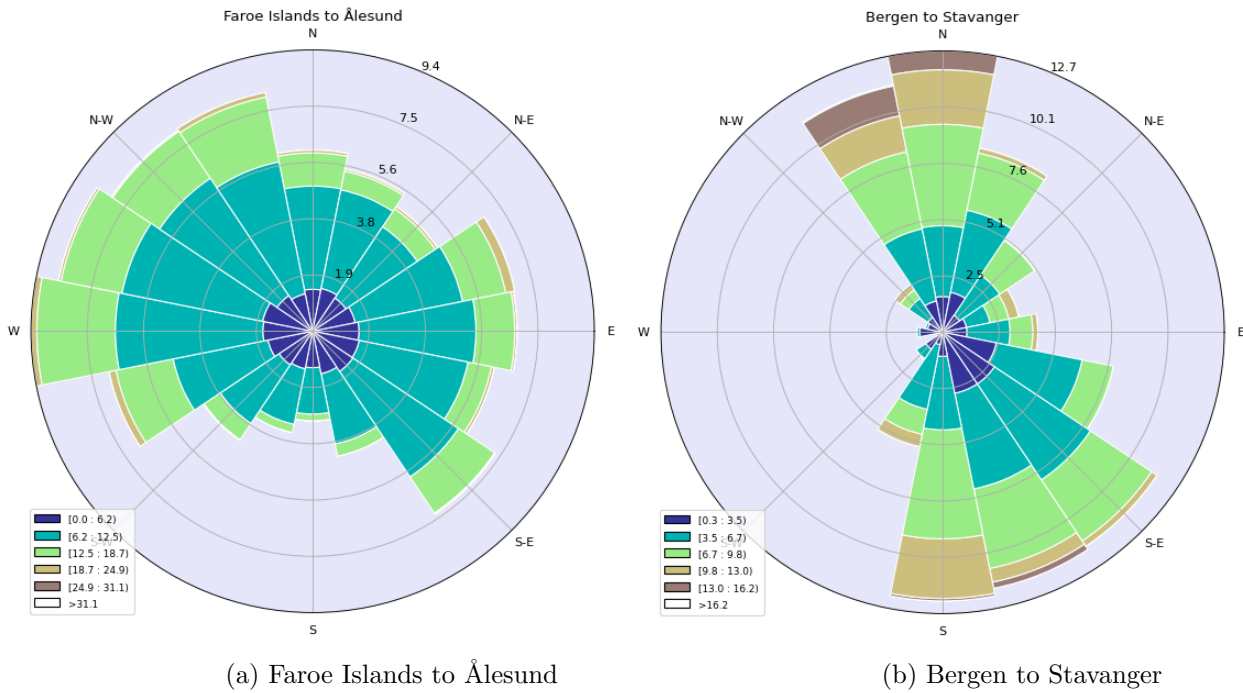
Figure 4.2: National vs. international wind roses

In contrast to the route from the Faroe Islands to Ålesund, which shows high speeds, the Bergen to Stavanger route has more than 65 percent recorded sailing speeds between 0-3 knots. The rose plots here may seem a bit misleading due to their color coding, but the winds are weaker on the national route compared to the international route. The color coding and windroses are further discussed in section 4.4 Wind analysis later. They are also in an unfavorable direction, as the vessel does not encounter side winds, but mostly head and aft winds when it sails due south.

Another example of this dependency on wind directions and speeds is the routes from Newcastle to Aberdeen and from Ålesund to Florø. Both sail quite close to shore, but the Norwegian route has a much higher wind speed, and, as such, sees better performance. This is reflected in the rose plots shown below for the wind speeds. Again, the wind direction may be optimal, coming primarily from the east, but since there is so little wind, little power is produced by the FRs.
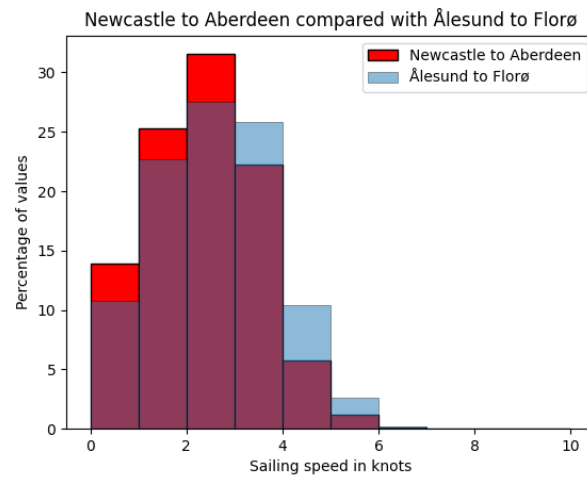
Figure 4.3: Sailing speed on routes Newcastle to Aberdeen vs. Ålesund to Florø

(a) Newcastle to Aberdeen

(b) Ålesund to Florø
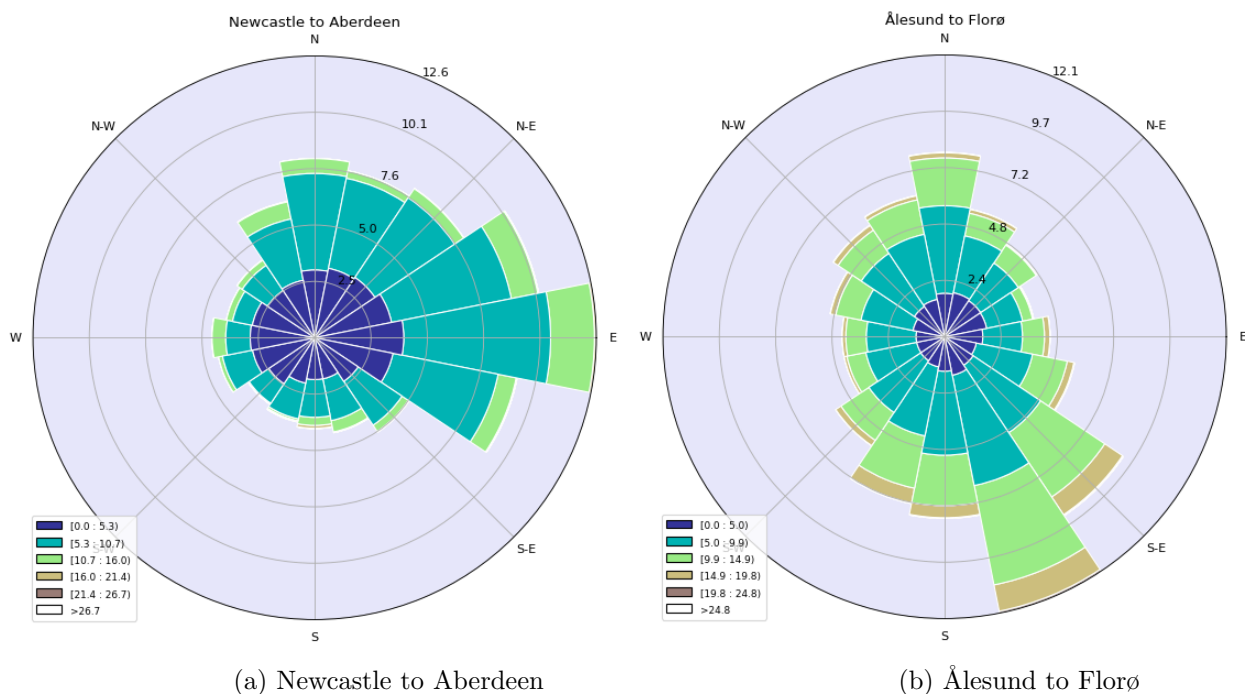
Figure 4.4: National versus international wind roses

Weather patterns change over a year. Therefore, one would expect the sailing speed data to show a trend corresponding to the time of the year the vessel sails. In the graph below, one may observe this pattern change. The graph starts and ends in July. The blue line shows sailing in the period 2020-2021, and the red line for 2021-2022. One can clearly see higher sailing speeds for the winter months. One should note that hydrodynamic resistance is not based on wind and wave conditions, but primarily on the vessel's speed. Therefore, one should expect a lower speed with higher waves. This added resistance is, however, not included in the simulation. Including wave and wind resistance could be an interesting topic for further work.
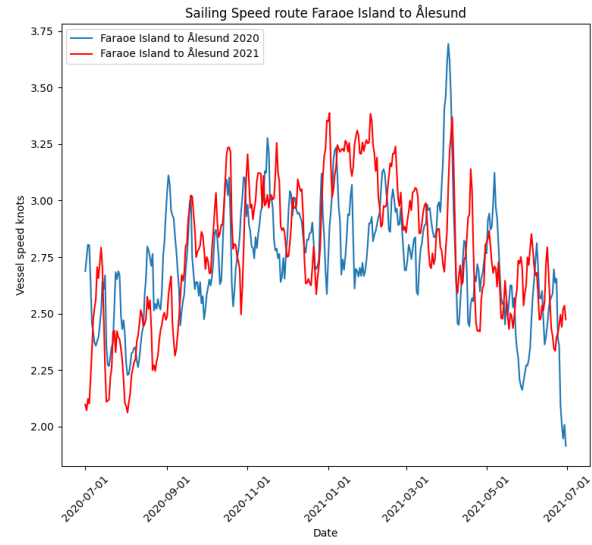
Figure 4.5: Seasonal changes on the trip from the Faroe Islands to Ålesund

4.2 KPI 2: Schedule reliability

The schedule reliability of a vessel as part of a business is seen as its ability to provide service at a scheduled time. This could, for example, mean that the ship would be required to sail at a speed of 14 knots. However, in the case of a vessel powered purely by wind, it is unreasonable to demand such speeds. As seen in section 4.1, 2 knots is a more plausible speed that can be demanded by the WPSP vessel on most routes. Whether this is enough to serve a market is another question.

The reliability on each route is given in table 4.2. Naturally, reliability improves when sailing on routes with better wind conditions. Results shown in section 4.4 shed light on the conditions that lead to individual reliabilities. The results show that the vessel's reliability varies within a range of 10 percentage points. A large concentration is found around 65 percent, which means that 35 percent of the time, speeds are limited between 0 and 1.99 knots. The route between the Faroe Islands and Ålesund is the most promising regarding reliability, with 71 percent of speeds sailing above 2 knots.

Table 4.2: Reliability on defined routes

Route	Reliability in percent
Ålesund - Denmark	65
Ålesund - Florø	66
Aberdeen - Faroe Islands	64
Amsterdam - Newcastle	65
Bergen - Stavanger	63
Denmark - Amsterdam	65
Faroe Islands - Ålesund	71
Florø - Bergen	68
Newcastle - Aberdeen	61
Trondheim - Ålesund	61

4.3 KPI 3: Return on investments

The investment costs of retrofitting a bulk vessel with FRs lie between 2.8 to 4.7 MUSD. Comparatively, the newbuilding cost of a bulk vessel of this size is between 5 and 20 MUSD est. While the OPEX of the two is assumed to be comparatively similar, returns on investments are made by differences in the daily VOYEX from fuel consumption reduction. The rotors require power to spin, and therefore a calculation has been performed to evaluate an estimated VOYEX. The graph below shows the VOYEX of a vessel with different fuel configurations for generators or batteries for energy production for FRs, with that of a vessel using VLSFO only without an FR configuration. Only the VLSFO option is without FRs in this graph.
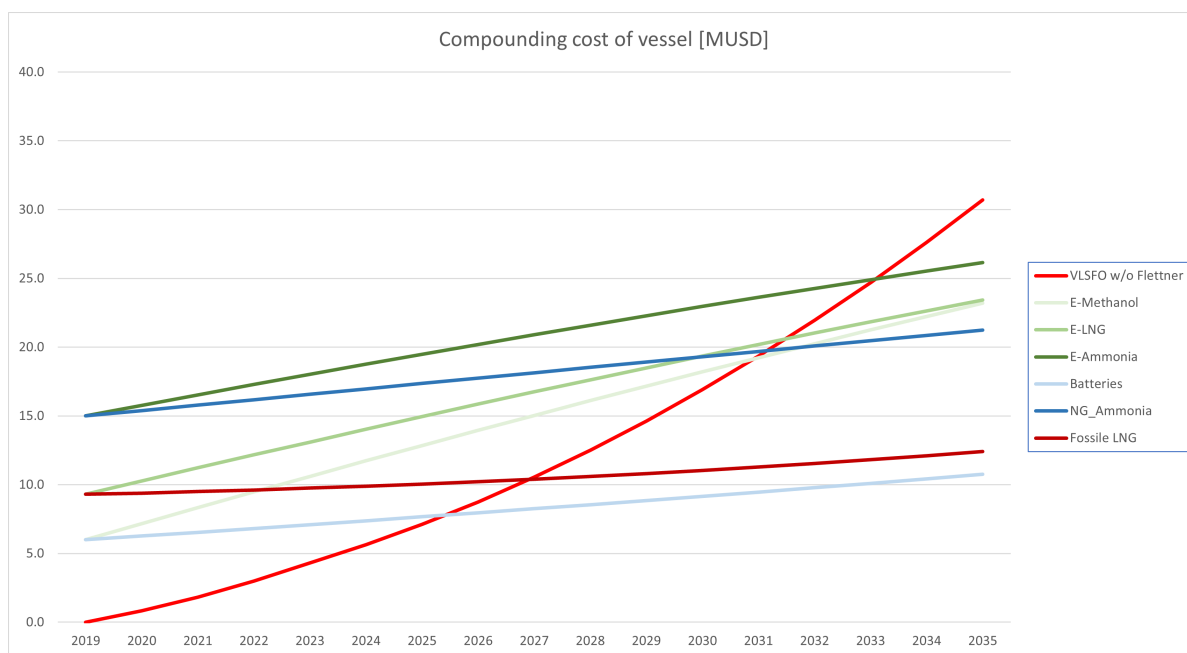
Figure 4.6: Compounding cost of vessel

The most expensive retrofit is ammonia, probably due to the novelty of the technology in addition to requiring a new engine and tank type compared to the other fuels. For batteries, an investment cost of 500 USD/kWh, corresponding to the medium price estimate established by (MAN Energy Solutions, 2019), is used. Methanol or batteries are the cheapest options today, with a low electricity price and a medium to low installation price. At the current price assumptions, the most expensive fuel over time is methanol, even though it has the lowest starting price. In the long run, methanol is the most expensive fuel, passing E-ammonia in around 2043. However, as the graph clearly shows, if a shipbuilder is interested in a positive return on investment, they may see that after 7 to 8 years, a retrofit is favorable compared to sailing with only a conventional system. The graph is based on several assumptions regarding fuel cost, electricity prices, carbon tax levels, energy densities, and battery prices (eia, 2023; Lageman, 2022; Lindstad et al., 2022a; Man Energy Solutions, 2020).

4.4 Wind analysis

The vessel's performance over the different routes presented in section 3.1.2 relies on the experienced wind conditions relative to the vessel heading. If the vessel sails due north, and the wind rose shows mainly wind from the north, then the vessel will experience headwinds, which is suboptimal. If the route, however, is due mainly eastwards and the wind rose still shows dominating winds from the north, then the wind direction relative to the vessel is more optimal for the use of FRs, and the vessel will most likely experience higher sailing speeds. The use of wind roses can visualize these conditions. A wind rose is a graphical representation of the frequency and intensity of wind directions. The concentric circles within the wind rose are numbered to show the

Figure 4.7: Color coding used in wind roses

percentage-wise distribution of the different intensities and directions. All segments within the wind rose indicate the direction that the wind is blowing. For example, if a segment is located in front of the letter "E", the wind comes from the east and blows towards the west.

The roses are also color-coded, as shown in figure 4.7. It ranges between dark blue, turquoise, green, light brown, brown, and white. The dark blue indicates weak wind, and the wind speed increases following down the list. Wind marked with a white color indicates stormy weather and high wind speeds. The specific values in each graph vary, so one must also observe the legends of each graph to understand them.

The following sections will respectively present conditions found on the routes along the Norwegian coast and the international routes.

4.4.1 Short-sea shipping routes along Norway

Figure 4.8 shows the wind experienced on the route between Stavanger and Bergen. Wind from the north and southerly direction dominates the route. The conditions are not optimal for Flettner rotors.

(a) Bergen to Stavanger

(b) Stavanger to Bergen
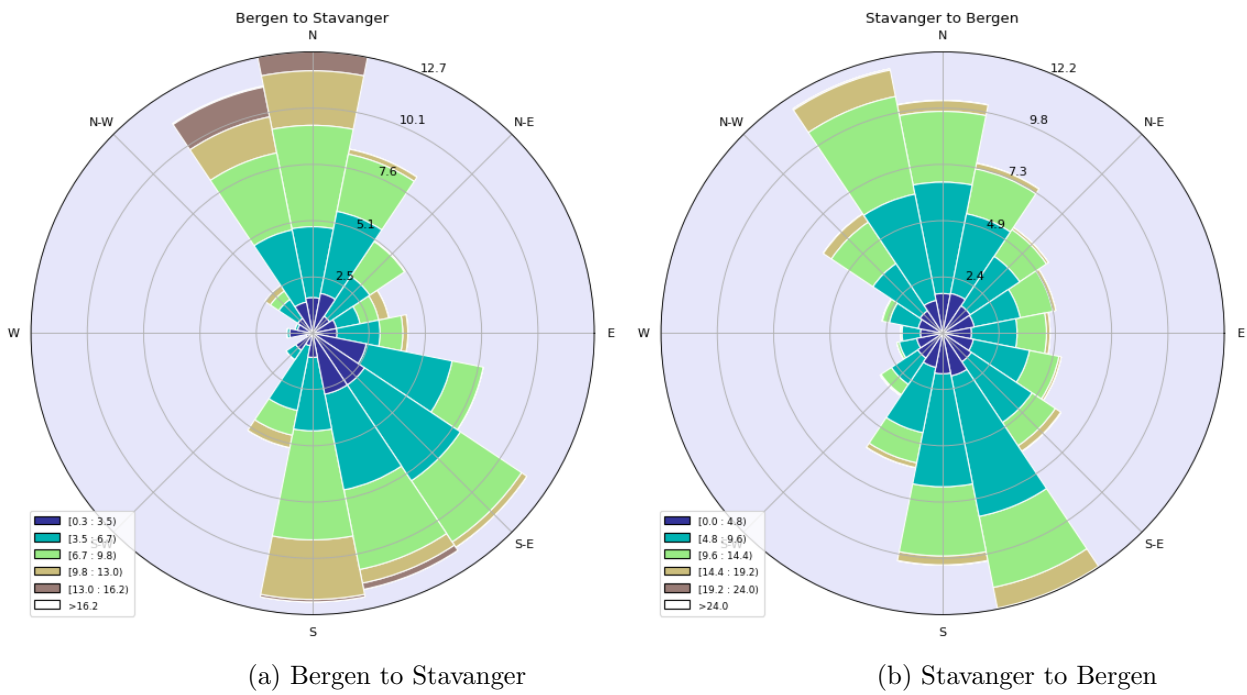
Figure 4.8: Wind experienced by the vessel on route Bergen-Stavanger

Similar conditions apply to the voyage between Florø and Bergen. Winds are not optimal for Flettner rotors.

(a) Florø to Bergen

(b) Bergen to Florø
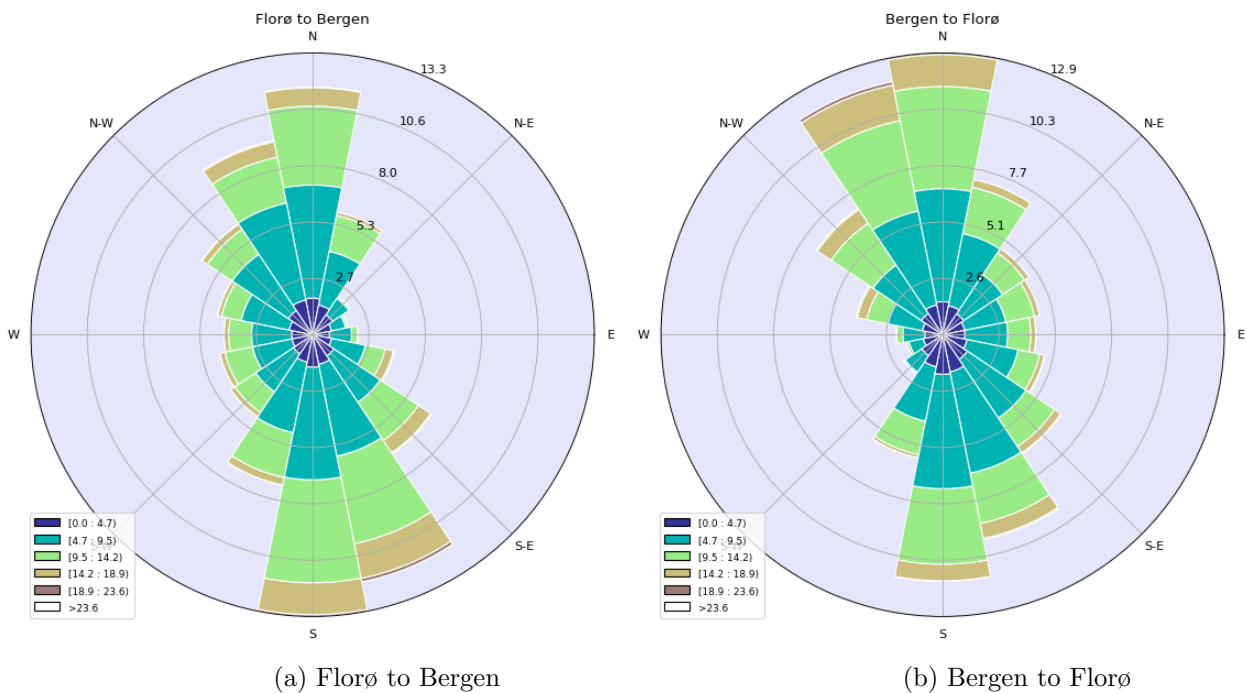
Figure 4.9: Wind experienced by the vessel on route Florø-Bergen

On the route between Trondheim and Ålesund, the vessel experiences a slightly wider range of wind directions. Therefore, the vessel can more often take advantage of the

Flettner rotors. The dominant directions are, however, still as on the other coastal routes.

(a) Trondheim to Ålesund

(b) Ålesund to Trondheim
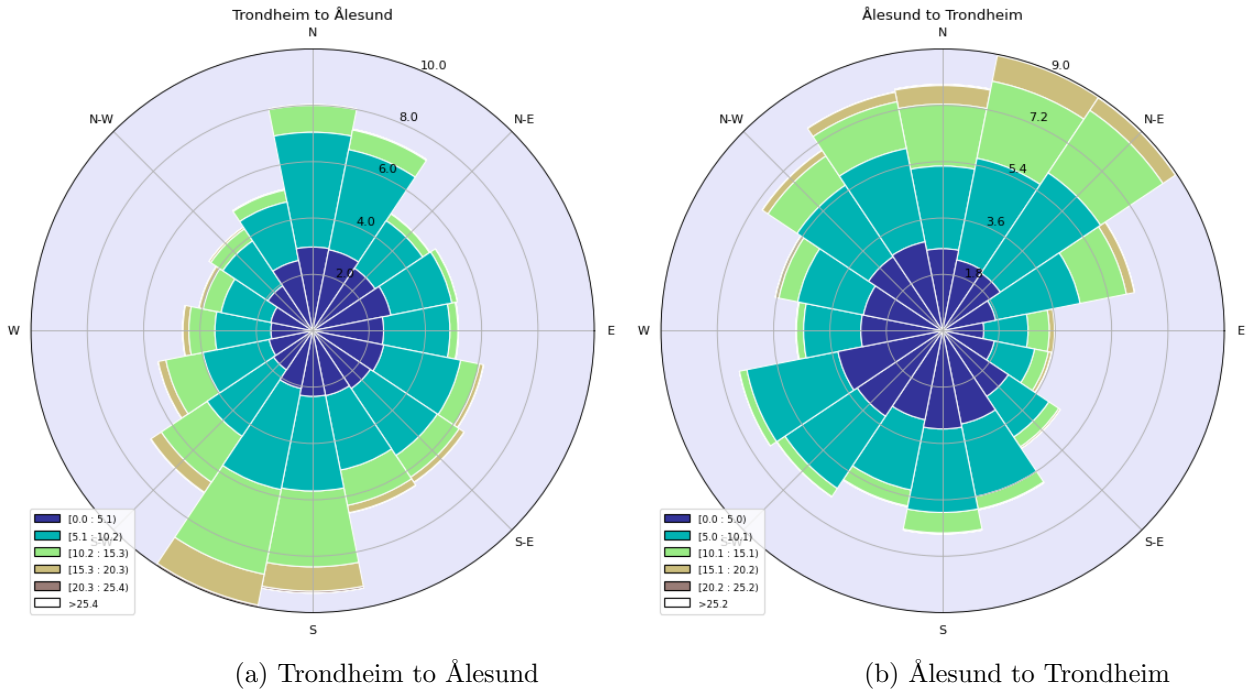
Figure 4.10: Wind experienced by the vessel on route Trondheim-Ålesund

4.4.2 International routes

The international routes presented in section 3.1.2 offer a chance to establish the performance of the Flettner-powered vessel in other geographical areas. The experienced winds along these routes are presented in this section. First, as shown below, one may see that the route between Amsterdam and Newcastle has more optimal conditions for using Flettner rotors. This is due to the fact that the dominant wind directions are between east and southeast as well as west and northwest.

(a) Amsterdam to Newcastle

(b) Newcastle to Amsterdam
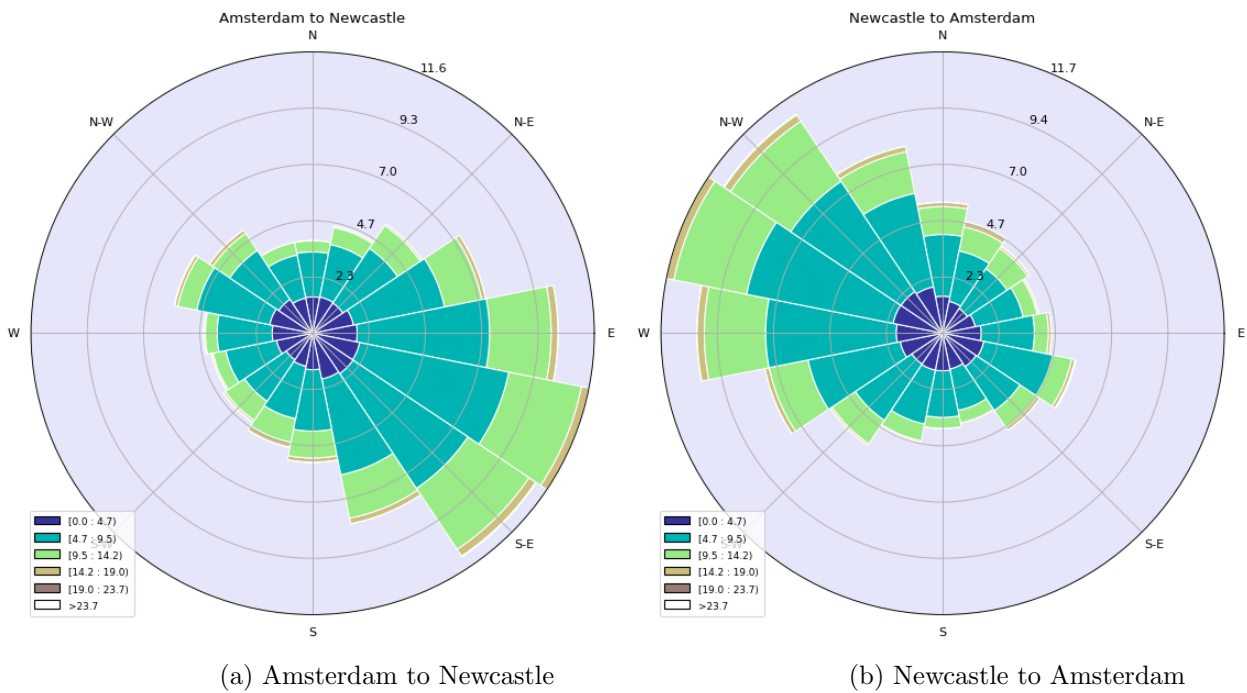
Figure 4.11: Wind experienced by the vessel on route Amsterdam-Newcastle

Another route that has promising results is the route between Newcastle and Aberdeen. The winds blowing in from the North Sea mainly strike the vessel perpendicularly.

(a) Newcastle to Aberdeen

(b) Aberdeen to Newcastle
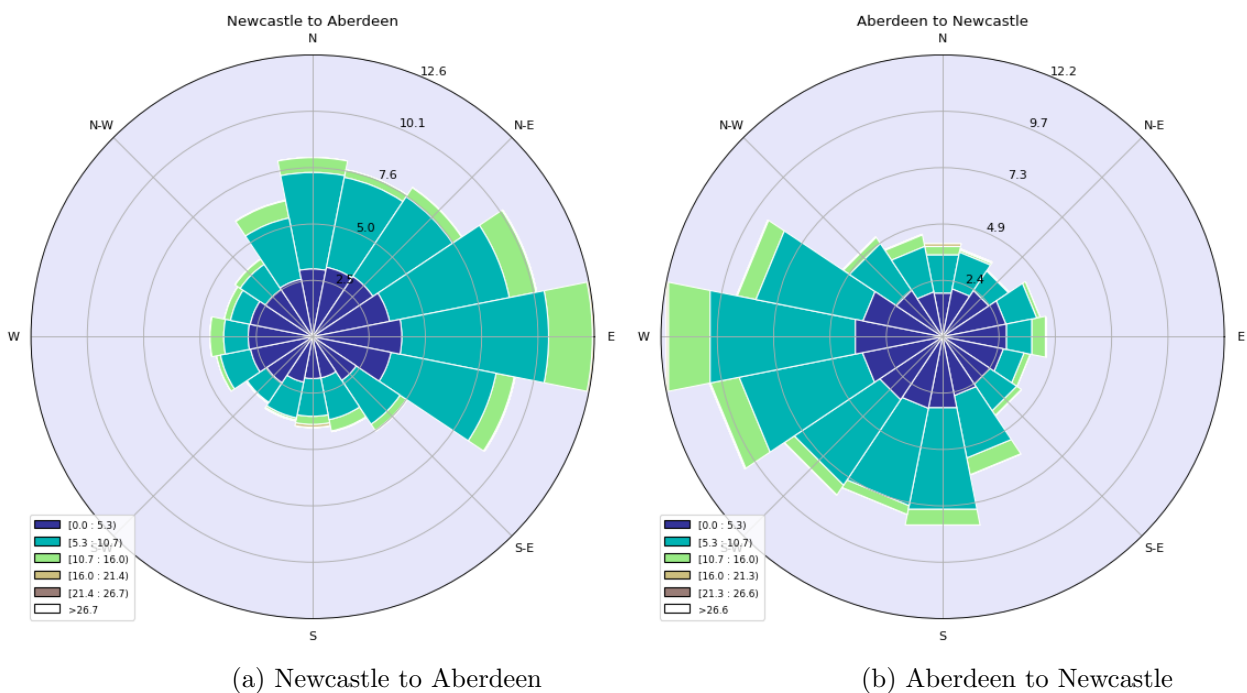
Figure 4.12: Wind experienced by the vessel on route Newcastle-Aberdeen

Results from the other international routes are seen in appendix II. Typical for these routes is a greater spread in wind directions. This does, however, not exclude them from being

viable routes for wind-powered vessels. For example, the Aberdeen and Faroe Islands route offers far stronger winds than many other routes. It could therefore result in good speeds even though the direction of the wind is less optimal.

Chapter 5

Discussion

Introduction

In this chapter, a discussion of the findings presented in chapter 4 of this thesis will be performed with a basis in the method outlined in chapter 3 and the theory presented in chapter 2. The main research objective of this thesis was to evaluate the consequences of utilizing a fully wind-powered ship propulsion system for a vessel. The second objective was to establish methods of improving this base case by introducing complementary technologies to the system. A simulation model was created to evaluate this research objective based mainly on three key performance indices. The main findings show that only using FRs results in a system whose reliability is on par with industry-standard, given a slow sailing speed. The results also show that the return on investment for installing FRs is positively low, performing even better when compared to the introduction of alternative zero-carbon fuels. This chapter first discusses the simulation results in relation to the three KPIs. It then validates the simulation results themselves before discussing a series of improvements that may be applied to the system.

5.1   KPI 1: Vessel speed

As stated in subsection 2.8.1, vessel speed is one of the most important, and perhaps most difficult, KPIs to score well on for a sailing vessel. As conventional vessels typically sail at around 10-15 knots using traditional machinery, achieving a comparable speed while only using FRs is assumed to be difficult, even before running the simulations and verifying their results. Many authors have, as discussed in the "previous work" section of this thesis 2.1, used FRs as a method for saving fuel. In those cases, a theoretical maximum of 22 percent on fuel expenditure is saved. 22 percent, however, came with the assumption of no drifting, which has been discussed in depth in section 2.4.2. It is stated that this may overestimate savings by up to 40 percent. Assuming then that the pure WPSP vessel would be able to perform on par with a conventional vessel, is highly improbable. Presuming a 22 percent theoretical performance is optimistic but practically unfeasible. It is more reasonable to consider a 12 percent saving obtained by accounting for the 40

percent overestimation. This would align with what is seen in practice already, as in the Timberwolf vessel (Norsepower, 2023). In any case, knowing what the base performance is, and later building on this knowledge to see if there are ways to improve it with different additions, is beneficial and one of the main goals of this thesis.

The KPI "vessel speed" is suitable for "quantifying the performance difference of a pure WASP solution compared to an existing transport system", as stated in this thesis' main objective. What could be established as a base case or base speed observed for the pure WPSP system? What can be done to improve the results after establishing a base case? How do the expected sailing speeds change with different locations and routes? Should sailing speed be a KPI for comparing a sailing vessel with conventional vessels? Could, for example, energy consumption per unit of transported goods be a better KPI? Sailing time could for instance be a KPI that is just as suitable to show the performance of the vessel as vessel speed is.

Establishing a base case from which to improve is essential for this exercise. A base case may be the simulation results from different national routes sailed, as these were the first routes studied in the thesis. Small bulk carriers are usually used for short-route shipping, and these routes are therefore befitting the system that the simulations were based upon in the first place. In the graphs below, one can see the results obtained by sailing the routes Trondheim to Ålesund, Ålesund to Florø, Florø to Bergen, and Bergen to Stavanger. The routes are between 65-180 nautical miles approximately. They have been combined in pairs to compare them below more easily, and to observe their differences. The routes have also been run in reverse, where the route plotted is flipped, allowing for sailing back to the port of origin. These results are not included here, but are shown in appendix III, together with all other histograms not included in the discussion.
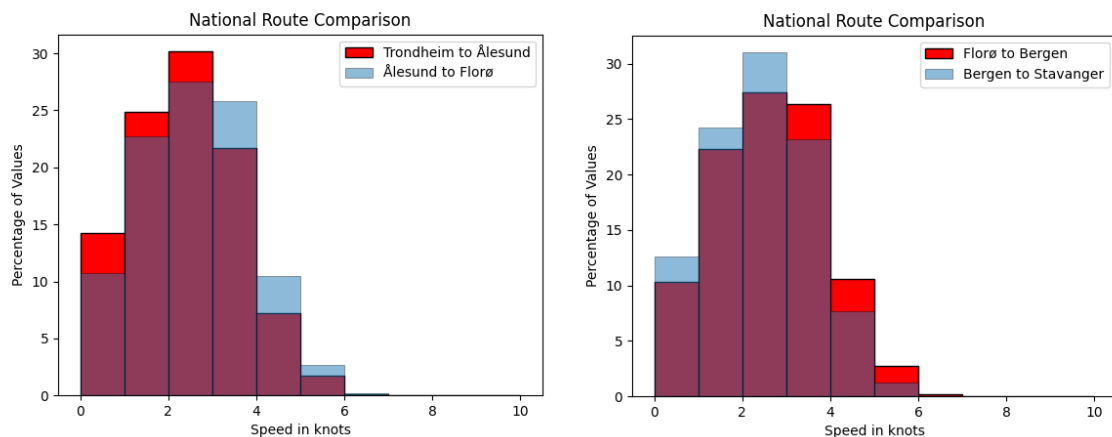
(a) Trondheim to Ålesund vs. Ålesund to Florø   (b) Florø to Bergen vs. Bergen to Stavanger

Figure 5.1: Two national routes compared

As one may see in the images above, sailing speeds at different national routes vary, but only slightly. The difference is around 10 percent in both graphs. The table below shows the different averaged speeds observed, including on routes sailed internationally. They vary between 2.3 and 2.6 knots, a fairly low sailing speed compared to the industry standard.

The results, as shown in table 4.1 in chapter 3 Results, are feasible because they reflect earlier assumptions of low sailing speeds. The results show that using only FRs on national and international routes around the Norwegian coast and in the North Sea is probably not a stand-alone solution that can replace conventional sailing methods without losing productivity. When traveling internationally, for example between the Faroe Islands and Ålesund, one sees higher speeds, as expected, but only slightly so. The route crosses the North Sea at an angle compared to the dominating wind patterns so that the FRs can be utilized well. In appendix II figure A.2b, the rose plot shows higher velocity and dominating side winds that the vessel observes on this route. Despite this preferable wind condition, the results still show low sailing speeds.
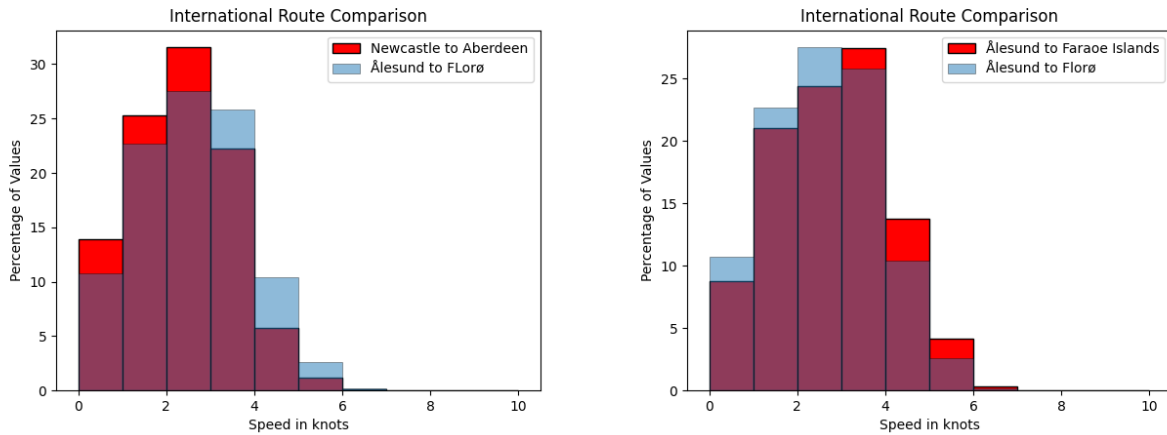
(a) Newcastle to Aberdeen vs. Ålesund to Florø   (b) Ålesund to Florø vs. Ålesund to Faraoe Islands

Figure 5.2: Route comparisons

Generally, when sailing far from shore, one would expect to see higher wind speeds and, as a result, a higher sailing speed. The results from the simulation, on the other hand, show that even though this is true on many routes, see figure 5.2b above, it is not always the case. For example, as seen in figure 5.2a, the speed obtained when sailing along the east coast of Great Britain results in much lower observed sailing speeds versus when sailing from Ålesund to Florø. One may conclude that sailing far offshore is often better than close to shore, but it is no given rule. Studying weather patterns and planning routes based on what weather is found is deemed more important than just sailing far from land.

As seen in table 4.1 in chapter 4, the best route to sail is the route from Faroe Islands to Ålesund, but at what time is this route the best? With seasonal weather, one should expect higher winds and better results at different times of the year. This is shown in figure 4.5 in chapter 4 Results as well. Visual evaluation shows a 0.5-knot difference in speed, corresponding to around 20 percent quicker sailing during the winter season. This should be taken into account when planning routes as well.

5.2   KPI 2: Schedule reliability

When accepting speeds as low as 2 knots, the WPSP vessel's reliability is competitive compared to shipping companies worldwide. Maersk was the leading company in 2022, with schedule reliability at 48 percent (TLME News Service, 2022). How can the schedule reliability of the WPSP vessel be higher than that of the conventional shipping vessels? The answer is found in the difference between the simplifications of simulations compared to the real world, and the fact that a very low sailing speed is assumed. For the WPSP vessel, the cause of poorer reliability is the inability to maintain sufficient speeds. This can also be a problem for conventional vessels due to bad weather, but other important factors are port congestion, labor strikes, and poor management (Cheng-Chi and Chao-Hung, 2011).

The factors such as bad weather, port congestion, and labor strikes are beyond the control of the vessel's operators. Therefore, the simulation results would likely worsen in real operation since unforeseen events have not been accounted for in the WPSP schedule reliability. Regardless, a positive finding from the discussion on schedule reliability is that shipping companies, ports, and entire supply chains are used to varying degrees of reliability from marine vessels. This suggests that the players involved can adapt to the ever-changing arrival times of the WPSP vessel.

As seen in section 4.2, the reliability is at its highest when sailing from the Faroe Islands to Ålesund. Generally, the routes closer to shore have poorer reliability than those that exploit winds on the open sea. Interestingly, one might find that these schedule reliabilities could shift in real operation. This is because the larger international ports are far busier than smaller national ports (Inbound Logistics, 2020). For example, the port of Amsterdam and surrounding ports such as Rotterdam are the busiest ports in Europe. As a result, the risk of port congestion and delays increase when sailing to these destinations.

Busy ports raise another concern for the WPSP vessel. Port administrators create berthing plans to handle all ships arriving at the port systematically. These plans are commonly drawn up a month before, and contain all information on the upcoming activities in the port. This includes arrival times, departure times, amount and type of cargo, service needs, and other factors regarding the ships arriving at the port (Menon, 2021). The schedule reliability of the different routes shows that a WPSP vessel sailing on these routes will likely struggle to keep a set schedule. This results in a difficulty concerning reporting arrival times to port authorities in advance. Consequently, WPSP vessels might find it difficult to conduct operations efficiently in busy ports.

To summarize, several factors indicate that the WPSP vessel will have worse schedule reliability when entering real operation. Ports and companies are used to delays, but may need to adapt significantly to accommodate WPSP vessels that, on a regular basis, cannot report and deliver on a set schedule.

5.3   KPI 3: Return on investment

The investment cost analysis of a WPSP compared to the continued usage of a conventional propulsion system should cover the vessel's CAPEX, OPEX, and VOYEX costs in both a retrofitted and unchanged version. CAPEX is short for capital expenditures, and covers the costs of creating the new vessel, from acquiring the raw materials to planning and producing the vessel itself. This cost will, in retrofits, cover the conversion costs and not the construction from the ground up. The OPEX, or Operational Costs, are expenditures related to the vessel's operations incurred to keep the vessel running. Employee salaries, rents, taxes, fees, port costs, and so on fall under this category (Twin, 2023). VOYEX is short for Voyage expenditures, and relates to the fuel costs of sailing a vessel (Ulstein and Brett, 2016).

5.3.1   CAPEX

According to Lindstad et al. (2022a), the installation of four FRs, 26 meters tall, 4 meters in diameter, including all the technology needed to use them, is estimated at 3.5 million United States dollars (MUSD) in 2022. In this thesis, four 35 meter tall FRs are installed, and for simplicity, assuming a linear relationship between size and cost, the total cost of the retrofit would be around 4.7 MUSD. According to Sclavounos (2020), the price in 2020 was estimated at about 2 MUSD total for four rotors of a size between 3 to 5 meters in diameter and 20 to 30 meters tall. Using the exact conversion as the other source, this means that installing 35 meter tall FRs would cost around 2.8 MUSD in 2020. Installing an FR configuration lands somewhere in the domain of 2.8 to 4.7 MUSD. This is a large spread and may come as a result of many factors, including the inclusion of port fees, geographical location, and general deviations in raw material costs. Therefore, 3.5 MUSD is used as a base price for the following plots.

More challenging is finding the newbuild price of the vessel itself. According to Jessen and Møller (2018), the compensated gross tonnage (CGT) price of a small bulk carrier is on average 3999 USD, with a range from 3100 to 4500 USD. Larger bulk carriers have a much lower cost per CGT at around 2500 USD. The CGT of the conventional vessel may be found using the simple formula presented by the OECD in (2007,p.6), where "a" and "b" are constants derived by the OECD for specific vessel types. For this case vessel, the CGT is around 5800 using the formula below.

$$CGT = a \cdot GT^b \tag{5.1}$$

For the vessel size in this thesis, a total contract price shy of 20 MUSD may therefore be expected. However, in the *System Based Ship Design* compendium, Kai Levander presents the graph below of trending ship-building prices based on their Gross Tonnage. Here, one sees that bulk carriers with a GT below 5000 cost around 5 MUSD (Levander, 2012, p.204).
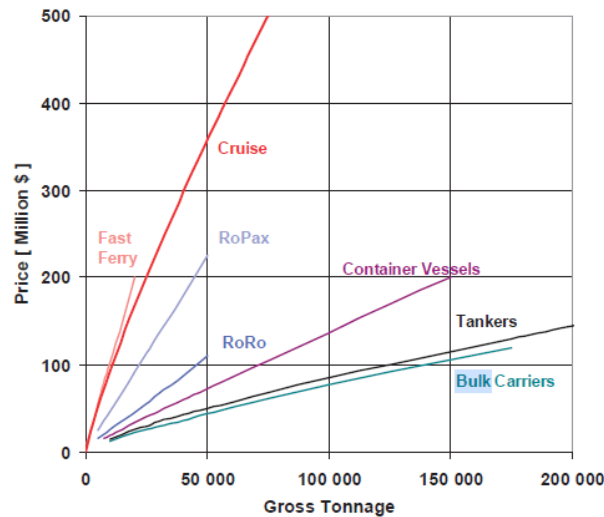
Figure 10.1.1: Ship prices

Figure 5.3: Ship price by GT (Levander, 2012, p.204)

To summarize, the bulk carrier's exact newbuild price is difficult to accurately establish with limited access to data, but anywhere between 5 to 20 MUSD may be expected. This means that the FR installation will increase the newbuild price anywhere between 25 and 100 percent. In any case, the cost is not that high when considering the time it would take to recuperate the investment, as will be studied further in subsection 5.3.2.

The retrofit price of alternative fuels for power production has been studied by Lagemann et al. (2022) for a 63 000 dwt Supramax bulker. Their findings show specific prices for retrofitting a vessel from a VLSFO vessel to an alternative fuel; see graph 5.4 below. The retrofit price for a battery is missing, which again was found through using MAN Energy Solutions and eia (2023; 2019). It is acknowledged that retrofitting a vessel more than ten times the size of the vessel used in the simulations is imprecise. However, due to the lack of logical scaling possibilities for newbuilds with regard to size, the original price has been used. This is understood to be a weakness, but as observed in chapter 4 Results, a retrofit may be favorable even with a high cost estimate.

from/to	VLSFO ship	LNG ship	LPG ship	Methanol ship	Ammonia ship	LH2 ship
VLSFO ship	0.0	9.3	9.3	6.0	15.0	24.6
LNG ship	3.5	0.0	2.5	6.7	11.3	22.6
LPG ship	4.0	7.8	0.0	6.7	8.2	22.6
Methanol ship	1.0	9.3	9.3	0.0	15.0	24.6
Ammonia ship					0.0	22.6
LH2 ship					6.7	0.0

Figure 5.4: Retrofit cost for alternative fuels (Lagemann et al., 2022)

5.3.2 VOYEX and OPEX

Lindstad et al. (2022) state that the total OPEX of a vessel with or without an FR configuration remains mostly the same. In contrast, the VOYEX cost of a rotor config-

uration only depends on the price of the energy input needed for the rotors. This energy consumption by the rotors is studied in this section.

The VOYEX of an FR configuration will consist mainly of a generator's fuel price or batteries' electricity price. To compare the VOYEX of the FR version with the unmodified vessel, one needs to compare the workload and the resulting transported capacity. The comparison vessel sails less than 1/5 the speed of the normal vessel, specifically 14.8 knots, see figure 2.15. This is compared to around 2.57 knots for the modified vessel according to the simulation results averaged over all routes. On the other hand, the modified vessel uses approximately 1/8 of the input energy. The comparison vessel uses a 4500 kW output engine to sail at 14.8 knots, while the FRs have a rated power of 572 kW to provide maximum output. However, an FR only uses 40 percent of this rated power according to the FR producer Anemoi (2023). Over a year, a vessel sails effectively for 237 days (Lindstad et al., 2022a). Using optimal speeds as a condition, this provides a power consumption of 25.6 GWh for the conventional vessel and 7.5 GWh for the modified vessel over a year.

$$4500[kW] \cdot 237[days] \cdot 24[hours/day] \approx 25.6 GWh \tag{5.2}$$

$$\frac{228.8[kW] \cdot 237[days] \cdot 24[hours/day]}{\frac{2.57}{14.8}[Transported\ volume\ factor]} \approx 7.5 GWh \tag{5.3}$$

The "Transported Volume Factor" (TVF) is a factor introduced to adjust the payload delivered by the amount of power used by the vessel. This is to compare the different systems on more similar grounds. The way that the gap in the payload transported should be closed is not discussed in this thesis. This could be studied later. When adjusting power consumption over an equal total payload transported, the energy consumption of the FR configuration is $7.5/25.6 \approx 29$ percent of the conventional vessel. Note that the "Transported Volume Factor" does not consider changes in payload due to specifications from retrofitting with new technology, which is especially important for low energy density power systems like batteries. Summarized, the fuel efficiency of the FR configuration is 71 percent better.

With a basis for the energy consumption of the different concepts established, an evaluation of a comparable VOYEX with varying types of fuel may be conducted. Price data concerning alternative fuel costs (DNV, 2022c; Global Petrol Prices, 2023; IMO, 2021; Lagemann et al., 2022) could provide an answer into what the vessel's VOYEX may be, both by year and aggregated over time to see what propulsion system combination may be expected to have the highest ROI over time. Several key points should be noted when studying the chart. First, the carbon tax significantly impacts the VLSFO and LNG prices. This tax is assumed linearly increasing from $0/tCO_2$ equivalent in 2020 to $288/tCO_2$ in 2050. Based on the assumption that VLSFO and Fossil LNG emit approximately 0.3 and 0.2 tCO_2/MWh, respectively, the carbon tax increases their price to 30 percent over the period. The increasing price difference between conventional fossil fuels and combinations with FRs comes from increased fuel consumption and fuel price, primarily from increased tax rates. Tax rates are assumed to experience almost a quintuple increase in the period 2025 to 2045, while fuel prices alone only increase by around 125 percent (from 49 to 110

USD per MWh). Secondly, the battery price reflects the average electricity price assuming a yearly linear trend as recorded in the US industrial power price average by the Energy Information Association USA (eia, 2023). Third, bio-fuels have been neglected due to their assessed lack of availability/readiness for shipping. Finally, e-fuel prices are based on lower bound electricity prices from completely green electricity, while NG ammonia is assumed to include carbon capture and storage (CCS) (DNV, 2022c; Global Petrol Prices, 2023; IMO, 2021; Lagemann et al., 2022).
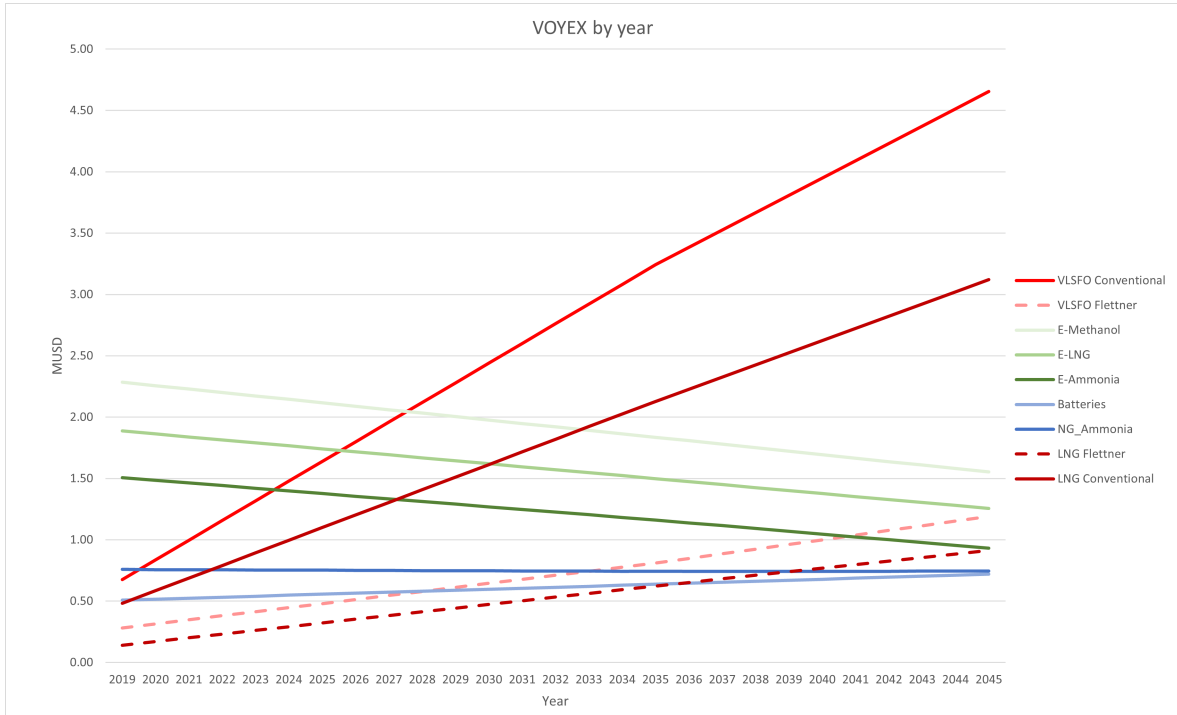
Figure 5.5: VOYEX by year, linearly interpolated (DNV, 2022c; Global Petrol Prices, 2023; IMO, 2021; Lagemann et al., 2022)

The full, red lines display conventional fuels used for main propulsion, and the dashed, red lines show the same fuels used for generating power for the FRs. The blue and green lines represent energy compositions without carbon emissions or with CCS technology. The green lines assume zero emissions from the electric grid and a steadily decreasing price for producing the respective specific fuels. Assuming the CAPEX established above in subsection 5.3.1, the VOYEX makes up anywhere between 10-60 percent of the CAPEX in just one year, mainly depending on what fuel is utilized for the rotors.
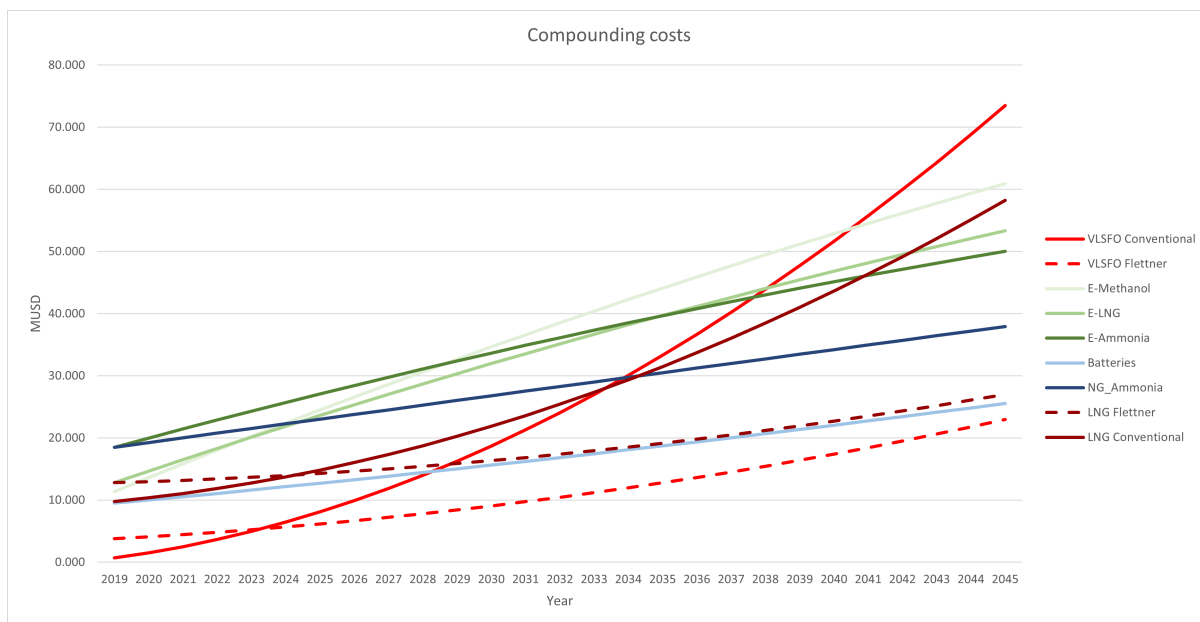
Figure 5.6: Compounding cost of vessel

Figure 5.6 shows the compounding costs of having a vessel operating at status quo (in full, red and dark red lines), with no system change and an FR configuration with different complementing fuels to drive Flettner rotation. One sees that only after around four years of operation has the cost of Flettners been regained. This may be seen in the intersection between the dashed and full red lines. The graph assumes a start in 2019, where a retrofit happens to all except the VLSFO and LNG conventional systems. From 2019, the different fuel prices, combined with lower fuel consumption from the FRs, show how the compounding costs of the vessel develop. All retrofits are assumed to be from a vessel running on VLSFO. The bottom-most alternative on the left is this VLSFO vessel with no retrofit and costs, therefore zero in 2019. However, the compounded cost increased at its most rapidly rate due to high fuel prices and an increasing carbon tax. The dark red line is with a retrofit to LNG with and without a Flettner configuration. The light green lines, e-methanol and e-LNG, as well as fossil LNG have the lowest retrofit cost due to their ability to work with most dual-fuel engines without significant changes. The retrofit cost consists here almost only of the rotor installation. Using blue or green ammonia, blue from the assumption of CCS entails a retrofit estimated to cost about 1 MUSD more, where the green ammonia is decisively more expensive to buy than the blue (MAN Energy Solutions, 2019). Interesting to note may be the low price of utilizing both LNG and Flettner. If a method for CCS with LNG is made possible and readily available, with resulting zero net emissions from the combination, then this fuel type may be the most optimal.

Once again, the assumption that using batteries does not change the payload is a simplification, and should be studied further if they are to be used. One must consider that the power system's effect on the payload has not been established. The battery option is known to have the lowest energy density of all the options provided above, at 0.14 MWh/mt (ESAU, 2021), and thus requires more space and weight, compared to the second least energy-dense fuel ammonia, at 5.17 MWh/mt. Bulk vessels are usually weight sensitive, and a heavy battery system will result in a lower payload. A marine battery pack at the system level will weigh between 11 and 30 kg/kWh. Running the simulations over the route Faroe Islands to Ålesund and measuring the average battery need shows

a consumption per trip of approximately 4500 kWh. This means that a battery with no extra power capacity will weigh at least 90 tonnes, all of which must be taken from the payload.

5.3.3 ROI reflections

As proposed in section 5.3.1, the cost of installing FRs is by linear deduction of around 3.5 MUSD. In shipbuilding, this is not necessarily a high price, and with increasing bunker prices, any technology that helps reduce the total fuel consumption may be beneficial. The cheapest fuel retrofit with batteries costs around 10 MUSD, around 3 times the FR installation cost. With 237 sailing days during a year, one can see that the first fully carbon-neutral alternative using batteries is cheaper after ten years. After 15 years, NG ammonia will be the more affordable alternative for the other fuel types. This is when using VLSFO fuel as a base case. However, better results develop with nonconventional fuels as a base case.

If calculated concerning the usage of other, greener fuel types, installing FRs has a positive ROI much earlier. So much earlier that to show the difference clearly, the vessel is assumed not to sail the first year, and the plot shows only the first six years of sailing. This way, the CAPEX difference is more readily observable with how quickly it diminishes. Below, in figure 5.7, only zero-emission alternatives are given. The graph shows that all vessel types with FRs outperform those without Flettners within two years due to the high VOYEX of alternative fuels.
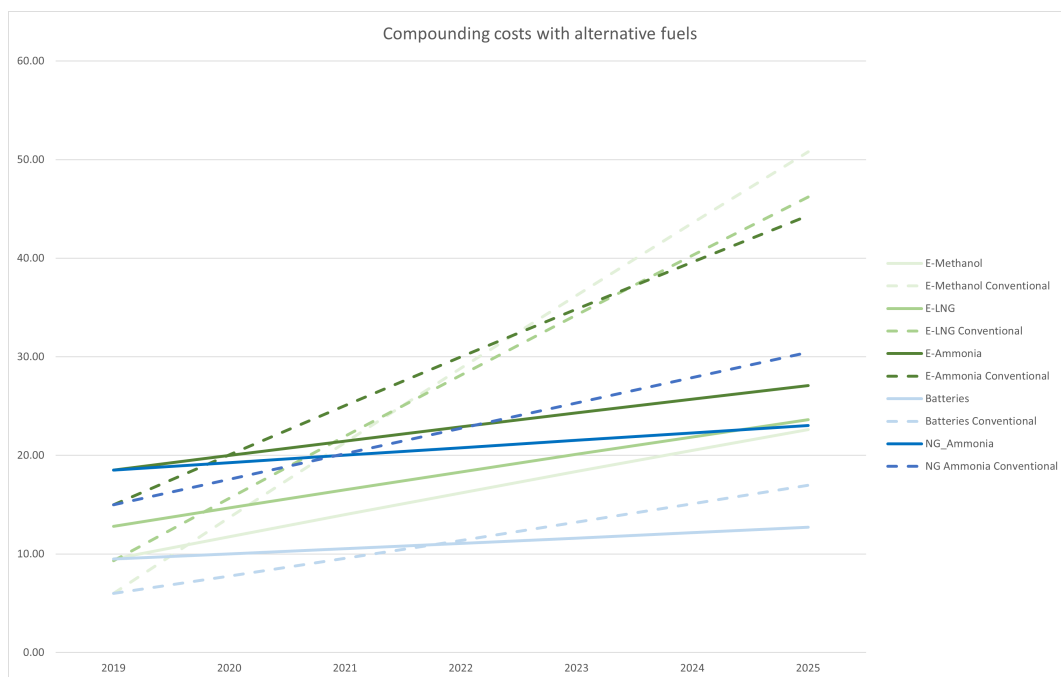

Figure 5.7: Compounding cost with alternative fuels only

5.3.4 Economic benefits

An ongoing challenge in the modernization of the maritime industry is how the distribution of economic gains is distributed. In most cases, a vessel's financial aspect is split between two or three beneficiaries: the shipbuilder or yard (from now on, shipbuilder), the shipbroker or owner (from now on, broker), and the customer or lender of the vessel, (from now on, customer). The customer and owner may be the same entity. The shipbuilder has no trouble installing FRs as this will increase their contract price and, thus, income margin. The problem, however, arises when the shipowner and the customer are two different entities. While the owner must bear the retrofit cost burden, the customer will reap the gains of the fuel reduction as the customer is the one paying for the bunker. This may mean that the vessel's owner increases the leasing rate. This increase, on the other hand, must cover both the actual investment and the risk from this investment, representing a premium that must be provided for the vessel's owner to want to invest in the upgrade. With this premium, the increased cost will result in losses for the customer that chooses the modified, upgraded WASP vessel. As a result of free market forces, the customer will understand that they will have to take this loss themselves, and seeing as they have no incentive to gain other than the non-monetary premium that comes with "sailing green", many customers may well choose the cheaper, more polluting alternative.

According to Schinas and Metzger (2019), the financial models in place to aid in the transition to greener shipping are lacking regardless of the technology chosen to reduce fuel consumption. There are no guiding economic benefits in place to supplement implementations of greener solutions, and only a non-monetary premium is gained to outweigh the economic and technological uncertainties that come with innovation when the vessel's owner and contractor are different entities. As mentioned earlier, the CAPEX is higher in retrofits due to their novelty and lack of scale. OPEX for green versus conventional machinery is assumed to be more or less the same. So only VOYEX is expected to tilt the scale for greener technologies, especially WASP technologies. To remedy this challenge where the risk premium of green innovation falls on the customer, who may easily choose a cheaper alternative, external incentives could effectively drive change. Once customers see the economic benefit of bearing the green risk premium, they may be more prone to choosing the green alternative. Although this discussion is beyond the scope of this thesis, it should be mentioned and could serve as a basis for further studies.

A small note may be added here in this regard. Although this non-monetary premium may have had little value historically, more recent examples show that some customers are willing to pay the price anyway. For instance, with the announcement of the Polestar 3 fully electric vehicle, Polestar states that their goal is to make the entire lifecycle of each car to have zero emissions of CO_2. In an article written in Teknisk Ukeblad, they state that this may mean using rotor ships to transport cars and raw materials (Haugstad, 2023). A suitable match for the vessel being studied in this thesis. In other words, although monetary gains have almost always been the center of focus for most businesses historically, with the green movement seen today, more and more companies may be comfortable with choosing a more expensive alternative. This may be part of the answer to the following question: Is there a market for a slower vessel with zero emissions?

5.4 Validation of simulation results

In addition to discussing the results obtained from the simulation, it is interesting to attempt to validate them. There are several ways of doing this. This section will evaluate the results using results from other reports and real data from ships operating with FR installed. Since the comparable results come from vessels using FR for assisted propulsion, a comparison will be performed on achieved fuel savings. For the case of the WPSP vessel in this thesis, it is assumed that the vessel sails at 14.8 knots with a combination of conventional propulsion and the four FRs.

Considering the simulation results, the case vessel has fuel savings of 6.8 percent when sailing with four FRs. The fuel savings calculations are based on a 591 kN thrust from the 4500 kW machinery when sailing at 14.8 knots. The FRs have an output of 40.38 kN on average over the favorable route described in section 5.5.2.

Flettner rotors are one of the few WASP technologies currently installed and in operation on several ships worldwide. Because of this, many reports on real-world gains of the FRs are available for comparison with simulation results. Tanker vessel Timberwolf (previously Maersk Pelican) is one such vessel, and is currently in operation with two FRs with a height of 30 meters and 5 meters in diameter. Independent measurements were done by Lloyd's Register and showed a yearly fuel reduction of 8.2 percent (Norsepower, 2023). It is worth noting that the Timberwolf sails at a speed of 8 knots.

In a case where the Timberwolf had 4 FRs installed, a fuel saving of 16.4 percent could optimistically be assumed. Compared to the simulation results, the Timberwolf achieves a 9.6 percentage points higher fuel saving when equipped with the same number of FRs. At first, this might seem to indicate that the simulation vessel performs worse than what one would see in the real world. However, the fuel consumption increases exponentially with higher speeds. As figure 5.8 from NAPA shows, the difference from a speed of 8 knots to 14 knots can mean that the fuel consumption can multiply by four. Subsequently, a given FR system will be unable to cut the same percentage-wise amount of fuel for two different speeds.
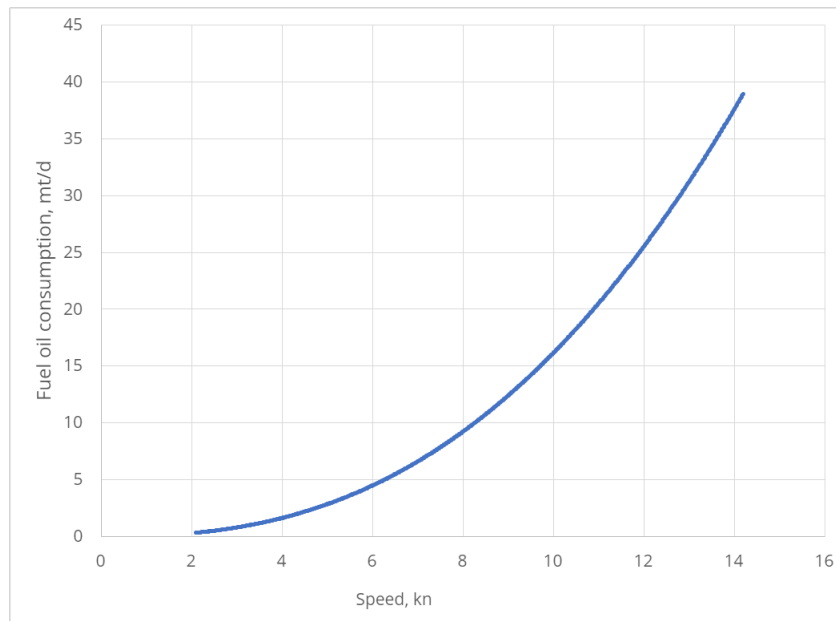
Figure 5.8: Typical fuel consumption (NAPA, 2023)

If the simulation vessel was to sail at 8 knots with a four times lower fuel consumption, the fuel savings could amount to 15 percent. This is a rough estimate based on the plot in figure 5.8 above, but highlights that a fair comparison between achieved fuel savings with and without FRs, requires information on sailing speeds and type of vessel. When considering the difference in speed between the two vessels, it seems that the simulation results are realistic figures on possible performance.

Seddiek and Ammar (2021) have modeled and performed calculations on the use of four FRs on board the bulk carrier Wadi Alkarm. Wadi Alkarm is an 80 000 DWT vessel with a sailing speed of 13.5 knots. After simulating sailing on a route between Egypt and France, the fuel saving from the four FRs is 22.28 percent. These results strongly outperform the findings in the simulations created in this thesis. Although there may be differences in weather conditions and sailing routes, the histograms in appendix III suggest that different routes should not alter performance quite as drastically. The large difference in performance may then be explained by differences in the models used in the simulation. Seddiek and Ammar (2021) do not reveal their entire simulation model, but importantly they state several simplifications. One of the simplifications is that the drift angle and the resulting drift resistance are neglected. As presented in section 2.4.2, Lindstad et al. (2022) estimate that performance can be overestimated by 40 percent when not including the resistance due to drift.

As a result of the simplifications regarding drift resistance, it could be argued that Seddiek and Ammar (2021) could have had up to 40 percent lower savings. This would result in savings of about 13 instead of 22 percent. Therefore, the neglection of drift resistance could help explain why the results of Seddiek and Ammar outperform both the simulations in this thesis and real measurements from the tanker vessel Timberwolf. The discussion above seems to indicate that results from the simulations are more conservative than they are optimistic. However, in terms of validating the results, it may be concluded that they are within a reasonable range of what independent sources have found.

5.4.1 Data reliability

In this section a look into the reliability of the data used is performed. The source behind the data, Copernicus Marine, has been studied to evaluate whether or not the source is reliable, and a comparison into the data found is performed with exact measurements.

Measurements versus numerical calculations

Theoretically, the best way to check if the weather data is reliable is to cross-reference the data with other measurements taken at the same place and time. If the datasets are similar, then one could argue that they are as reliable as needed. In Copernicus, the weather data is provided by combining a large mixture of different *in situ* measurement platforms, including buoys, gliders, drifters, sail drones, and minilogers, and combining them with satellite data. These data collection devices feed data into the Copernicus database, providing "state-of-the-art analyses and forecasts". Together, they provide a basis for users to study weather patterns and wind behaviors (Copernicus Marine, 2022). The database uses all these data points and estimates the weather found at all different positions on the map. Therefore, checking the data that is found using the Copernicus script with data taken from a specific measurement buoy or mooring in the exact location and time, and seeing if they correlate with the data estimated by Copernicus, will provide a basis of reliability. The result will show how close to reality the program works when calculating the weather. This is precisely what has been done, and the results are provided below. In the code, "WSPD_Measured" and all other variables with "Measured" is the data measured precisely at a specific location. The data preceded by "Calculated" is data that Copernicus estimates based on all their available data.

First, by going to the CMEMS In Situ TAC website, one may find the recorded weather data from specific measurement areas. Then, to cross-reference this data with what is found and used in the code, one may access one or more specific measurement stations, and compare the real-time measurements with the combined data calculations done by Copernicus. The first measurement station used is the Troll-A platform fixed buoy and mooring time series data set. The platform is located at (60.64350, 3.71930). The second station compared is from the Sleipner-A platform at (58.37110, 1.90910). Both these platforms provide wind speed and wind direction data for 10-minute intervals as ".nc" files. The weather data for June 2020 has been compared to the data from Troll-A, and weather data for March 2021 has been compared with the Sleipner measurements. The locations of these platforms are shown below and overlap with the routes used in the calculations earlier.
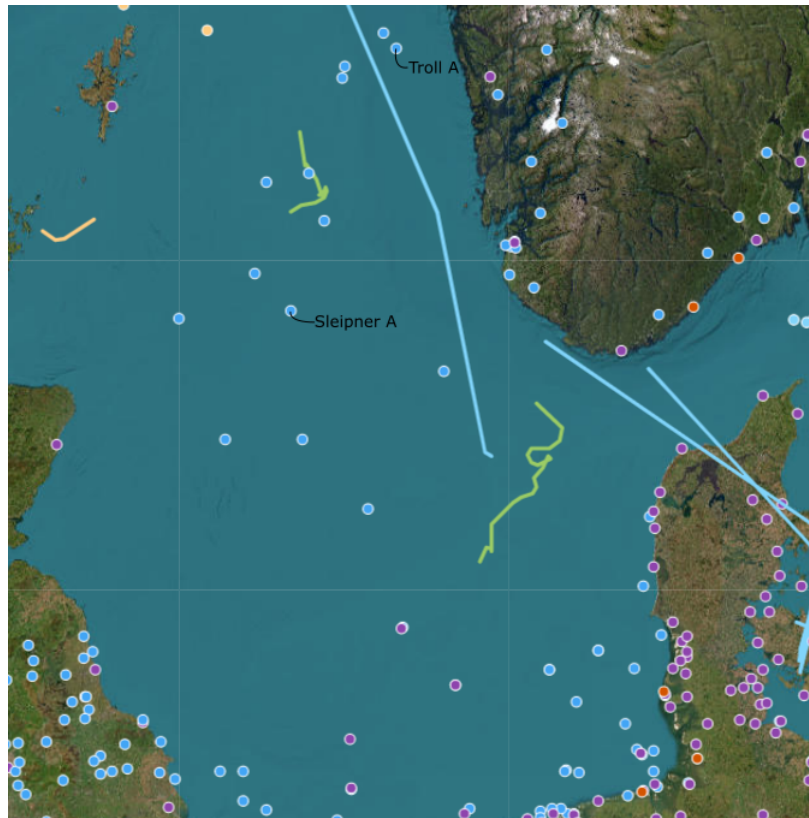
Figure 5.9: Map of weather measurement stations

The results of these comparisons produce highly similar results in terms of average wind speeds. The data found using the Copernicus database calculations shows an average wind speed for the Troll platform of 8.28 knots. Using the data directly from the measurement station on the Troll platform, an average wind speed of 8.66 knots is shown. Furthermore, the data gathered by calculation from the Sleipner field gives an average wind speed of 7.45 knots, while the wind speed measured is close, at 8.55 knots. The fact that the exact observed data correspond so closely with the modeled data for both stations at two different times is positive. However, as averages may hide important information in the data, the distribution and variance of the data are studied next. As a note, the time segments studied were chosen randomly, not because they happened to correlate.

Plotting the measured and calculated data has been done to further try to analyze the data. The weather data for the entire year at the Sleipner field was missing several time intervals, perhaps due to measurement failures, and thus only the Troll field focused upon. The top plot (a) below shows what direct plotting from Copernicus' textitin situ database gives. The middle plot (b) shows this same data plotted in Python, and the bottom plot (c) shows the measured data overlapped with calculated data for this field. The y-axis shows wind speed in meters per second, and the x-axis is time in July (given as dates in the first plots and hours in the second and third).
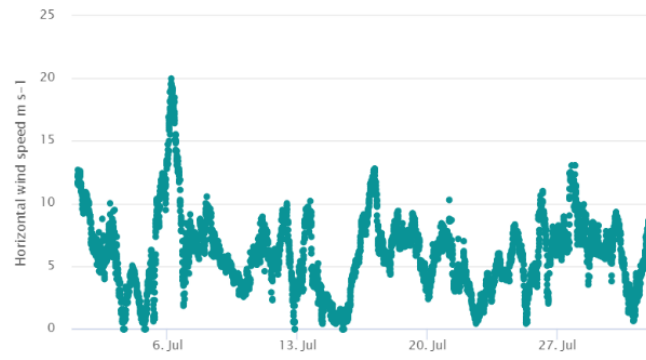
(a) *In situ* from Copernicus Marine (2023) directly
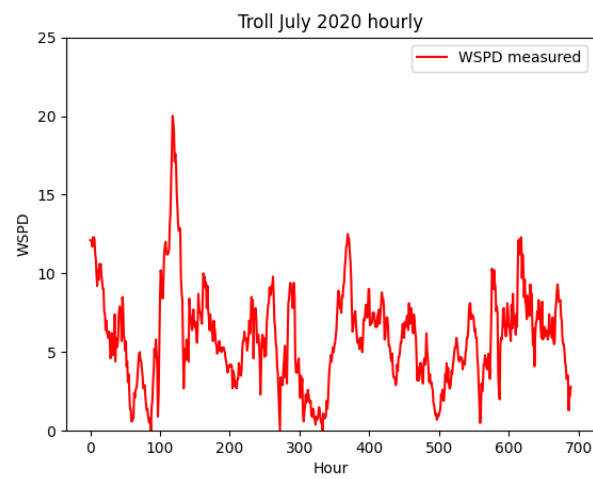
(b) Python plot
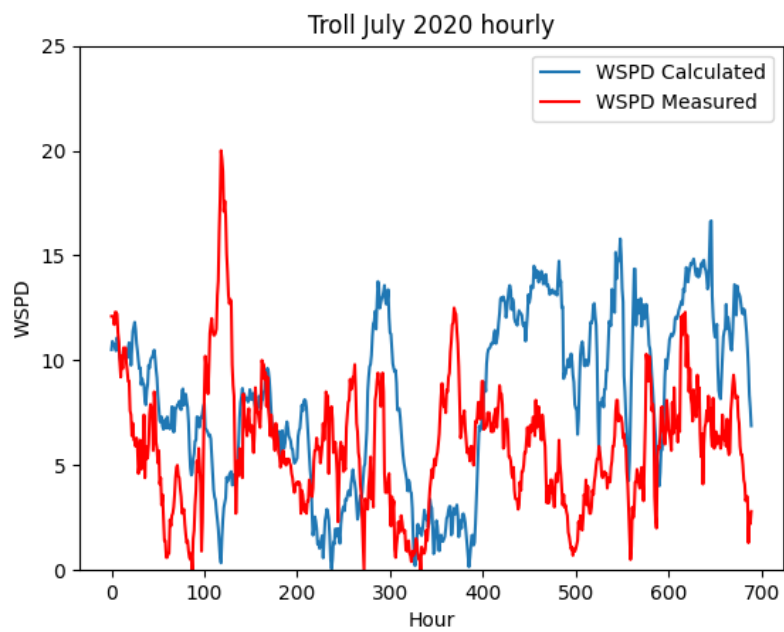
(c) Comparison

Figure 5.10: Comparison of calculated vs. measured plots

Immediately, one sees no high degree of correlation between the measured data and the calculated one. However, this should not be expected due to several reasons. Firstly, the measured data is collected at ten-minute intervals, while the calculated data is found at one-hour intervals. Secondly, the data calculated is based on numerical calculations of satellite data, discrepancies must be expected due to simplification and estimations done in these calculations (Copernicus Marine, 2023). Nevertheless, as the datasets contain no remarkable differences, except perhaps once around 120 hours into July, they may be assumed to be trustworthy. This one discrepancy not found in the calculated data may either come from a faulty measurement or a mistake in the calculation, but without a third source of data, this is difficult to know for sure. In any case, since the underlying picture found from the remaining data shows mostly similar trends, then this singular large discrepancy may be ignored.

Specific variations in the weather may not be as important to evaluate the system's effectiveness, compared to the trends in weather that one sees. As discussed earlier, the data from Copernicus is already too coarse to predict the behavior of a vessel exactly. Nevertheless, as long as the simulation captures the trend both in wind speeds and directions over a specific route, then the outcomes from the simulations should give an accurate representation of the underlying problem. Therefore, plotting the trends will provide a more complete look into the aptness of the data. Below, a histogram has been plotted, showing the percentage of windspeeds observed through measurements versus calculations. The correlation here is much higher, showing that although the two datasets disagree on the specific weather, they both show the same trends. The speeds observed in the graph below show a typical Weibull distribution, just as one expects from weather data, according to Bergfjord (2011).
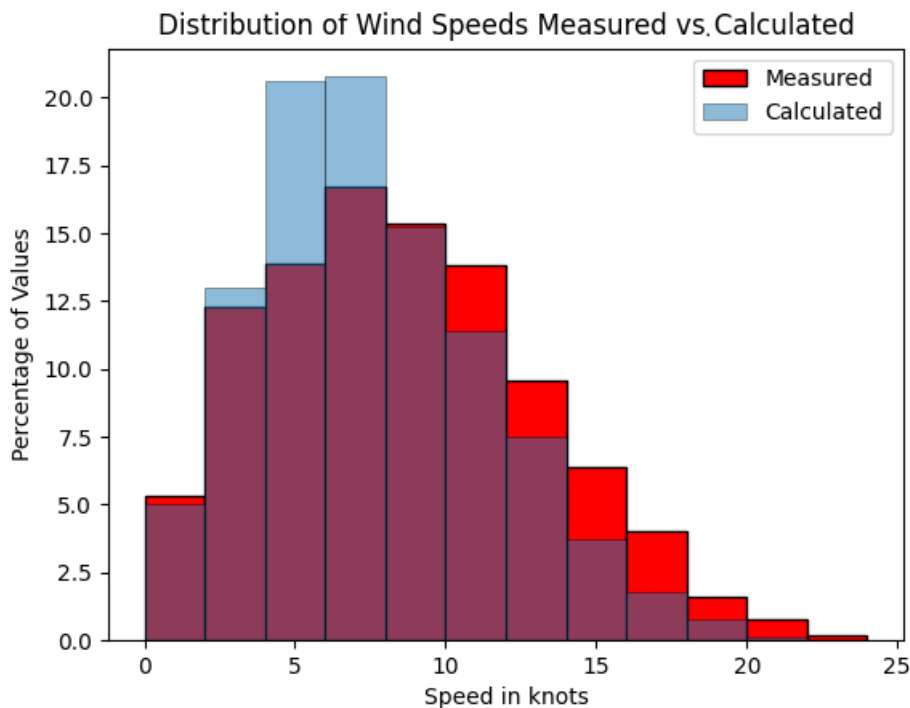

Figure 5.11: Histogram of wind speeds

The fact that the weather trends used in the simulations are comparable to those measured is important. This means that the simulation results may be an early indication of which areas are more suitable for sailing with FRs. The histogram above shows the percentage-wise distribution of calculated and measured wind speeds observed to show their similarity. Worth noticing is that the measured calculations show higher average speeds than the calculated ones, with a smaller percentage found in the 5-8 knot range. Nevertheless, because these two graphs are so similar, and the measured windspeeds are even higher than what is assumed in the program, one could reason that the results discussed in chapter 4 are conservative. In any case, the results may be trusted for their current usage.

Quality control

Any information provider's quality should be considered when utilizing their data for research. The quality of the Copernicus Marine database is regarded by the company as a critical task, and as such, they have established a specific "Product Quality Strategy" summarized in the "Product Quality Strategy Document". This document provides insight into the multitude of ways that Copernicus works to ensure that their information is reliable. Product quality is considered a core of the service.

Transparency

Evaluating the reliability of the data may be done by assessing how transparent the processes behind the data function and how to open the data itself. Firstly, all changes implemented in the database are made known through the Copernicus Ocean State Reports. All code and data are also open-source, and everything is provided for free. Access to all data, as well as help from people working at Copernicus to access specific data, increases the reliability of the database.

Feedback

The database is open to peer review, and with an extensive user database, feedback from users is continuously gathered, monitored, and addressed. One of the authors of this master's thesis sent feedback to the database regarding probable errors in the results, and after only a couple of days, these errors had been addressed. With any data collection process involving human interaction, mistakes are bound to happen, and having a database that actively addresses and fixes mistakes when they are found and reported increases reliability.

Endorsements

The Copernicus Marine database is endorsed by several governmental organizations, such as the Intergovernmental Oceanographic Commission (IOC) of UNESCO and the European Space Agency (ESA), both of which utilize data from the database for their operations.

5.4.2 Comparing simulation results with AIS analysis

The basis for the routes along the Norwegian coast comes from the initial AIS analysis. The properties of the AIS vessel are used in the simulations, which enables a comparison between the performance of a marine diesel engine and pure wind-propulsion on an equal vessel and the same routes. Speed profiles from the simulations have been presented in section 4 Results and appendix III Histograms. Figure 5.12 presents the speed profile of the AIS vessel, with percentages of the different occurrences of sailed speeds observed. One might find it interesting that the AIS vessel has almost twice the number of occurrences at 0 knots than what is found in the simulations. This is explained by the fact that the AIS vessel, in total, stops at 11 different ports on its short-sea shipping route. Many hours are spent maneuvering and handling cargo in port at such low speeds that the AIS registers zero knots. This is reflected in the AIS data.
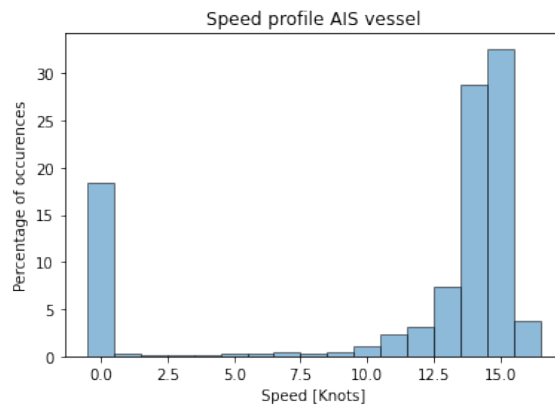

Figure 5.12: Speed profile percentages for AIS vessel

Time in port is not considered in the simulations, neither are delays and unexpected events. The results in figure 5.12 highlight the difference between simulations and the real world. From these discussions, one can expect the speed profile of the pure wind-powered vessels to have far more recordings of low speeds than what the simulation shows. In addition, the speed profiles of the two vessels are fundamentally different. For the purely FR-powered vessel, sailing speeds fluctuate between a range of speeds, while the conventional vessel can sail at a set speed.

When the WPSP vessel sails the exact route of the AIS vessel, one may see that the average speed is about 3 knots, depending on the route and time of year. A result of the reduction in sailing speed is that the annual transport volume is cut by 80 percent. Therefore, to sustain the current rate of deliveries, one would need to have a fleet of 5 WPSP vessels on the short sea shipping routes. However, this is without using tools such as route optimization and combinations with other propulsion technologies.

Figure 5.13 shows how the AIS vessel chooses its sailing route between Stavanger and Bergen. As seen in section 4.4.1, the wind conditions along this route are mainly directed toward the north, south, and southeast. If the WPSP vessel is to follow the same route close to the shore, it will experience both weak wind speeds and nonoptimal wind directions. Proper routing will be further discussed in section 5.5.2.

Figure 5.13: Route taken by AIS vessel between Stavanger and Bergen

The discussion above points out several important aspects to remember when introducing a WPSP vessel on a route previously serviced by a conventional diesel-powered vessel. The speed and reliability are lowered. If WPSP is introduced, the discussion above further highlights how all aspects of the operation would need to adapt. For example, sailing patterns would need to change dynamically to optimize sailing times. As a result, port operators would have to prepare for changing arrival times. Consequently, this has an impact on businesses and entire value chains.

5.4.3 Data fidelity

The choice of data fidelity in this simulation was made based on the desire for as much accuracy as possible, not the amount of time the simulations would take. For this reason, weather data for every hour and positional data of 0.125 degrees were utilized. This was the most fine-grained data fidelity available, and it was therefore used. Furthermore, the simulation was run for every single hour over the course of 2 years, this means that all routes were traveled by the same vessel 17520 times. This was done to make sure that no trends in the weather were lost by chance. However, with such a high level of precision, the code took a very long time to run. Therefore, improving simulation efficiency was evaluated.

5.4.4 Increasing simulation efficiency

The simulations were performed for every hour of every day over two years. However, as mentioned in section 2.5 there are no rules or mathematical laws that govern the exact fidelity one should use when simulating over a given dataset. One must use experience and knowledge of the data to evaluate this. In terms of weather patterns, for example, running a simulation once every year over a thousand years would provide no input into seasonal changes. Further, running the simulation once every day would not show whether changes occurred between night and day. To be safe, the simulation in this thesis was run

as often as possible given the data that was available, As seen below, running the same simulation with larger time intervals would result in more or less the same conclusions, up to a certain point.
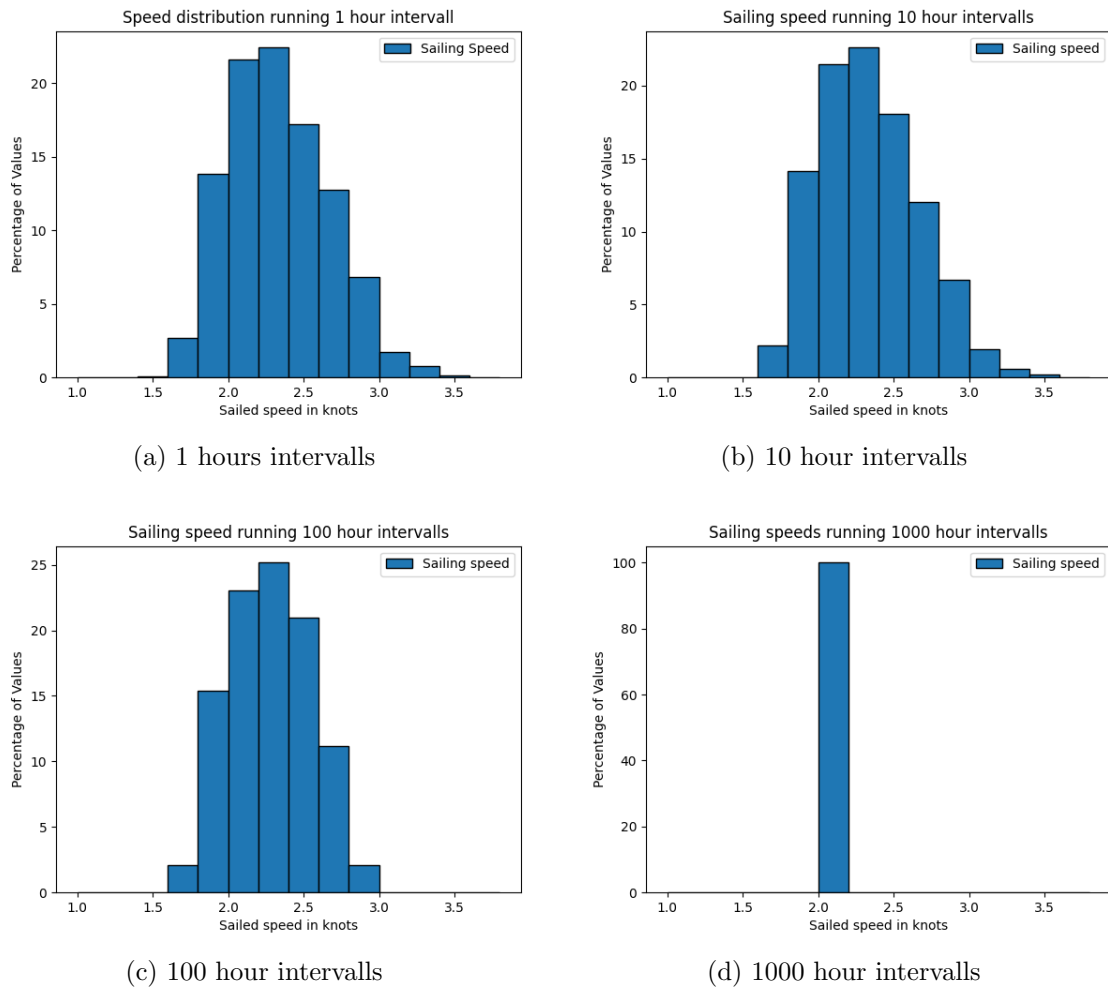

(a) 1 hours intervalls

(b) 10 hour intervalls

(c) 100 hour intervalls

(d) 1000 hour intervalls

Figure 5.14: Simulation run with different time intervalls

The results as plotted in figure 5.14 above show that running the simulation with gradually decreasing granularity or larger and larger time intervals provides at first little difference to the observed results. Running the simulation for every 10 hours over a year for example, gives a very close approximation to the simulation run for every single hour. This means that the simulated system may use 1/10 of the time to run, and still produce results that are similar to the most exact simulation. When pushing the simulation intervals to 100 hours, one sees that some of the higher sailing speeds observed in the first graphs disappear. This means that one will not see the full potential of the vessel, however, the shape of the results, and thereby the underlying trend is still visible. Running the simulation only 17 times, once every 1000 hours results in a graph that provides hardly any information at all. What may be learned from these results is that running the simulations for every hour is not necessary for these simulations to provide useful results. Somewhere between 10 and 100 hours is likely sufficient.

5.5 Possible improvements to a WPSP vessel

In this section, different methods of improving the effectiveness of only sailing with FRs will be evaluated. This is done by using the WPSP system as a base case and adding complementary technologies, as well as creating operational policies to see how big of an impact they may have on the observed results from the simulation. When looking at how much of an improvement a small addition to a pure WPSP system can make, one can introduce solutions that may not have been feasible on modified conventional vessels. Several questions will be attempted answered in this section, using the simulated results and several sources as a basis. Does the area of operation that a WPSP vessel operates in have much to say on its performance? Are there certain areas or types of areas that should be avoided? How important is route planning in the use of WPSP? Would it be favorable to avoid a retrofit and instead create a newbuild, specifically designed for the use of FRs? How much better would a WPSP vessel work if a kite, a rigid wing sail, a small battery pack, a generator, or similar is added? Could one establish a series of operational policies when batteries or similar are introduced? Is there a market for a vessel that, according to simulations, only sails at around 2.6 knots on average?

5.5.1 Area of operation

Because of the specifications of the Flettner rotor, the performance of the WPSP vessel will vary with the weather conditions in each geographical area. As described in section 2.2, the introduction of WASP technology re-introduces the need to understand the centuries-old term "trade winds". How a vessel needs to relate to and utilize trade winds depends on which WASP technology is used. Discussions and results presented in this section are, therefore, mainly applicable to vessels fitted with FRs.

The initial simulations and investigations of the thesis are based on a short-sea shipping route along the Norwegian coast. This is the route of the case vessel, and enables the comparison between a WPSP vessel and one with conventional machinery. However, several short-sea shipping routes offer poor conditions for a Flettner rotor. For example, Stavanger-Bergen and Florø-Bergen have especially poor wind conditions, which is reflected in the speeds at which the WPSP vessel can sail. Furthermore, not only are the wind directions unsuitable for FRs but it is also known that winds are weaker close to shore. This is because the flat surface of the sea enables the wind to maintain its strength, while closer to land, more obstructions slow the winds down (Oblack, 2019).

Figure 5.15 compares the route between Bergen-Stavanger and Faroe Islands-Ålesund. This highlights the differences between a poor route close to shore and a route across the open ocean. Bergen-Stavanger has a reliability of 63 percent, and Faroe Islands-Ålesund has 71 percent reliability. Regarding speed distribution, higher speeds are achieved on the route Faroe Islands - Ålesund. As seen in appendix III and below in figure 5.15, this is a common trend when comparing such routes. The vessel would be better off sailing on the open sea in order to score better on KPIs such as speed and reliability.
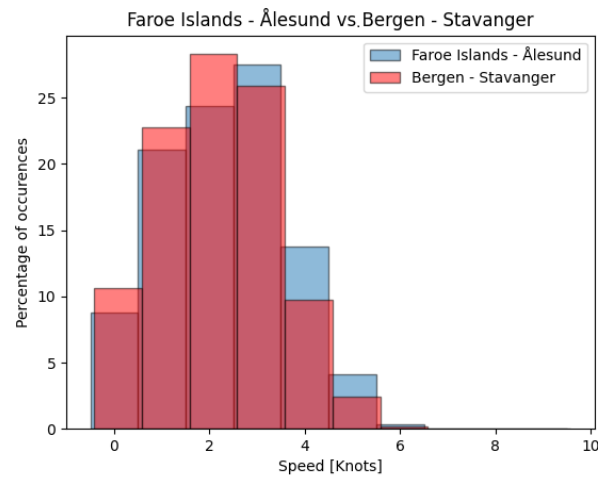
Figure 5.15: Faroe Islands-Ålesund compared to Bergen-Stavanger

Recommending areas of operation purely on performance and KPIs is not always necessary. Varying speeds and low reliability regarding the ability to arrive on a set schedule are not concerns in all businesses. This could, for example, be businesses such as tourist vessels and cargo vessels sailing between islands. For instance, tourist vessels in the Caribbean travel relatively short distances between the islands. The area is also known for good wind conditions, and sailing vessels frequently visit the area. Many of the islands house unique wildlife in addition to a large marine ecosystem. Traditional cruise vessels and pleasure boats have been criticized for damaging wildlife with their emissions in recent years. Emissions include wastewater, garbage, and CO_2 emissions (Diez et al., 2019). Areas sensitive to these emissions may more easily be ready to accept the tradeoff of losing some speed from their vessels in return for emission-free sailing. The worldwide push for a reduction in emissions has changed the requirements and thoughts on vessel performance, and the large cut in fuel consumption can defend the reduction in speed or reliability on its own.

5.5.2 Route planning

Route planning is essential when working with WPSP and any other weather-dependent propulsion system. While most vessels may only plan their routes differently if storms are forecasted, and seldom travel longer distances to find better weather, WPSP vessels must consider the weather when planning a route. A quick comparison of two potential routes in the North Sea is presented below to exemplify this. Due to poor planning and utilization of dominating weather patterns, one yields better results than the other. The program used for this comparison is an openly available "Flettner Savings Calculator" (Lloyd's Register, 2023). This calculator uses a vessel with conventional machinery and plots power savings in percent. Since the code behind this data is unknown, the program has only been used to illustrate the point that route planning is important. The point of departure in the picture below is from the Faroe Islands, but the islands do not appear on the map.
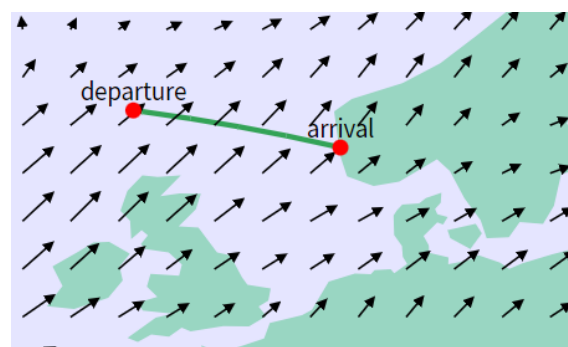
(a) Favourable route (Lloyd's Register, 2023)
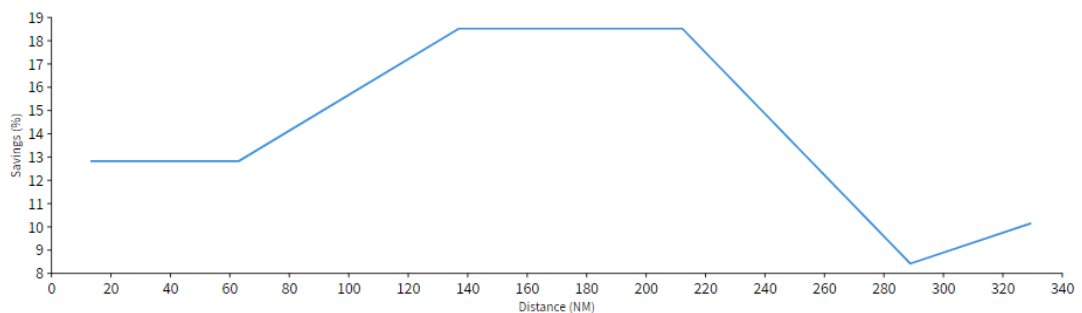
(b) Favourable route output assumed (Lloyd's Register, 2023)

What may be seen in the images above is a route chosen for the use of FRs as the wind conditions are close to optimal for the technology. Specifically, a route traveling across the North Sea from the Faroe Islands to Ålesund. This route utilizes strong side winds to achieve good power savings. The line plot shows this power saving in percent. One should note that the y-axis on this plot goes from 8 to 19 percent. In comparison, the route plotted below sails from Aberdeen to Ålesund. This route hardly saves any power, notice the axis is changed from around 0 to 2 percent. Despite sailing with the wind, this route performs poorly. FRs perform at their best in side winds, not tailwinds, as may be seen in the polar diagram presented earlier in section 2.3.2.
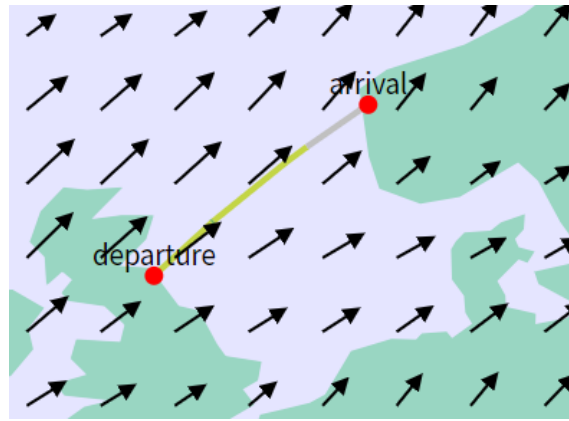
(a) Bad route planning(Lloyd's Register, 2023)
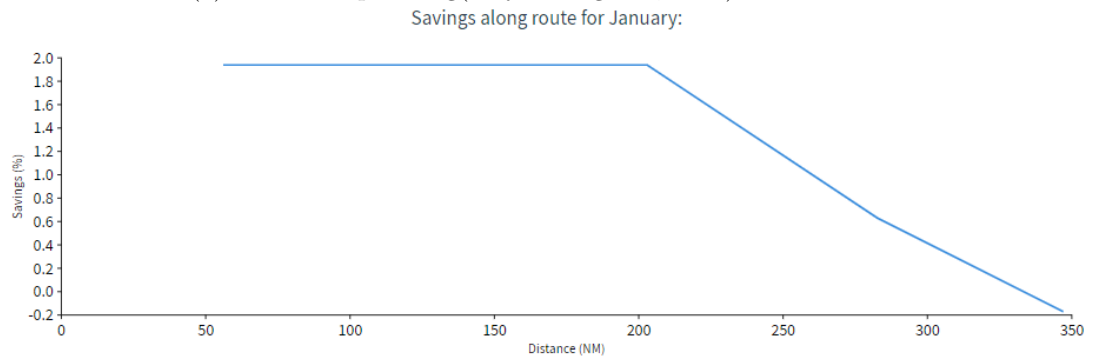
(b) Bad route planning output (Lloyd's Register, 2023)

Running the simulations over these routes shows a smaller difference compared to what is found by Lloyd's Register in their calculations, as seen in image 5.18 below. While the program created by Lloyd's Register only shows the average savings over one month, the simulation runs the routes over a two-year period. Therefore, as one can see in figure 5.18, the difference is smaller than what the program from Lloyd's Register shows. A reduction in averaged sailed speeds of about eight percentage points (from 2.76 knots to 2.54 knots), however, will still amount to a large loss of revenue in the long run. In summary, choosing a route that suits the FRs is important to be able to get the best results from the system.
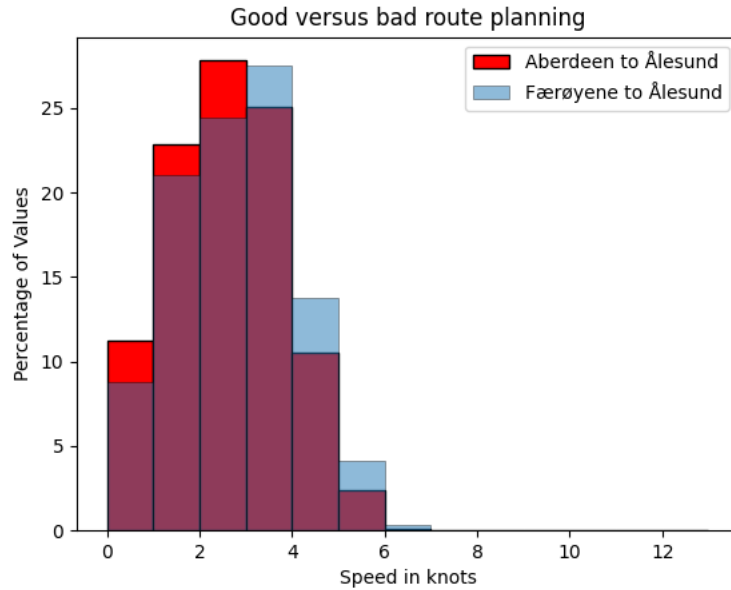
Figure 5.18: Good vs. bad route using simulation

5.5.3 Newbuild of specialized WPSP vessel

In this thesis, the focus has not been on implementing a partial energy mix where WASP technologies reduce fuel consumption, but rather on a complete transition to the usage of FRs. Therefore, utilizing a vessel with a conventional propulsion system is an inherently poor decision, as all space and weight from the conventional system will either need to be retrofitted or removed, which may result in a high retrofit premium. Therefore, Lindstad et al. (2022) performed a study into the possibility of constructing a Supramax carrier with a lower beam and higher draft to compensate for the discussed lost power production. This hull form was supposed to be better at counteracting drift forces, and perform generally better with FRs due to, amongst other, reduced drag from a lower beam and a smaller drift angle from the longer hull. The CAPEX of the newbuild remains more or less the same compared to a conventional build, but results in a vessel with a lower VOYEX (Lindstad et al., 2022a). Stating that a slimmer vessel has less sailing resistance is not revolutionary, but it provides the basis for a second conclusion found in the study.

With the implementation of FRs on a vessel, side forces due to perpendicular forces created by the rotors need to be counteracted by a rudder, see section 2.4.2 "Added resistance due to drift angle". This causes a substantial reduction in power output, and creates a drifting angle that increases drag. Lindstad et al. (2022) state that a longer and slimmer vessel specifically designed to use a WPSP system will be able to counteract much of this potential drifting by utilizing the hull's shape. They conclude that a vessel that is not retrofit but built specifically for a WPSP system will utilize up to 2 to 3 times more power from the wind to propel itself forward as it will drift less (Lindstad et al., 2022a). From the simulations, achieving speeds of around 2 to 4 knots is not especially competitive in the business, even when OPEX savings are accounted for. However, with a 2.5-time increase in power output, the resulting speed would increase decidedly, as one sees in plot 5.19 below. The average speed increase to 4 to 5 knots compared to an industry average of 10

to 15 knots is by far better. This increase in speed may be a defining factor as to whether or not FR technology will be utilized. To show the results of a 2.5-time increase in power utilization, the simulation has been run once more for the Ålesund - Faroe Islands route. The results are plotted below. To simplify the calculations, only the forces obtained from the FRs have been multiplied by 2.5. Neither the drifting angle nor the hydrodynamic drag has been changed. The results are as such, only to be treated as an indication, and may perhaps be conservative.
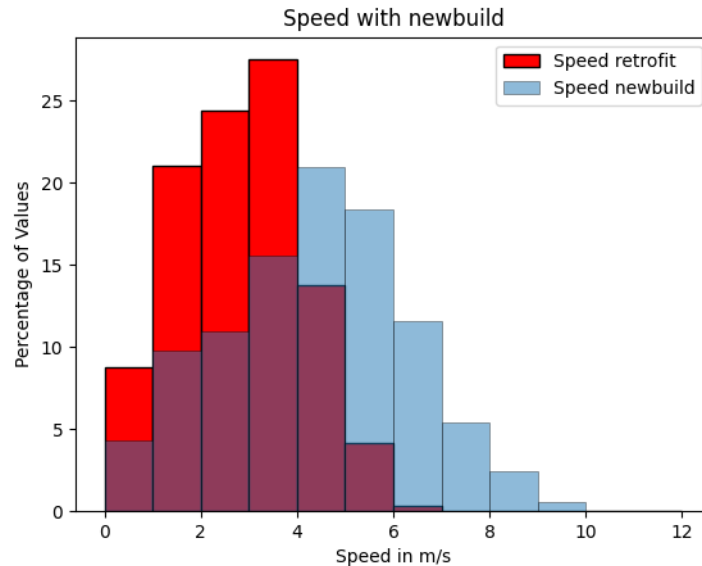

Figure 5.19: Speed distribution for route between Faroe Islands and Ålesund with newbuild

To summarize, using a new design as a base for an FR configuration provides significant gains in FR efficiency. The retrofit clearly provides the best output from the FRs, resulting in a much higher average sailing speed. Combining a newbuild with other technologies as well, in order to remove periods of sailing below a certain speed, is even more favorable. Specifically, combining a newbuild with a battery pack has been studied and is discussed at the end of section 5.5.4 below.

5.5.4 Combining technologies

The analysis in section 4.4 shows that several routes have conditions that disfavor the FR. A possibility is, therefore, to combine the FRs with other means of propulsion that can achieve a better performance where the FR configuration works poorly. Even when conditions are favorable for the FR, achieved speeds are not great. For this reason, it is also interesting to look at combinations that can at least eliminate the times that the vessel obtains speeds below 2 knots, and see the speed distribution shift upwards.

Combination with kite

A combination of FRs and kite is interesting because of their ability to complement each other. The kite can utilize the tailwind that provides no output from the FRs, and the FRs will use side winds that the kite fails to extract performance from. Figure 5.20 compares the polar plots of the FR and a kite. The plots show the power delivered as a function of the true wind angle. The black arrows indicate a vessel direction of 0°.

The kite works particularly well when the speed of the tailwind is significant compared to the vessel's speed. This may be seen from the red plot in figure 5.20 b. When the vessel's speed is 6 m/s, and the wind speed is 15 m/s, the power output is at its largest. When the wind speed is 5 m/s, the output from the kite is nearly 0. The blue-colored plot illustrates the reduced power output as the vessel sails faster. Fortunately, the vessel's speed is not especially high when powered by FRs. This means that the kite will be able to extract more power and help increase the overall speed of the vessel, given favorable wind conditions. Formosa et al. (2023) highlight this concept in their report "Wind-Assisted Ship Propulsion of a Series 60 Ship Using a Static Kite Sail". They conclude that slow steaming is beneficial when using a kite for propulsion assistance.
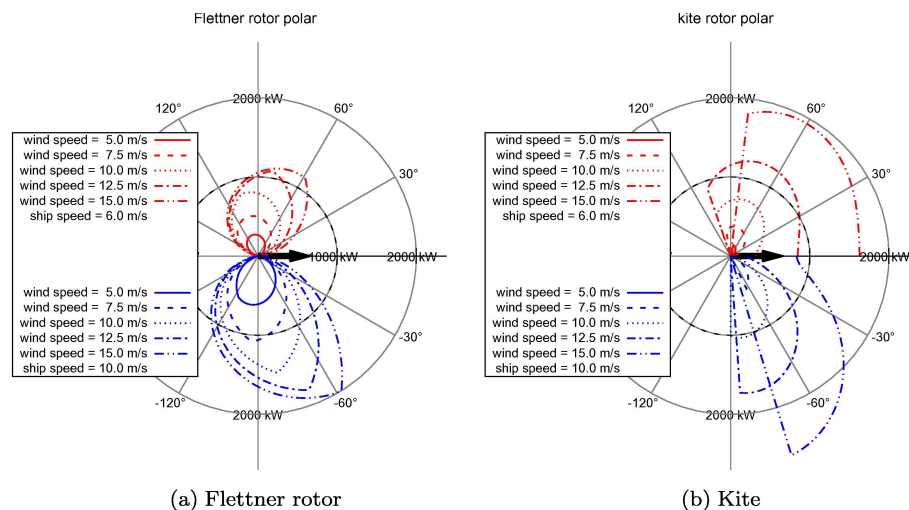

(a) Flettner rotor (b) Kite

Figure 5.20: Polar plot comparison between FRs and kite (Traut et al., 2014)

To investigate the combination of the FR and a kite, findings from two research papers are implemented into the simulation program. Leloup et al. (2015) have published a paper on using kites as auxiliary propulsion for vessels. The main topics discussed include the optimal wind window, formulas for calculating the contribution by the kite, and the influence of the vessel's speed and wind speed. The other paper has researched the case of using a static kite sail as WASP on a Series 60 ship. Formosa et al. (2023) present relevant background theory for simulation, the influence of kite area, optimal kite elevation, and the performance of the different configurations.

Routes such as Bergen-Stavanger and Florø-Bergen have shown especially poor conditions for the FR. With dominating wind directions being with or against the direction of travel, using kites could be beneficial as they provide thrust in tailwinds, and may be stored away in headwinds, causing no added aerodynamic resistance. How much the kite contributes to

the vessel's speed depends on the type of vessel, type of kite, and weather conditions. For a 50 000 dwt tanker, a 50 percent fuel reduction is possible given Beaufort 7 (15 m/s wind speed) and optimal tailwind conditions (Leloup et al., 2015). Conditions on the routes mentioned above are, for the most part, between Beaufort 5-6 on the Beaufort wind scale. Considering this, a 40 percent fuel saving is applied as a contribution to the performance of the FR in the simulation on the route between Bergen-Stavanger. Even though this might be an optimistic estimate of the kite contribution, it is interesting to see how such a combination of technologies could improve performance.

As figure 5.21 illustrates, optimizing the combination of FR and kite can dramatically shift the speed profile of the vessel. The mean speed achieved changes from 2.8 knots to 3.9 knots. Lower speeds in the range of 0 to 2 knots will, however, still occur when the wind speed is low, or the wind direction is towards the bow, etc. Even though a combination of FR and kite can use wind coming from the aft or sides, the vessel will still perform poorly in headwinds.
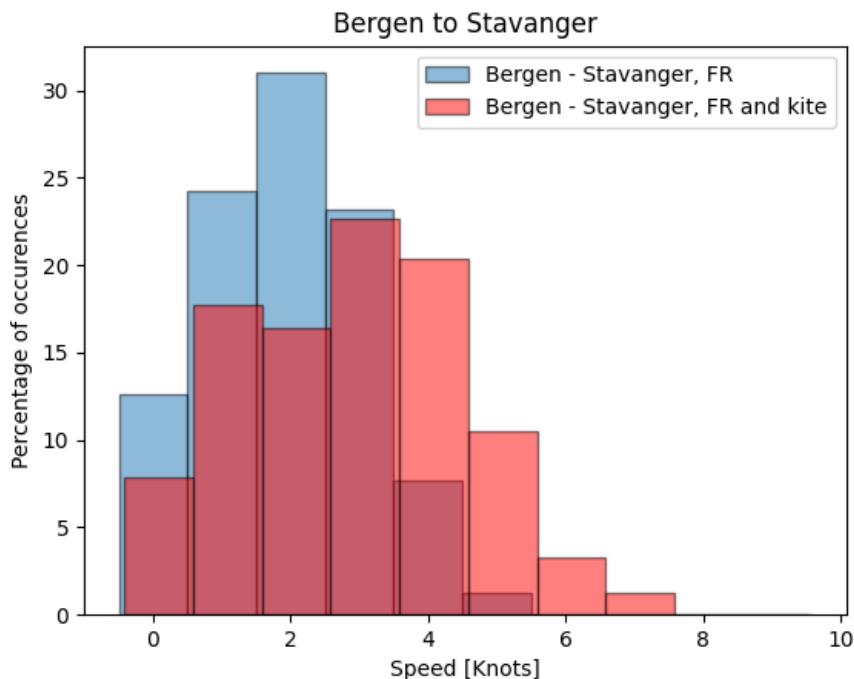
Figure 5.21: Speed profile with only FR compared to FR and kite

Combination with Rigid wing sail

Rigid wing sails have gained interest in recent years. Different companies offer different designs, and some have additional flaps in addition to the wing to optimize the angle of attack from the wind. Published research on the power output from these sails is limited, so it is unclear how it would influence the simulated vessel's performance. However, polar plots for a rigid sail are available and will indicate which routes and areas at which the sail can contribute to propulsive performance.

Figure 5.22 shows a polar plot for a rigid wing sail (Atkinson, 2018). An interesting point

is that the rigid sail can extract power from the same range as the combination of FR and kite. Combining the FR with rigid wing sails is a viable option when considering the desire to utilize a more significant part of the experienced wind directions. Despite this, several factors suggest that such a combination would be complex. Firstly, both the FR and the rigid wing sail require significant deck space. In addition, both technologies typically have solutions that fold down to enable port operations and passings under bridges. As a result of this, one may see that this combination would require an excessive amount of deck space.
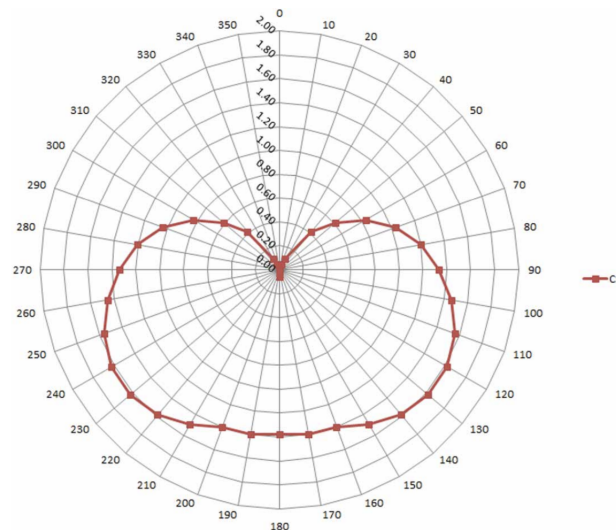

Figure 5.22: Polar plot of propulsive force for 4 m x 2.5 m rigid sail (Atkinson, 2018)

Combining FR and rigid sails also introduces topics such as wind flow interference and cost-benefit. In an article from DNV, the cost of rigid-wing sails is pointed out as one of its disadvantages (Hochkirck and Bertram, 2021). According to Bloomberg, rigid sails and kites could have system costs of around 1.5 MUSD (Ha, 2022). On the other hand, it is common to have several sails installed, meaning that the price will exceed that of the kite system.

Combination with battery

A battery solution installed on a WPSP vessel has several positive contributions to the vessel's operability. Firstly, it allows for onboard electrical energy storage, which can be used for both critical systems, powering the FRs, and propelling the vessel forward. This may increase the overall reliability of the vessel, as battery power may be utilized when there is little or no wind. For example, the vessel can use battery power to ensure a minimum speed at all times, only providing power when the wind is insufficient.

The amount of propulsion that the battery solution can deliver is determined by the system's state of charge (SOC). A percentage describes SOC between 0 and 100, where 100 percent indicates that the charge is equal to the capacity of the battery system. The SOC is an important factor in relation to the operability and the health of the battery system. If batteries experience large fluctuations in SOC, an increase in the rate of battery

aging is seen. Under regular operation, the expected lifetime of marine batteries is about ten years. Therefore, paying attention to the SOC is important to limit the number of necessary battery changes (Man Energy Solutions, 2020).

A battery system consists of several components. On the lowest level, there are individual battery cells. As several cells are connected in parallel or series, they form modules. Several modules form battery packs, and several battery packs form battery strings. These are the components that together form a marine battery system. To manage this system properly, the vessel needs a battery management system (BMS). The BMS controls charging and discharging, protects against overloading, and monitors the SOC. In addition to the management system, there is a need for a thermal management system (TMS). Thermal Runaway is a significant threat to every battery system. According to Man Energy Solutions, this is where battery temperature increases uncontrollably due to a chain chemical reaction (2020).

How may batteries be implemented in the code?

A central part of this thesis revolves around using the performance prediction model to simulate how the vessel would handle different routes at different times. Implementing a battery option to the code has therefore been done. The usage of a battery pack is to be sure that the vessel never sails below a specific threshold speed, and to evaluate how much of an effect this will have on the KPIs. The code has been run where this threshold is set to 2 knots. Battery power has been implemented by creating a pseudo-power function that provides extra power output from the FRs when needed to sustain a two-knot base speed. This is a simplified assumption that has been made for two reasons. Firstly, simplicity leads to a code that is more easily understood. Secondly, finding exact results with corresponding effect losses, added resistances, power losses, and so on would lead to arbitrarily inaccurate results. Simply stating that the power utilized is without loss, a future study may be conducted where the actual battery power needed to provide the effectual power output may be studied. This added power function is implemented in the code as follows.

First, the speed achieved using only power from the Flettners is found, with the corresponding resistance that this speed entails. Then, a new resistance measurement is taken with the wind parameters found at the specified time and place, given a speed of 2 knots. The difference in the power output needed to sail at 2 knots and whichever speed the FRs provide is then the amount of power that the battery pack needs to provide, again assuming a battery propulsion system without losses. The resulting power needed is recorded in an array and stored. Finally, the speed at which the vessel ends up sailing is set to 2 knots. The results when simulating this would be that all speeds below 2 knots are instead equal to 2 knots, and a specified amount of battery storage capacity is returned for the entire trip. When simulating the whole two-year period, insight into how large the battery capacity would be to support the vessel may be examined. To easily see the difference a battery makes, the plot below shows the histogram of speeds found without using a battery on the Faroe Islands to Ålesund voyage compared to that of sailing with batteries. As one sees, all speeds below 2 knots are removed, and a slight shift is observed for the other speed segments.
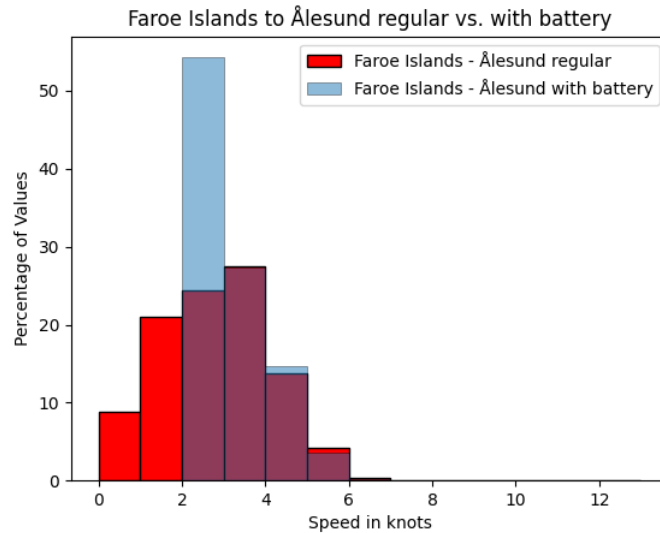
Figure 5.23: WPSP vessel with and without battery support

A graph showing the relation between averaged speed and battery power consumption may be created to see that the battery is used when needed and also how much power is provided. The graph below shows that the battery is turned on whenever the FRs do not produce enough force. The plot shows data over only 4 days to more easily show how the battery turns on and off. One sees how each time the vessel maintains a speed higher than 2 knots, the battery stops being used.

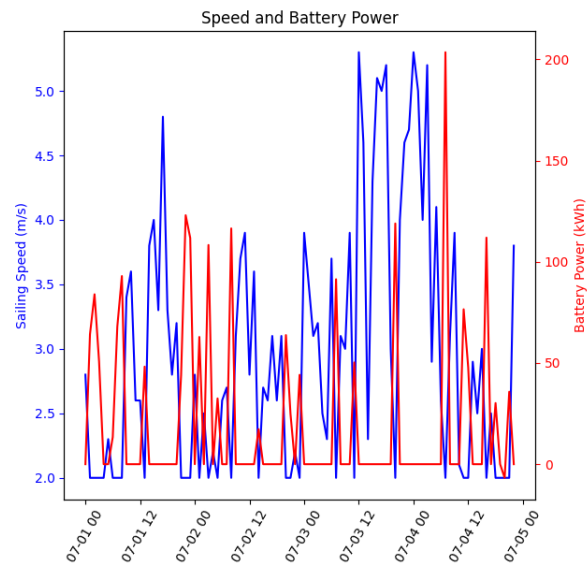Figure 5.24: Battery usage over one route, sailing from 01/07 - 05/07

Now that the battery function works as intended, one may ask several interesting questions about the vessel's behavior. First, how much battery capacity would be needed, when sailing the vessel on one of the routes simulated? Second, how does the battery need fluctuate with time? Additionally, how will the battery function influence the vessel's

speed? Finally, one may want to know how a battery pack would combine with a newbuild, as a natural addition to a newbuild would be implementing a green propulsion solution that may work both as backup and as a way to provide both that extra thrust while sailing in poor wind conditions as well as provide reliable power when docking. All these questions may be answered using the two graphs below. Plot "a" shows the influence of a battery system on the retrofit vessel, and plot "b" shows the same plot for the newbuild. The average speed sailed and averaged battery usage may be seen for both plots as a dotted line. The left y-axes in blue show the battery power the vessel needs for each iteration of the route, plotted over the two-year period. The right y-axes in red show the vessel's average sailing speeds over the whole route. The plots show how the amount of battery power needed changes with seasons and is inversely proportional to the sailed speed. One may notice that these plots correlate directly for sailed speed and inversely for battery power with the seasons and dominating windspeeds observed during those seasons. Sailed speeds are at a maximum during the summer and a minimum during the winter.
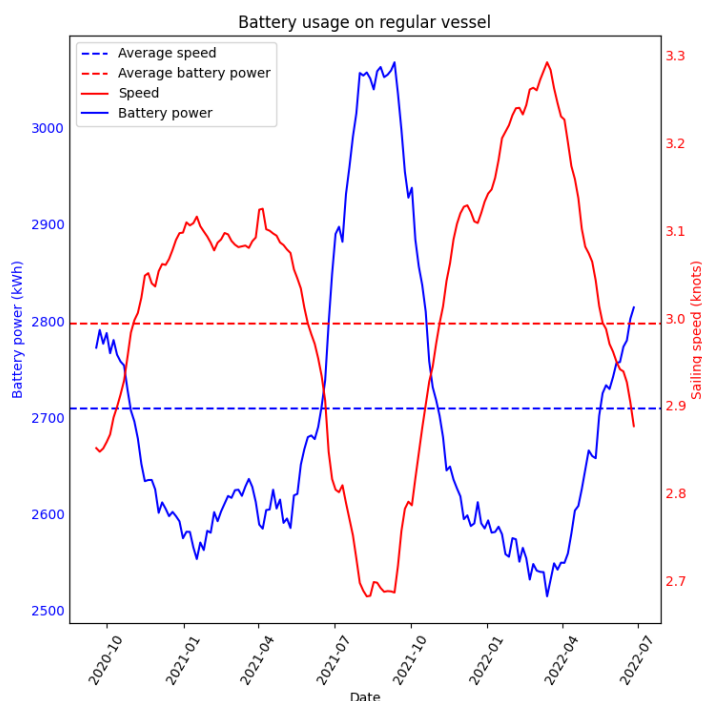

Figure 5.25: Retrofit vessel battery usage vs. sailing speed
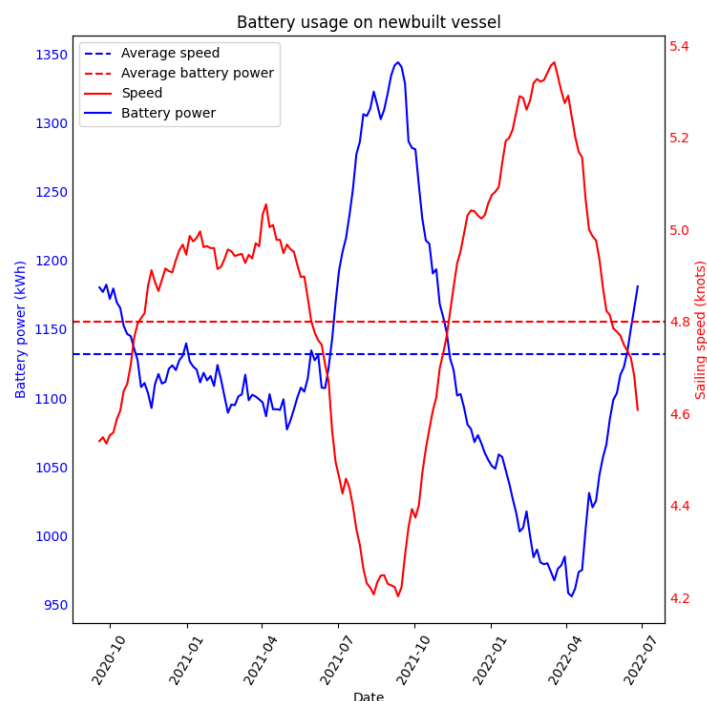
Figure 5.26: Newbuildt vessel battery usage vs. sailing speed

The average battery capacity for the retrofit vessel to sail the route from the Faroe Islands to Ålesund is 2709 kWh. With this power input, the vessel can maintain an average speed of 3 knots, about 10 percent quicker than the vessel sailing without a battery pack. This vessel would need a maximum of 4500 kWh on one trip, which may be used as a design criterion. A smaller battery pack is required for the newbuild to maintain a speed above 2 knots, as the vessel is more effective. Using 3000 kWh, the vessel manages to sail an average of 4.8 knots, compared to 4.7 knots when not using a battery. In the case of a newbuild, a higher target minimum speed may be set, as there is only a minimal speed increase of 2 percent. When dealing with higher speeds, more power is needed to further increase speeds, so adding a battery to remove low speeds will have a decreasing marginal

return on investment. A study into the optimal combination of technologies to improve WPSP as a propulsion system could be done as further work.

5.5.5 Policies for decision-making

To make decisions on when to utilize additional propulsion, decision-making policies could be beneficial. The procedures must describe the available systems, their capabilities, and the situations that may arise when using them. The following section will introduce policies that can be applied when utilizing a hybrid system consisting of wind-propulsion and batteries. These policies are developed based on the simulation results of the pure Flettner propulsion system and on the operational capabilities of the batteries as described in section 5.5.4. The policies could also consider port calls and traffic in port. To limit the complexity, these will not be accounted for here.

Policies for decision-making

1. **Power demand**

   Propulsion power from the battery system is initiated when the power demand exceeds what the FRs can deliver. Whether or not there is a lack of power is determined by the desired sailing speed.

2. **Battery state of charge**

   Propulsion power from the battery system is initiated when the battery state of charge is within a specific range. This range promotes good battery health and possibly ensures some capacity is reserved for emergencies.

3. **Emergency**

   Propulsion power from the battery system is initiated when the vessel is experiencing an emergency. A certain amount of SOC is dedicated to emergencies.

Power demand as a policy for decision-making is the most apparent policy when wind propulsion is used. With varying winds comes varying output from the wind-propulsion technology. Therefore, WPSP vessels will have cases where the sailing speed is significantly lower than the desired mean sailing speed. The fluctuations in sailing speed cause challenges to the entire value chain surrounding the vessel. The main challenge is that a pure WPSP vessel cannot offer good reliability and predictability in terms of deliveries compared to conventional vessels.

State of charge as a policy is mainly enforced by setting operational limits x and y, which gives SOCs lower and upper limits. As described in section 5.5.4, these limits are needed to ensure good battery health and preserve energy for a potential emergency. The state of charge policy facilitates the existence of the emergency policy since the vessel on every voyage will have stored electrical power available.

5.5.6 Reflections on WPSP improvements

The simulations in this thesis show that a WPSP vessel can struggle with performance when having the same operational constraints as conventional vessels. The previous sections have focused on improvements for the WPSP vessel base case. Discussed improvements are illustrated in figure 5.27. The most crucial implementation that all WPSP vessels need is route optimization. This needs to be synchronized with the type of wind propulsion technology that is installed. More flexibility is added when a combination such as Flettner rotors and kite is used. Added flexibility in this respect refers to route optimization. If wind conditions change during sailing, combining technologies can allow the vessel to continue on the same course.

An important lesson from the discussion is that many aspects of a vessel's characteristics and operations must change to promote pure wind propulsion. As discussed, Lindstad et al. 2022 find that the best configuration is to combine routing, smart FR (Flettner rotors that can fold down), and a slim hull [Lindstad et al., 2022a]. To have WPSP vessels with the best possible performance, these vessels should be purpose-built newbuilds. This would allow for a slim hull that reduces drift forces, systems for route optimization, and a layout that enables optimal placement of wind propulsion systems.

Figure 5.27 illustrates the different improvements that could be made to the WPSP vessel. In addition to the pure wind elements, a battery solution is included. The improvement in performance from the battery is, of course, dependent on the capacity of the battery system. Battery solutions or zero-emission fuels could at least work as backup to eliminate speeds close to zero knots when the wind is absent. No matter how many improvements one makes to the WPSP vessel, the absence of wind leads to zero speed.
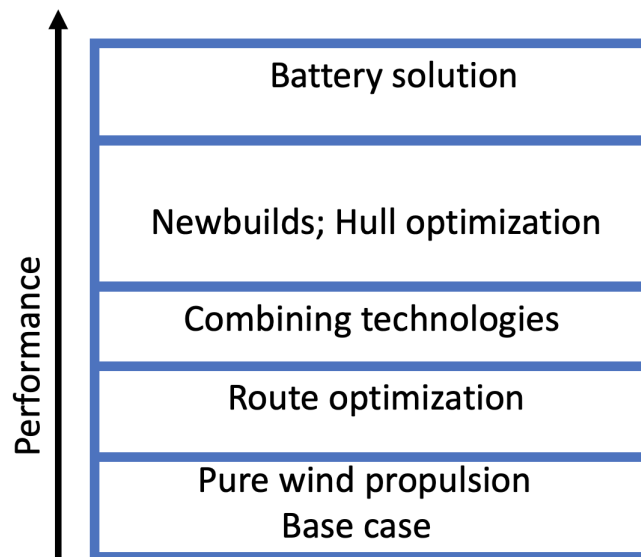

Figure 5.27: Performance enhancement of WPSP vessel

5.6 Business areas suitable to WPSP

The discussions on KPIs and the need for improvements to the WPSP vessel suggest that pure wind will often be outcompeted. This raises the question; Are there businesses and cases where the performance of the WPSP vessel is acceptable and desired? The main goal for a WPSP vessel and vessels fitted with WASP technologies is to cut emissions. The International Maritime Organization (IMO) has announced its mandate to cut emissions by 50 percent by 2050. Stakeholders intending to share this mandate are all possible candidates that can use WPSP vessels.

One concept that seeks to cut emissions from marine transport is the introduction of green corridors. A green corridor is defined as a shipping route between two major port hubs (including intermediary stopovers) on which the technological, economic, and regulatory feasibility of the operation of zero-emissions ships is catalyzed through public and private actions (Zero Coalition, 2021). The definition is presented in a paper by the Getting to Zero Coalition. Contributors to the coalition include a wide range of players within the maritime shipping industry, such as Maersk, Port of Rotterdam, Yara, and Kuehne+Nagel, to mention a few. The paper suggests several points that are needed to establish green corridors. Cross-value-chain collaboration is mentioned as one of the most important factors that are needed. For WPSP vessels, this could mean that stakeholders need to adapt to the performance of the WPSP vessel to reach the goal of zero emissions in the corridor. Introducing green corridors creates a market for WPSP vessels where conventional shipping vessels cannot compete because of their emissions.

A central point in the "Getting to Zero Coalition" report is that green corridors need to be implemented on routes with high emissions. Introducing green corridors on a route such as Bergen to Stavanger would have a negligible effect on world emissions. Therefore, feasible candidate routes must be identified. Figure 5.28 presents findings from a feasibility study conducted by the coalition. The figure shows that the route between Australia and Japan and between Asia and Europe are highlighted as routes with both high impact and feasibility. The route between Asia and the US has a low impact but can easily be implemented. For the WPSP vessel, the bulk transport of iron ore between Australia and Japan is the most viable out of the three routes mentioned. As mentioned throughout the thesis, this is because bulk vessels have available deck space where Flettne rotors and other wind propulsion technologies can be fitted.

Green corridor prioritisation framework

IMPACT

Low — High

FEASIBILITY

High

"QUICK" WINS
9 Asia-US automotive

10 Saudi-China methanol

GAME CHANGERS
3 Aus-Japan iron ore
6 Transatlantic containers
1 Aus-China iron ore
5 Asia-Europe containers

8 Saudi-India ammonia

Low

LOW PRIORITY

7 North-South containers

4 Transpacific containers

2 Brazil-Asia iron ore

LONG PLAYS

3 **Australia-Japan iron ore:** Favourable location for fuel production along with an **enabling regulatory environment and willing stakeholders**

5 **Asia-Europe containerships:** Stakeholder complexity creates implementation challenges but **high volumes and potential impact** provide a case for implementation

9 **Asia-US automotive:** Narrow set of stakeholders with strong **stakeholder willingness and end-customer alignment** (e.g., shift to EVs)
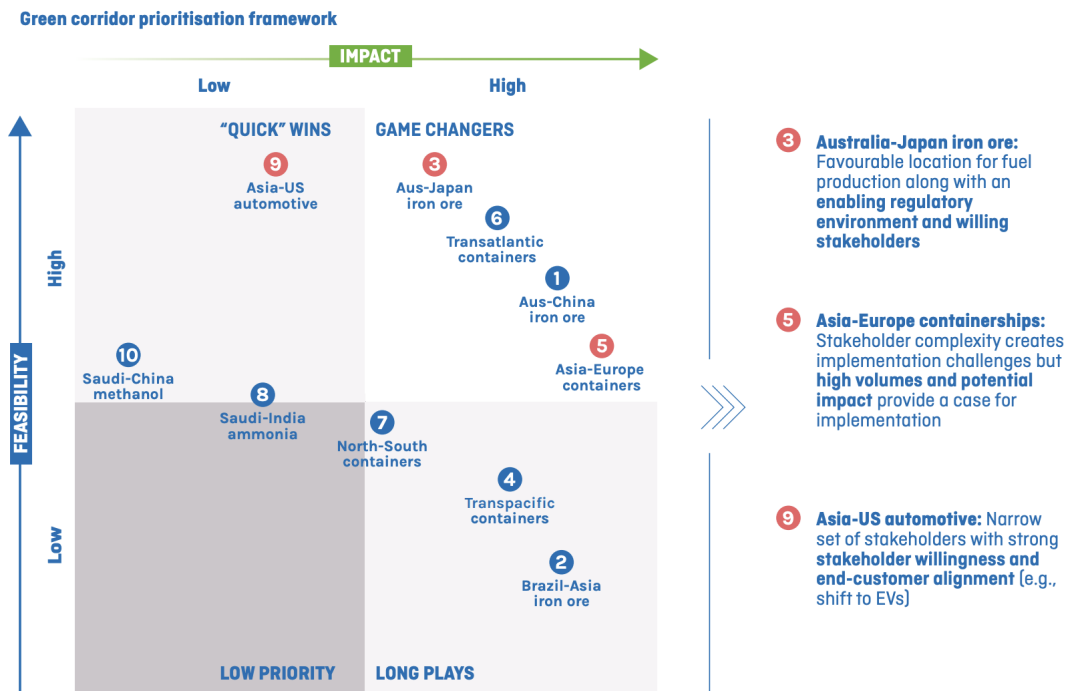
Figure 5.28: Green corridor candidate routes (Zero Coalition, 2021)

The bulk vessels themselves are not the only reason bulk transport is a business well-suited to WPSP. The very nature of bulk goods means that there will be arbitrarily sized cargo loads at both ends of the logistics chain. For the iron ore transport between Australia and Japan, these loads or piles will look like the ones seen in figure 5.29. Stakeholders in both Australia and Japan are willing to contribute to establishing green corridors. One of the reasons might be that they are not restricted to current transport solutions. As long as one sustains a transport flow, slower or irregular sailing times will not disrupt either stakeholder's operations. These arguments are valid independent of green corridors. WPSP vessels should therefore be able to service many routes where bulk is transported, and stakeholders are willing to cut emissions.

Figure 5.29: Yandi mine, Australia (BHP, 2023)

The transport of non-perishable goods is also a business area where the characteristics of the WPSP vessel can be accepted. These goods do not require fast sailing times because their state won't decay. Examples of such goods are furniture, machinery, and spare parts. Typically, these goods are stored in warehouses and stockpiled on both ends of the logistics chain. As long as the customers have availability of goods from their storages, their businesses will not suffer from the possible variations in arrival times from the WPSP vessel.

Chapter 6

Conclusion

The goal of this thesis was to answer the following main question. *What are the consequences of utilizing Flettner rotors as the only source of propulsion for a vessel?*. A simulation model was established to solve this question, a set of KPIs were created, and general improvements to the pure wind propulsion solution were proposed. The main conclusion that may be drawn from the case study used in the simulation was that using a pure WPSP system will provide insufficient results for sailing speeds, but competitive schedule reliability compared to existing conventional vessel solutions. The study also shows that implementing Flettner rotors provides a positive return on investments after only four years, given a transported value factor to account for reduced sailing speed. In reality, the vessel sailing with FRs will use a much longer time to move payload as it will sail at a reduced speed. However, the energy needed to sail the vessel at this lower speed is relatively lower, meaning fuel consumption per goods transported is lower for the retrofitted vessel. The simulations also show that this result may be significantly improved if the construction of a newbuilt vessel meant specifically for sailing with WPSP, combined with proper route planning and selection, is utilized.

The retrofitted vessel shows poor results regarding sailing speed and only shows decent results on reliability when essential factors such as port delays, port calls, and preplanned port time slots are left unaccounted for. The newbuilt vessel performs much better on the KPI reliability, and when combined with an external power source, such as a battery pack, the solution is improved even further. Whatever technological combinations are chosen for a WPSP vessel, industry demands, stakeholder willingness, and customer flexibility are the most significant obstacles. Suppose these beforementioned actors show willingness, both economically and strategically, to plan for a more volatile transportation system, where vessels do not necessarily have the capacity or possibility to plan their route schedules ahead of time. In that case, WPSP will have a place in the transportation sector. The simulations and literature findings show that a vessel built to sail with WPSP could provide a service that is both needed and sought after in the market.

It is the opinion of the authors that a solution combining the use of Flettner rotors for primary propulsion with a secondary propulsion unit, such as a battery pack or kite, added to complement the areas where FRs provide insufficient thrust could provide the basis for a feasible transportation system. If this basis is then combined with a specialized hull design, where an appropriately chosen route combining weather planning and predeter-

mined policies for decision-making are used, then the base case result may be improved upon to such an extent that it in itself provides a viable option for customers. The thesis showcases practical examples illustrating the acceptance of a trade-off in transportation capacity and flexibility as a requisite compromise to enable zero-emission transport. The authors contend that the proposed solution not only holds relevance for the future but also immediate significance today. With increasing fuel prices, carbon taxes, and general societal acceptance of the need to change the status quo, a WPSP solution such as the one proposed in this thesis may provide a solution.

Chapter 7

Further work

This chapter summarizes potential further work that may be conducted from the results found in this thesis. The authors believe several areas in this thesis may be improved if more time is devoted to their study. Some of these areas are mentioned here.

First, the potential size of the market for this vessel. To further evaluate the specific consequences the vessel may have for the economy and surrounding infrastructure is interesting to focus on. Looking more into how ports and customers have to deal with slower sailing ships and how they have to plan their operations correspondingly could be done. When looking into the vessel's specifics and what customers choose most fitting for the WPSP system, applying pre-planned routes for the vessel would be interesting. When a specific route requirement is found, carrying a particular load to or from a specific customer, a realistic result may be found using the simulations. This result should then be studied and evaluated regarding the customer's needs.

When sailing with WPSP, studying methods of improving the sailed route through either the optimization of policies for decision-making or through the utilization of observed wind may be looked into. For example, if sailing in direct headwinds, a sailing vessel will use a technique called "tacking", as the sails need to be positioned at a certain angle to provide thrust. This same technique will also be required with FRs, but the rate of turning and the specific angles sailed need to be studied. How much should a vessel deviate from its planned route when using FRs in these situations? Further, how much deviation should a WPSP vessel sail to obtain more optimal winds, not just to position itself correctly against the wind? These questions may be studied further using the simulation developed in this thesis.

As seen, studying ways of improving the results found in the simulations by looking into optimizations for vessel handling is possible. Many parts of the code are based on assumptions, simplifications, and generalizations that may be further studied to improve accuracy and useability for specific vessels. For example, generalizing the code so that input for specific vessels is used is a feasible future outcome. The resistances are calculated by using simplified formulas that use approximations of, amongst others, the block coefficient, hull shape, rudder and propeller resistances, and so on. Finding exact coefficients and using actual input for existing vessels for their resistances could improve the accuracy of the results. Furthermore, including both wind and wave resistances should be done to take

into account the negative effect of sailing in high winds. The assumption that neither wave nor wind resistance acts on the vessel will provide misleading results for higher winds.

Further investigating the force produced by the Flettners and the impact vessel angles and rolling have on these forces should also be investigated further. Where does the force vector from the Flettners apply, and what consequences does it have on propulsion? How do the different rotors influence each other with regard to wake and turbulence, for example? How do endplates and the size of Flettners affect each other, and what combinations should be used with specific vessel sizes? Studying the observed output of the Flettners themselves deserves a thesis in itself.

Regarding vessel economics, and the choice between constructing a newbuild or retrofits, the influence of using alternative fuels or batteries for energy production aboard is a topic that could be studied more closely. For example, what payload reductions must be expected using different propulsion combinations? How large must a potential battery pack account for load shedding, SOC, and so on? If batteries are not used, then what generators should be used? On the other hand, how can excess propulsion be created if a newbuild is used? What kind of propellers are most beneficial when sailing slower and with less power needed?

As summarized in the paragraphs above, many new questions and work may be further built upon from the findings in this thesis. With the introduction of new technologies and methods to change the modus operandi, many new problems and solutions will arise. The authors hope that their work be utilized in the future study of FRs and their implementation in marine transportation.

Bibliography

Ahlborn, H., (1930). *The Magnus Effect in Theory and in Reality*. Ed. by Natrional Advisory committee for Aeronautics. Zeitschrift fur Flugtechnik und Moto.

Airseas, (2022). *Airseas solution*. URL: https://www.airseas.com/.

Allwright, Gavin, (Apr. 2023). *The winds of change: One zero-emission dilemma for shipping solved?* SWZ—Maritime's March 2023 Energy Transition.

Anemoi, (Nov. 2020). *Anemoi Rotor Sails - Rail Deployment Demo*. URL: https://www.youtube.com/watch?v=5VE8yyVh3Nw.

— (2023). *Anemoi Rotor Sail Technology*. URL: https://anemoimarine.com/rotor-sail-technology/.

Atkinson, Gregory Mark, (July 2018). *Analysis of lift, drag and C_x polar graph for a 3D segment rigid sail using CFD analysis*. URL: https://www.tandfonline.com/doi/pdf/10.1080/20464177.2018.1494953.

Badalamenti, C. and Simon Prince, (Jan. 2008). "Vortex shedding from a rotating circular cylinder at moderate sub-critical reynolds numbers and high velocity ratio". In: *ICAS Secretariat - 26th Congress of International Council of the Aeronautical Sciences 2008, ICAS 2008* 6, pp. 404–414.

Bergfjord, Line, (2011). "Wind in the North Sea.: Effects of offshore grid design on power system operation." In: *NTNU Open*. URL: http://hdl.handle.net/11250/257214.

BHP, (2023). *What we do*. URL: https://www.bhp.com/what-we-do/global-locations/australia/western-australia/yandi.

Britannica, (2022). *History of ships*. Britannica. URL: https://seahistory.org/sea-history-for-kids/wind-and-the-sailor/.

Buitendijk, Mariska, (Aug. 2022). *MOL to build second bulk carrier with hard sail system*. SWZ Maritime. URL: https://swzmaritime.nl/news/2022/08/11/mol-to-build-second-bulk-carrier-with-hard-sail-system/.

Cambridge Dictionary, (2023). *Simulation*. URL: https://dictionary.cambridge.org/dictionary/english/simulation.

Cheng-Chi, Chung and Chiang Chao-Hung, (2011). *Critical factors in schedule reliability of container shipping carriers*. URL: https://www.iiis.org/CDs2011/CD2011SCI/MMMSE_2011/PapersPdf/NB272VW.pdf.

Chou, Todd, Kosmas Vasileios, Katharine Renken and Michele Acciaro, (2020). *New Wind Propulsion Technology - A Literature Review of Recent Adoptions*. NMTF. URL: https://vb.northsearegion.eu/public/files/repository/20210111083115_WASP-WP4.D5B-NewWPTALiteratureReviewofRecentAdoptions-Final.pdf.

Copernicus Marine, (Nov. 2022). *Copernicus Marine Service*. https://marine.copernicus.eu/about. URL: https://marine.copernicus.eu/about.

— (Apr. 2023). *Global Ocean Hourly Sea Surface Wind and Stress from Scatterometer and Model*. DOI: 10.48670/moi-00305.

Craft, Tim, Hector Iacovides, N Johnson and Brian Launder, (2012). "Back to the future: Flettner-Thom rotors for maritime propulsion?" In: *Proceeding of THMT-12. Proceedings of the Seventh International Symposium On Turbulence, Heat and Mass Transfer Palermo, Italy, 24-27 September, 2012*. Begellhouse. DOI: 10.1615/ichmt.2012.procsevintsympturbheattransfpal.1150.

De Marco, A, S Mancini, C Pensa, G Calise and F De Luca, (2016). "Flettner Rotor Concept for Marine Applications: A Systematic Study". In: *International Journal of Rotating Machinery* 2016, pp. 1–12. DOI: 10.1155/2016/3458750.

Diez, S.M, P.G Patil, J Morton, D.J Rodriguez, A Vanzella, D.V Robin, T. Maes and C. Corbin, (2019). "Marine Pollution in the Caribbeans: Not a Minutes to Waste". In.

DNV, (2020). *Rigid wing sails*. DNV. URL: https://www.dnv.com/expert-story/maritime-impact/Wind-assisted-propulsion-can-cut-fuel-costs-and-emissions.html.

— (2022a). *Energy Transition Outlook 2022*. DNV. URL: https://www.dnv.com/Publications/energy-transition-outlook-2022-232649.

— (2022b). *Maratime Forecast To 2050*. DNV. URL: https://www.dnv.com/maritime/publications/maritime-forecast-2022/index.html.

— (2022c). *Maritime Forecast to 2050*. Tech. rep. DNV.

eia, (May 2023). *Average industrial price of electricity US*. eia.gov. URL: https://www.eia.gov/electricity/data/.

Elger, David E., Marcus Bentin and Michael Vahs, (2020). "Comparison of different methods for predicting the drift angle and rudder resistance by wind propulsion systems on ships". In: *Ocean Engineering* 217, p. 108152. ISSN: 0029-8018. DOI: 10.1016/j.oceaneng.2020.108152. URL: https://www.sciencedirect.com/science/article/pii/S0029801820310878.

ESAU, Steve, (Sept. 2021). "Fuel Comparisons Must Consider Energy Density". In: *The Maritime Executive*. URL: https://maritime-executive.com/editorials/future-fuel-comparisons-must-consider-energy-density.

Fadai-Ghotbi, A, R Manceau and J Borée, (15th Mar. 2008). "Revisiting URANS Computations of the Backward-facing Step Flow Using Second Moment Closures. Influence of the Numerics". In: *Flow, Turbulence and Combustion* 81.3, pp. 395–414. DOI: 10.1007/s10494-008-9140-8.

Formosa, Wayne, Tonio Sant, Claire De Marco Muscat-Fenech and Massimo Figari, (2023). "Wind-Assisted Ship Propulsion of a Series 60 Ship Using a Static Kite Sail". In: URL: https://www.researchgate.net/publication/366938712_Wind-Assisted_Ship_Propulsion_of_a_Series_60_Ship_Using_a_Static_Kite_Sail.

Global Petrol Prices, (Apr. 2023). *Electricity Prices*. GlobalPetrolPrices.com.

Ha, K Oanh, (Aug. 2022). *The Future of Shipping Is ... Sails?* URL: https://www.bloomberg.com/news/articles/2022-08-24/wind-power-comes-to-cargo-ships-as-shipping-goes-green?leadSource=uverify%5C%20wall.

Haugstad, Tormod, (Feb. 2023). "Skal Lage Verdens første klimanøytrale bil". In: *Teknisk Ukeblad* 0223.170, pp. 36–42.

Hochkirck, Karsten and Volker Bertram, (Nov. 2021). *Wind-assisted propulsion: Economic and ecological considerations.* URL: https://www.researchgate.net/publication/357362304_Wind_assisted_propulsion_Economic_and_ecological_considerations.

Hofstede, Geert, (2004). "Business Goals and Corporate Governance". In: *Asia Pacific Business Review* 10.3-4, pp. 292–301. DOI: 10.1080/1360238042000264379. eprint: https://doi.org/10.1080/1360238042000264379. URL: https://doi.org/10.1080/1360238042000264379.

IMO, (Apr. 2021). "IMO MEPC 76". In: ed. by safety4sea. URL: https://safety4sea.com/imo-mepc-76-review-of-2020-marine-fuels-quality/.

Inbound Logistics, (2020). *Small Ports, Big Benefits.* URL: https://www.inboundlogistics.com/articles/small-ports-big-benefits/.

Inoue, S., M. Hirano, K. Kijima and J. Takashina, (1981). "A practical calculation method of ship maneuvering motion". In: *International Shipbuilding Progress* 28.325, pp. 207–222. ISSN: 1566-2829. DOI: 10.3233/ISP-1981-2832502.

IRENA, (Dec. 2022). *Levelized cost of energy by technology, World.* URL: https://ourworldindata.org/grapher/levelized-cost-of-energy.

Jessen Martin Stette; Møller, Håkon, (2018). "Integration of shipbuilding markets : a quantitvative study of the newbuilding prices for bulk carriers, tankers and containerships from 1994 to 2015". MA thesis. NHH.

Khan, L, (2021). *A review of Wind-Assisted Ship Propulsion For Sustainable Commercial Shipping: Latest Developments And Future Stakes.* Aston University. URL: https://publications.aston.ac.uk/id/eprint/43134/1/Khan_et_al_2021_RINA_Wind_Assisted_Ship_Review.pdf.

Kijima, Katsuro, Toshiyuki Katsuno, Yasuaki Nakiri and Yoshitaka Furukawa, (1990). "On the manoeuvring performance of a ship with theparameter of loading condition". In: *Journal of the Society of Naval Architects of Japan* 1990.168, pp. 141–148. DOI: 10.2534/jjasnaoe1968.1990.168_141.

Kim, Ekaterina and Bjørnar Brende Smestad, (2021). *Introduction to geospatial and temporal maritime data*. NTNU TMR4135. URL: Blackboard.

Kramer, Jarle, Sverre Steen and Luca Savio, (Oct. 2016). *Drift Forces - Wingsails vs Flettner Rotors*.

Kystverket, (2022). *AIS Norge*. Kystverket. URL: https://www.kystverket.no/navigasjonstjenester/ais/ais-artikkelside/.

Lageman, Benjamin, (Sept. 2022). *Metocean*. URL: https://github.com/NTNU-IMT/Metocean/blob/master/README.md.

Lagemann, Benjamin, Elizabeth Lindstad, Kjetil Fagerholt, Agathe Rialland and Stein Ove Erikstad, (Jan. 2022). "Optimal ship lifetime fuel and power system selection". In: *Transportation Research Part D: Transport and Environment* 102, p. 103145. DOI: 10.1016/j.trd.2021.103145.

Leloup, R., K. Roncin, M. Behrel, G. Bles, J.-B. Leroux, C. Jochum and Y. Parlier, (2015). "A continuous and analytical modeling for kites as auxiliary propulsion devoted to merchant ships, including fuel saving estimation". In: URL: https://www.sciencedirect.com/science/article/pii/S0960148115302366?ref=pdf_download&fr=RR-2&rr=7c06fa5faaedb52d.

Levander, Kai, (2012). *System Based Ship Deign*. seaKey Naval Achitecture.

Lindstad, Elizabeth, Polic Dražen, Agathe Rialland, Inge Sandaas and Tor Stokke, (Sept. 2022a). "Reaching IMO 2050 GHG Targets Exclusively through Energy efficiency measures". In: *Day 3 Thu, September 29, 2022*. SNAME. DOI: 10.5957/smc-2022-060.

Lindstad, Elizabeth, Dražen Polić, Agathe Rialland, Inge Sandaas and Tor Stokke, (Dec. 2022b). "Decarbonizing bulk shipping combining ship design and alternative power". In: *Ocean Engineering* 266, p. 112798. DOI: 10.1016/j.oceaneng.2022.112798.

Lloyd's Register, (May 2023). *Flettner rotor savings estimator*. URL: https://flettner.lr.org/KHbCZMdL#.

MAN Energy Solutions, (Sept. 2019). *Batteries onboard ocean going vessels*.

Man Energy Solutions, (2020). *Batteries on board ocean-going vessels*. MAN. URL: https://www.man-es.com/docs/default-source/marine/tools/batteries-on-board-ocean-going-vessels.pdf?sfvrsn=deaa76b8_14.

Menon, Ajay, (2021). *What are berthing plans - Everything you need to know*. URL: https://www.marineinsight.com/marine-navigation/berthing-plans/.

NAPA, (2023). *The basics of EEXI - from 2023, all existing ships must meet new energy efficiency standards.* URL: https://www.napa.fi/the-basics-of-eexi-from-2023-all-existing-ships-must-meet-new-energy-efficiency-standards/.

Norsepower, (Nov. 2022). *Rotor Sail solutions to save fuel - and the planet.* Flettner Technical Specifications. URL: https://www.norsepower.com/download/brochure.pdf.

— (2023). *Tankers.* URL: https://www.norsepower.com/tankers/.

Oblack, Rachelle, (Apr. 2019). *Why is wind speed slower over land than over ocean.* ThoughtCo. URL: https://www.thoughtco.com/wind-speed-slower-over-land-3444038.

Oceana, (2022). "Shipping pollution". In: *Asia Pacific Business Review.* URL: https://europe.oceana.org/shipping-pollution-1/.

OECD, (2007). "COMPENSATED GROSS TON (CGT) SYSTEM". In: COUNCIL WORKING PARTY ON SHIPBUILDING. DOI: 10.21428/cb6ab371.8b0ec66c. URL: https://www.oecd.org/industry/ind/37655301.pdf.

Ohmae, K., (1982). *The Mind Of The Strategist: The Art of Japanese Business.* Management & Leadership. McGraw-Hill Education. ISBN: 9780070479043. URL: https://books.google.no/books?id=xgVtpdx0FzQC.

Oldendorff, (Jan. 2021). *Wind Propulsion for Dry Bulk Carriers.* URL: https://www.oldendorff.com/news/wind-propulsion-for-dry-bulk-carriers.

Patowary, Kaushik, (2022). *Flettner Rotor: Sailing Ships Without Sails.* URL: https://www.amusingplanet.com/2021/02/flettner-rotor-sailing-ships-without.html.

Paul D. Sclavounos Nikos Mazarkis, Dimitris Katsanos, (Feb. 2020). "Flettner Totor Sails for Ship Propulsion". In: *StormGeo.* URL: https://www.stormgeo.com/solutions/shipping/articles/flettner-rotor-sails-for-ship-propulsion/.

Qin, Ruqiong and Chunyi Duan, (Oct. 2017). "The principle and applications of Bernoulli equation". In: *Journal of Physics: Conference Series* 916, p. 012038. DOI: 10.1088/1742-6596/916/1/012038.

Rawson, K.J. and E.C. Tupper, (2001). "Manoeuvrability". In: *Basic Ship Theory.* Elsevier, pp. 523–573. DOI: 10.1016/b978-075065398-5/50016-9.

Reche-Vilanova, Martina, Hansen Dr. Heikki and B. Bingham Dr. Harry, (2021). *Performance Prediction Program for Wind-Assisted Cargo Ships.* DTU. URL: https://www.researchgate.net/publication/344238090_Performance_Prediction_Program_for_Wind-Assisted_Cargo_Ships.

Riski, Tuomas, (Feb. 2021). *Norsepower.* URL: https://maritime-forum.ec.europa.eu/sites/default/files/r_cwl8uzhoma8ubyj_norsepower_investor_presentation_2021-02-24.pdf.

Schinas, O and D Metzger, (16th Oct. 2019). "FINANCING SHIPS WITH WIND-ASSISTED PROPULSION TECHNOLOGIES". In: *Wind Propulsion 2019.* DOI: 10.3940/rina.win.2019.13.

Seahistory, (2022). *Wind and the Sailor*. National maritime historical society. URL: https://seahistory.org/sea-history-for-kids/wind-and-the-sailor/.

Seddiek, Ibrahim and Nader Ammar, (2021). *Harnessing wind energy on merchant ships: Case study Flettner rotors onboard bulk carriers*. Springer. URL: https://link.springer.com/content/pdf/10.1007/s11356-021-12791-3.pdf.

Seddiek, Ibrahim S. and Nader R. Ammar, (2021). "Harnessing wind energy on merchant ships: case study Flettner rotors onboard bulk carriers". In: *Environmental Science and Pollution Research* 28.25, pp. 32695–32707. ISSN: 1614-7499. DOI: 10.1007/s11356-021-12791-3.

Tillig, Fabian and Jonas Ringsberg, (2019). "A 4 DOF simulation model developed for fuel consumption prediction of ships at sea". In: *Ships and Offshore Structures* 14.sup1, pp. 112–120. DOI: 10.1080/17445302.2018.1559912.

TLME News Service, (Aug. 2022). *Vessel Schedule Reliability Continues Its Upward Trend*. Transport & Logsitics ME. URL: https://www.transportandlogisticsme.com/smart-sea-freight/vessel-schedule-reliability-continues-on-an-upwards-trend.

Traut, Michael, Paul Gilbert, Conor Walsh, Alice Bows, Antonio Filippone, Peter Stansby and Ruth Wood, (Jan. 2014). "Propulsive power contribution of a kite and a Flettner rotor on selected shipping routes". In: vol. 113. Elsevier BV, pp. 362–372. DOI: 10.1016/j.apenergy.2013.07.026.

Traut, Michael, Alice Larkin, Paul Gilbert, Sarah Mander, Peter Stansby, Conor Walsh and Ruth Wood, (2022). *Low C for the High Seas Flettner rotor power contribution on a route Brazil to UK*. URL: https://www.researchgate.net/publication/233863726_Low_C_for_the_High_Seas_Flettner_rotor_power_contribution_on_a_route_Brazil_to_UK.

Twin, Alexandra, (Mar. 2023). *What Is a Key Performance Indicator (KPI)? Definition, Types, and Examples*. Investopedia. URL: https://www.investopedia.com/terms/k/kpi.asp.

Ulstein, Tore and Per Olaf Brett, (Mar. 2016). "What is a better ship? - It all depends". In: *12th International Marine Design Conference 2015*.

Weck, Prof. De and Prof. Willcox, (2004). *Multidisciplinary System Design Optimization*. URL: https://dspace.mit.edu/bitstream/handle/1721.1/68163/16-888-spring-2004/contents/lecture-notes/MSDO_L3_Simulation.pdf.

Zero Coalition, Getting to, (2021). *The Next Wave - Green Corridors*. URL: https://www.globalmaritimeforum.org/content/2021/11/The-Next-Wave-Green-Corridors.pdf.

Zhang, Shengming, Preben Terndrup Pedersen and Richard Villavicencio, (2019). *Probability and Mechanics of Ship Collision and Grounding*. English. Cambridge, MA: Butterworth-Heinemann. URL: https://search.ebscohost.com/login.aspx?direct=true&db=nlebk&AN=1986264&site=ehost-live&scope=site.

Appendix A

Appendix

I Code

Some of the more important codesnippets may be found below. All of the code may be accessed through GitHub using this link: https://github.com/HCaspari/Master-2.0.git

```python
1
2    #Input stats for code
3    mean_wind_speed = 10 #knots
4    mean_wind_direction = 90 #degrees
5    time_intervall =0.10 #hours
6    mesh_size = 10 #nautical miles
7    Start_east = 0
8    Start_north = 0
9    Start_position = (Start_east,Start_north) #Current Position
10   GlobalPositionVect = [(0,0)]
11   clock = 0
12
13   travel_iteration          = 0
14
15   #vessel parameters:
16   vessel_length             = 101.26
17   vessel_draft              = 10.15
18   vessel_weight_disp        = 8856
19   rho_air                   = 1.025
20   rho_water                 = 1025
21   rotor_amount = 4
22   h   = 35     #height flettner
23   d   = 5      #diameter of flettner
24   A   = h*d    #cross sectional area of flettner
25   Cl  = 12.5
26   Cd  = 0.2
27   Cm  = 0.2
28   alpha = 3.5
```

```
29
30
31
32    #Function that calculates time spent sailing from place to place, through route
33    def main(route, iteration, date_of_simulation,routenumber):
34        """
35        :param route: Vector of route coordinates [(x1,y1),(x2,y2),...,(xn,yn)]
36        :param iteration: Number of repetitions of simulation
37        :return:For each iteration of simulation:
38                total_time_sailed_route: float
39                tot_sailing_dist: vector of sailing distances over route
40                poor_sailing_time: float, time sailed less than 1 knot
41                poor_sailing_distance: float, distance sailed at less than 1 knot
42                sailing_speed_vector: vector of speed sailed at each point along route
43                TWS: Vector of true wind speed
44                TWD: Vector of true wind direction
45                Route sailing time: Time used to sail each route iteration
46                Coordinate sailing time: Time used to sail between two points on route
47                datestamp_vector: Vector containing times vessel is at each point over route
48                battery_use_vector: Total batterypower neeed for sailing this iteration
49        """
50        # initializing sailing speed of 4 knots (will change after one iteration)
51        vessel_speed                = 4
52        route_sailing_time          = iteration
53        tot_sailing_dist            = 0
54        poor_sailing_time           = 0
55        poor_sailing_distance       = 0
56        sailing_speed_vector        = []
57        coordinate_sailing_time     = []
58        apparent_wind_speed_observed = []
59        true_wind_speed_vector      = []
60        true_wind_direction_vector  = []
61        datestamp_vector            = [date_of_simulation]
62        battery_use_vector          = []
63        forward_force_vect          = []
64        total_time_sailed_route     = 0
65
66        for i in range(len(route)-1): #create itteration through route
67            position_first     = route[i]
68            position_next      = route[i+1]
69            sailing_distance   =
            ↪   geopy.distance.geodesic(position_first,position_next).nautical#In Nm
70            vessel_heading     = calc_vessel_heading_2(position_first, position_next)
71            WSE,WSN            =
            ↪   getweather(route_sailing_time,position_first[0],position_first[1])
72            TWS                = True_wind_speed(WSN,WSE)
73            TWD                = True_wind_direction(vessel_heading,WSN,WSE)
74            AWS                = Apparent_Wind_Speed(TWS,vessel_speed,TWD)
75            AWA                = alpha(vessel_speed,vessel_heading,WSN,WSE )
76            Forward_Force,Perp_Force = Force_produced(AWS, AWA)
77
78            #With Kite added aswell as Flettner, assume 1.4 times more force generated
```

```python
79              if routenumber == 14:
80                  Forward_Force       = 1.4*Forward_Force
81                  if iteration % 1000 == 0 and i == 1:
82                      print("Running kite (1.4 force)")
83
84              #With utilization of modern vessel design.
85              if routenumber == 16 or routenumber == 151 or routenumber == 152:
86                  Forward_Force       = 2.5*Forward_Force
87
88              #With Kite and Slimmer vessel aswell as Flettner,
89              # assume 3.5 (2.5*1.4) times more force generated
90              if routenumber == 17:
91                  if iteration % 1000 == 0 and i == 1:
92                      print("running Kite, and newbuild (3.5 force)")
93                  Forward_Force       = 3.5*Forward_Force
94
95              vessel_speed,total_resistance,battery_need_power = \
96                  Speed_achieved_Valid(Perp_Force, Forward_Force)
97
98              if type(Forward_Force) == MaskedConstant or type(Perp_Force) == MaskedConstant:
99                  print("ouchie, we have a mask", i)
100                 return 1
101
102             #If wind observed equals zero, sailing time is set to one
103             # and calculations are reated with new experienced wind at next intervall
104
105             # If ship experiences no wind, it waits an hour recalculating forces
106             if vessel_speed == 0:
107                 sailing_time = 1.00
108             else:
109                 sailing_time    = round(sailing_distance/vessel_speed,3)
110
111             # check for extreme time usage, whenever sailed speed is less than 1 knot.
112             if vessel_speed < 1:
113                 poor_sailing_time += sailing_time
114                 poor_sailing_distance += sailing_distance
115
116             #When batteries are not utilized, the batterypower calculated is set to 0
117             if routenumber != 15 and routenumber != 152:
118                 battery_need_power = 0
119
120             #When batteries are utilized, speeds below 2 knots are st to 2 knots
121             if routenumber == 15 or routenumber == 152:
122                 if vessel_speed < 2:
123                     vessel_speed = 2
124
125             #Append data to vectors
126             sailing_speed_vector.append(vessel_speed)
127             coordinate_sailing_time.append(sailing_time)
128             true_wind_speed_vector.append(TWS)
129             true_wind_direction_vector.append(TWD)
130             apparent_wind_speed_observed.append(AWS)
```

```python
131          tot_sailing_dist += sailing_distance
132          battery_use_vector.append(round(battery_need_power*(sailing_distance/2),3))
133          forward_force_vect.append(round(Forward_Force,3))
134
135
136          route_sailing_time += sailing_time   #Sailing time of total route
137          if len(coordinate_sailing_time) != 0:
138              total_time_sailed_route = sum(coordinate_sailing_time)
139
140          # Adding timestamp to first column
141          if i > 0:
142              time_beginning  = datestamp_vector[i-1]
143              time_new        = add_hours_to_date(time_beginning,sailing_time)
144              datestamp_vector.append(time_new)
145
146      return total_time_sailed_route,tot_sailing_dist, poor_sailing_time, \
147              poor_sailing_distance, sailing_speed_vector,true_wind_speed_vector,\
148              true_wind_direction_vector, route_sailing_time, coordinate_sailing_time, \
149              datestamp_vector, battery_use_vector
150
151  def getweather(tid,latitude, longditude):
152      """
153      :param tid: Time we want to access weather data
154      :param latitude: Latitude where we want to access weather data
155      :param longditude: Longdtitude where we want to access weather data
156      :return: WSN and WSE in m/s at time = tid, and position (lat,lon)
157      """
158      if tid >= 17520:  #if end of year 2 is reached while sailing, weatherdata from the
         ↪ beginning of year one is used
159          tid -= 17520
160
161      if tid <= 8742:
162
163          lat_pos = int((latitude-eastward_lat_1[0])*8)              #Access correct
             ↪ position in vector of north wind
164          lon_pos = int((longditude-eastward_lon_1[0])*8)            #Access correct
             ↪ position in vector of east wind
165
166          if latitude < eastward_lat_1[0] or latitude > eastward_lat_1[-1]:
167              print("latitude out of bounds, latitude between 58.9375 and 70.1875")
168              return 1
169          elif longditude < eastward_lon_1[0] or longditude > eastward_lon_1[-1]: #været må
             ↪ være hentet på posisjonen longditude
170              print("longditude out of bounds, longditude between 3.0625 and 20.9375")
171              return 1
172          elif lat_pos >= len(dataset_NW_1["northward_wind"][tid,:]):
173              print("yay")
174          elif lat_pos >= len(dataset_NW_1["northward_wind"][tid,:,lon_pos]):
175              print(f"lat posistion is out of bound at {lat_pos} degrees")
176              return 1
177          elif lon_pos >= len(dataset_NW_1["northward_wind"][tid, lat_pos, :]):
178              print(f"lon posistion is out of bound at {lon_pos} degrees")
```

```python
179                 return 1
180
181             WSN = dataset_NW_1["northward_wind"][tid,lat_pos,lon_pos]
182             WSE = dataset_EW_1["eastward_wind"][tid,lat_pos,lon_pos]
183
184         else:
185
186             tid -= 8743        #indekserer tiden i andre filen fra start igjen
187
188             lat_pos = int((latitude - eastward_lat_2[0]) * 8)  # Access correct position in
                ↪    vector of north wind
189             lon_pos = int((longditude - eastward_lon_2[0]) * 8)  # Access correct position in
                ↪    vector of east wind
190
191             WSN = dataset_NW_2["northward_wind"][tid, lat_pos, lon_pos]
192             WSE = dataset_EW_2["eastward_wind"][tid, lat_pos, lon_pos]
193
194         return WSN,WSE
195
196     def True_wind_speed(WSN,WSE):
197         """
198         :param WSN: Wind Speed North in m/s
199         :param WSE: Wind Speed East in m/s
200         :return: True wind speed in m/s
201         """
202         TWS = np.sqrt(WSN**2+WSE**2)
203
204         return TWS
205
206     #Function that return true wind direction in degrees from wind speed north/east
        ↪    (WSN/WSE)
207     def True_wind_direction(vessel_heading,wind_speed_north,wind_speed_east):
208         """
209         :param vessel_heading: Vessel heading in degrees
210         :param wind_speed_north: speed of wind in northward direction (negaitive means
        ↪    south)
211         :param wind_speed_east: speed of wind in eastern direction (negative means west)
212         :return: true wind direction [degrees]
213         """
214         wind_angle_rads = math.atan2(wind_speed_north,wind_speed_east)   # gives direction, 0
                ↪    degrees equals east, 90 degrees = north ....
215         wind_angle_degs = r2d(wind_angle_rads)
216         wind_angle_degs = (wind_angle_degs + 360) % 360           #normalizes degrees
217
218         true_wind_direction = wind_angle_degs-vessel_heading          #true wind direction in
                ↪    degrees
219
220         true_wind_direction = (true_wind_direction + 360) % 360
221
222         return true_wind_direction #in degrees
223
224
```

```
225
226    def Apparent_Wind_Speed(true_wind_speed, vessel_speed, true_wind_direction):
227        """
228
229        :param true_wind_speed: Wind speed in relation to vessel heading
230        :param vessel_speed: speed vessel sails
231        :param true_wind_direction: heading of wind in relation to vessel
232        :return: apparend wind speed m/s [float]: speed of wind in relation to vessel speed
     ↪  and heading
233        """
234
235        #AWS_func = TWS_func - sailing_speed_func * np.sin(np.pi / 180 *
           ↪  sailing_direction_func)
236        #from Seddiek et al. function 1 and 2
237        AWS = np.sqrt(true_wind_speed ** 2 +
           ↪  vessel_speed**2-2*true_wind_speed*vessel_speed*np.cos(true_wind_direction))
238
239        return AWS
240
241
242    #Function that calculates AWA selfmade
243    def Apparent_Wind_Angle(vessel_speed, vessel_heading, NWS, EWS):
244        """
245        :param vessel_speed: Speed of vessel
246        :param vessel_heading: Heading of vessel
247        :param NWS: Northern wind speed (decomposed)
248        :param EWS: Eastern wind speed (decomposed)
249        :return: Apparent wind angle in degrees
250        """
251        Vsx = np.cos(vessel_heading)*vessel_speed     #Decompose sailing speed
252        Vsy = np.sin(vessel_heading)*vessel_speed     #Decompose sailing speed
253        Wsx = EWS                                     #Decompose Wind speed
254        Wsy = NWS                                     #Decompose Wind speed
255        Vawx = Vsx + Wsx                              #Recombine speeds
256        Vawy = Vsy + Wsy                              #Recombine speeds
257        alpha_temp = r2d(math.atan2(Vawy,Vawx))       #Change to degrees, calculate angle
258        alpha     = (alpha_temp+360) % 360            #Normalize angle between 0 and 360
           ↪  degrees
259
260        return alpha
261
262    def Route_Creation(start_point_coordinates, end_point_coordinates, midpoint1 = (),
     ↪  midpoint2 = (), midpoint3 = (), midpoint4 = (), midpoint5 = ()):
263
264         """
265        :param start_point_coordinates: Coordinate of Starting port
266        :param end_point_coordinates: COordinate of destination location
267        :param midpoint1: Optional midpoint coordinate
268        :param midpoint2: Optional midpoint coordinate
269        :param midpoint3: Optional midpoint coordinate
270        :param midpoint4: Optional midpoint coordinate
271        :param midpoint5: Optional midpoint coordinate
```

```
272        :return: Route generated with equally spaced distances between all coordinates
273        """
274
275
276        #Route steps between points inputted
277        route_step_1 = [start_point_coordinates, midpoint1]  # first segment of 1 step route
278        route_step_2 = [midpoint1, midpoint2]  # second segment of 2. step route
279        route_step_3 = [midpoint2, midpoint3]  # second segment of 3. step route
280        route_step_4 = [midpoint3, midpoint4]  # second segment of 4. step route
281        route_step_5 = [midpoint4, midpoint5]  # second segment of 5. step route
282        route_step_6 = [midpoint5, end_point_coordinates]  # second segment of final step
       ↪  route
283
284        #Geodesic caluclates distances over a curved surface (the earth)
285        distance_step_1 = geodesic(start_point_coordinates, midpoint1).kilometers  # distance
       ↪  of 1. step
286        distance_step_2 = geodesic(midpoint1, midpoint2).kilometers  # distance of 2. step
287        distance_step_3 = geodesic(midpoint2, midpoint3).kilometers  # distance of 3. step
288        distance_step_4 = geodesic(midpoint3, midpoint4).kilometers  # distance of 4. step
289        distance_step_5 = geodesic(midpoint4, midpoint5).kilometers  # distance of 5. step
290        distance_step_6 = geodesic(midpoint5, end_point_coordinates).kilometers  # distance
       ↪  of final step
291
292        distance_tot = int(np.floor((distance_step_1 + distance_step_2 + distance_step_3 +
       ↪  distance_step_4 + distance_step_5 + distance_step_6) // 7))
293
294        #Generate_intricate_route splits route into equally spaces steps
295
296        Route1 = generate_intricate_route(route_step_1, distance_tot)  # route part 1
297        Route2 = generate_intricate_route(route_step_2, distance_tot)  # route part 2
298        Route3 = generate_intricate_route(route_step_3, distance_tot)  # route part 3
299        Route4 = generate_intricate_route(route_step_4, distance_tot)  # route part 4
300        Route5 = generate_intricate_route(route_step_5, distance_tot)  # route part 5
301        Route6 = generate_intricate_route(route_step_6, distance_tot)  # route part 6
302
303        #Completed route through all steps
304        Route = Route1 + Route2 + Route3 + Route4 + Route5 + Route6
305
306        return Route
307
308
309
```

II Wind roses

(a) Aberdeen to Faroe Islands

(b) Faroe Islands to Aberdeen
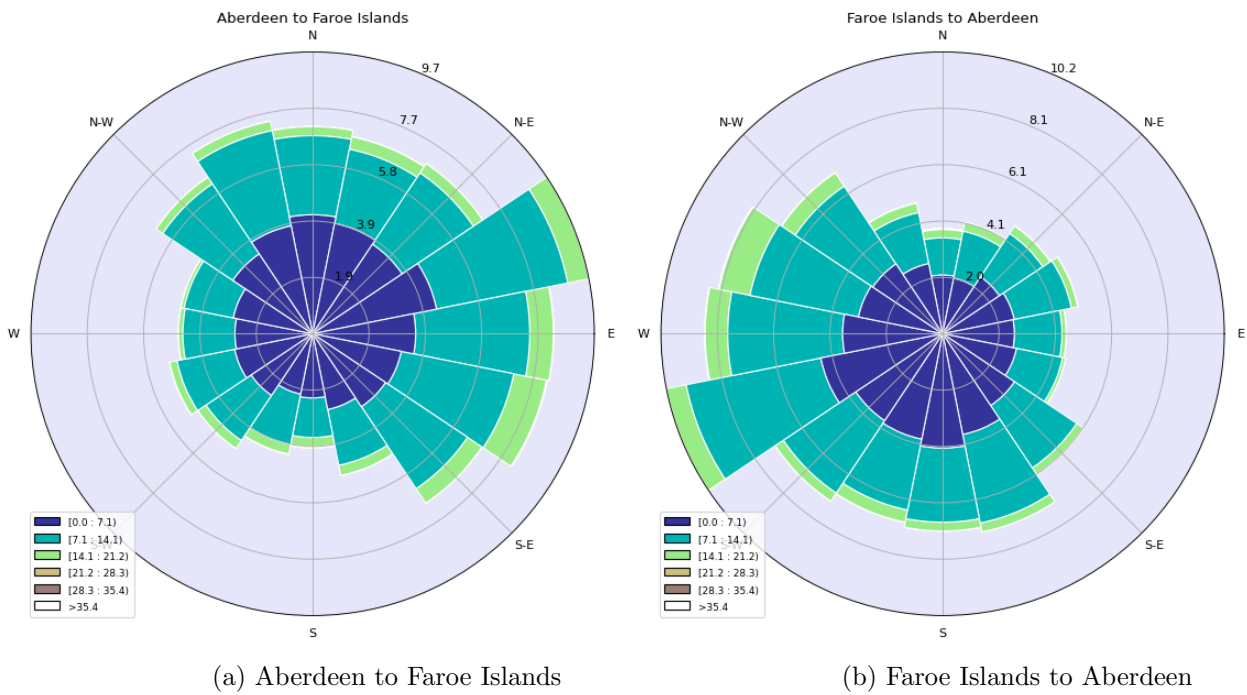
Figure A.1: Wind roses for route between Aberdeen and Faroe Islands

(a) Faroe Islands to Ålesund

(b) Ålesund to Faroe Islands
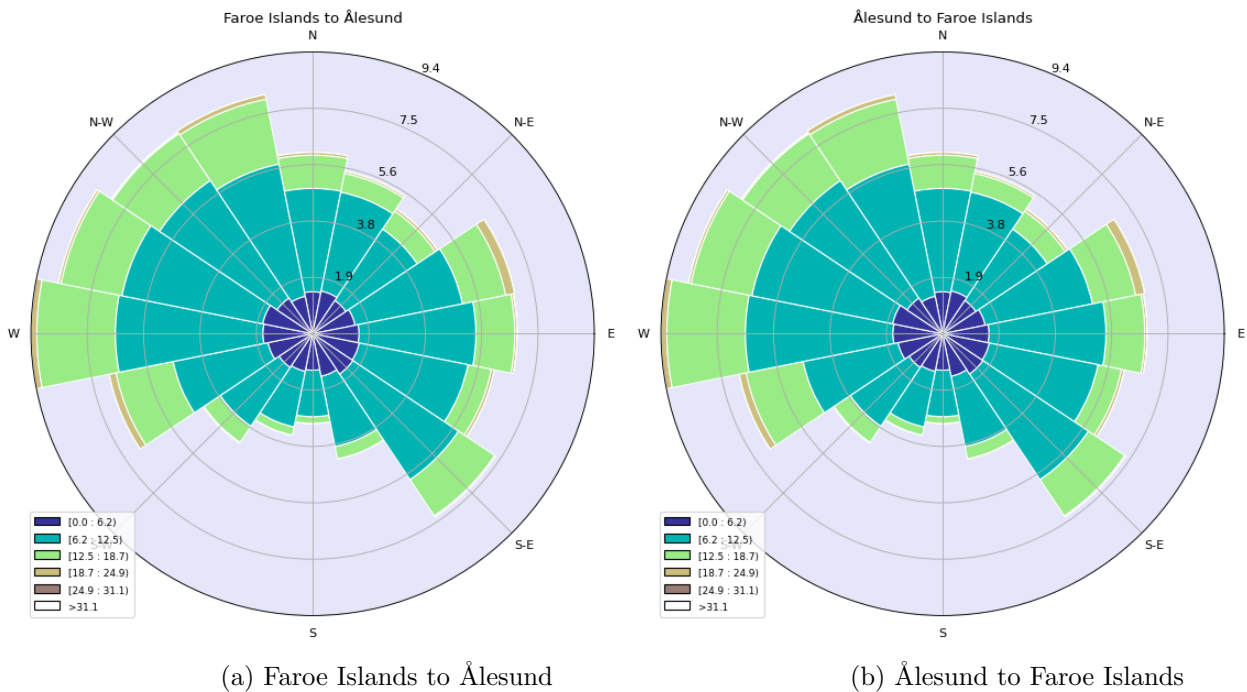
Figure A.2: Wind roses for route between Faroe Islands and Ålesund

(a) Denmark to Amsterdam

(b) Amsterdam to Denmark
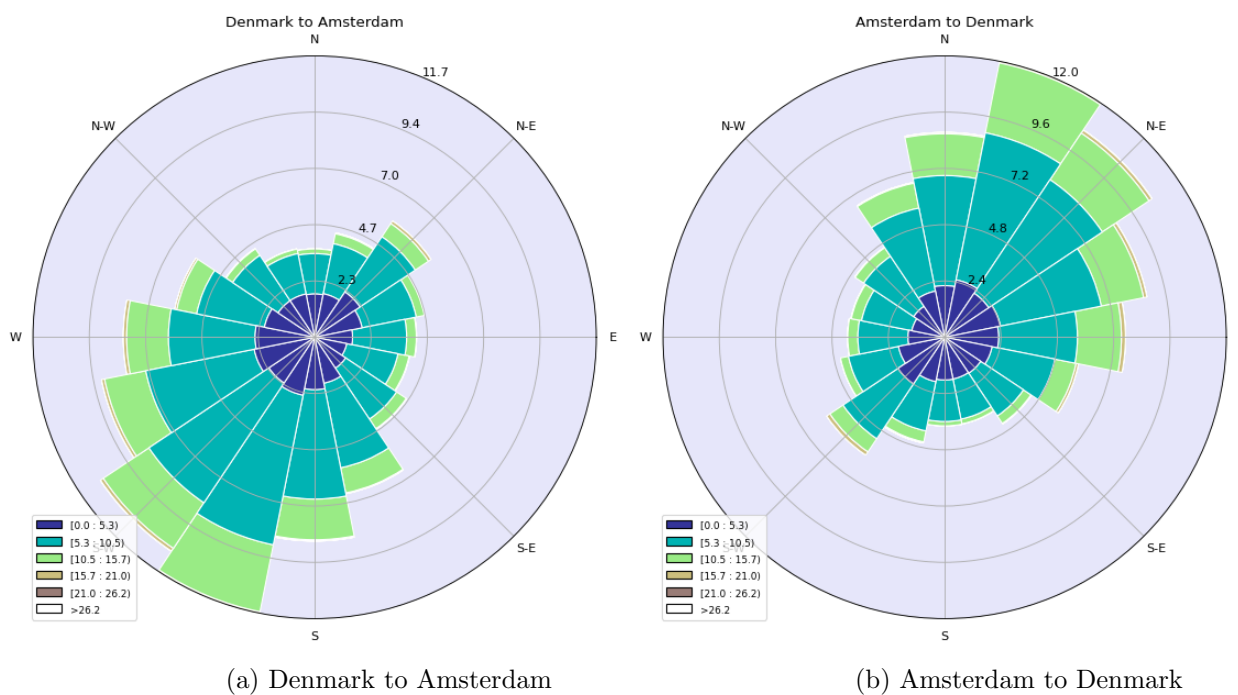
Figure A.3: Wind rose for route between Denmark and Amsterdam

(a) Ålesund to Denmark

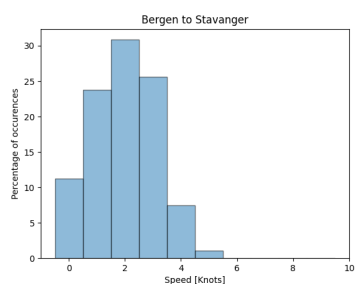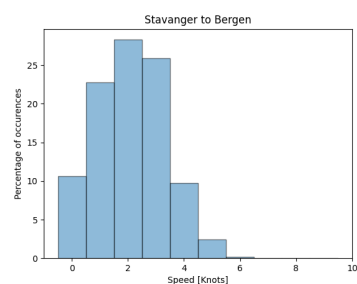(b) Denmark to Ålesund
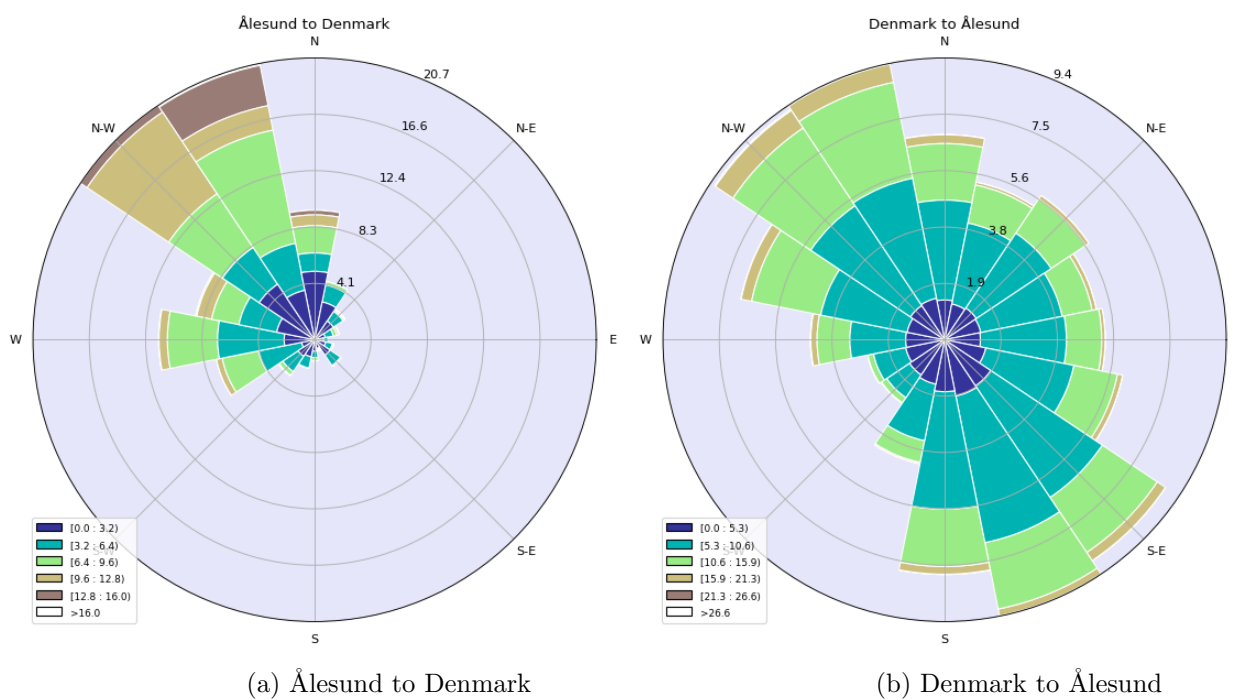
Figure A.4: Wind rose for route between Ålesund and Denmark

III   Histograms
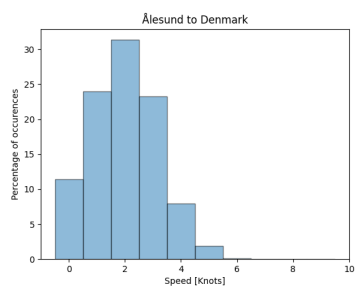
(a) Ålesund to Denmark
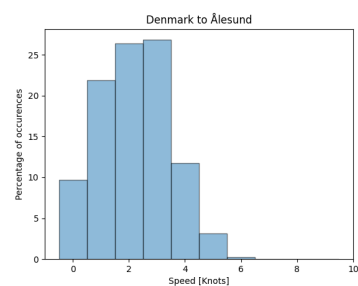
(b) Denmark to Ålesund

Figure A.5: Histogram for route between Ålesund and Denmark
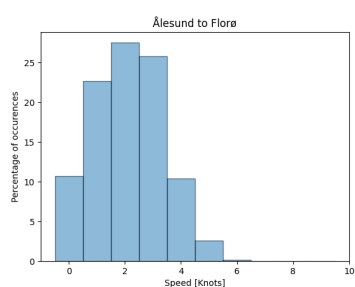
(a) Ålesund to Florø
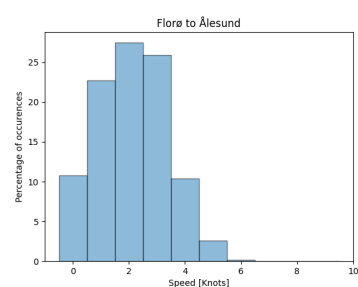
(b) Florø to Ålesund

Figure A.6: Histogram for route between Ålesund and Florø
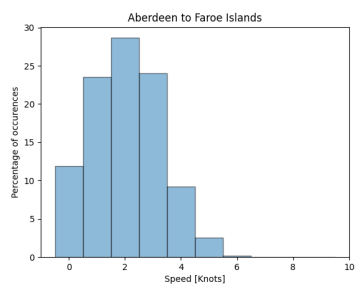
(a) Aberdeen to Faroe Islands
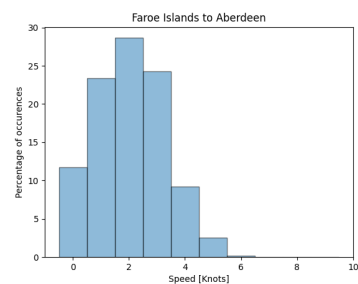
(b) Faroe Islands to Aberdeen

Figure A.7: Histogram for route between Aberdeen and Faroe Islands
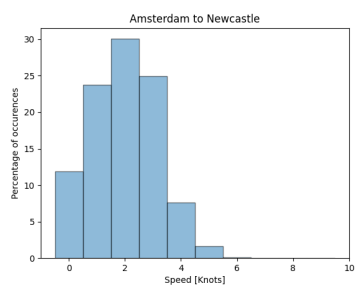
(a) Amsterdam to Newcastle
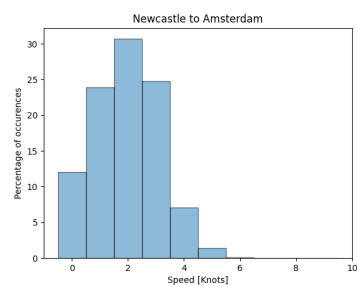
(b) Newcastle to Amsterdam

Figure A.8: Histogram for route between Amsterdam and Newcastle

(a) Bergen to Stavanger

(b) Stavanger to Bergen

Figure A.9: Histogram for route between Bergen and Stavanger
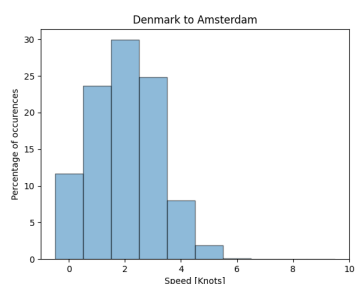
(a) Denmark to Amsterdam
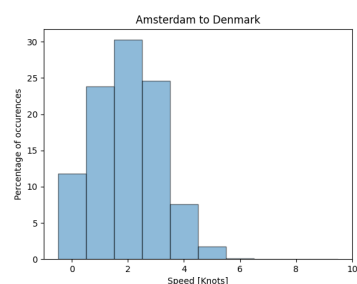
(b) Amsterdam to Denmark

Figure A.10: Histogram for route between Denmark and Amsterdam
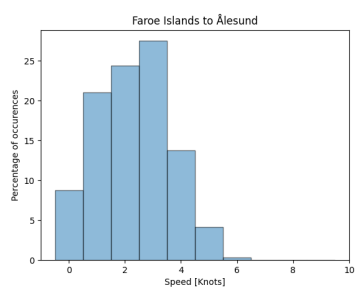
(a) Faroe Islands to Ålesund
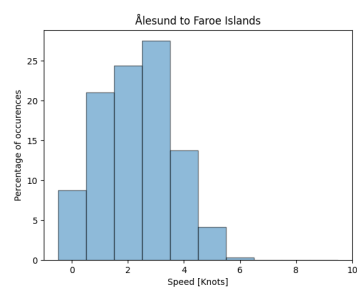
(b) Ålesund to Faroe Islands

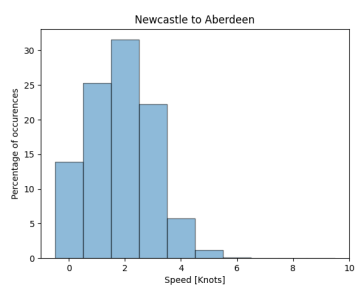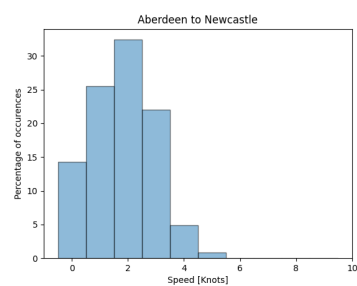Figure A.11: Histogram for route between Faroe Islands and Ålesund
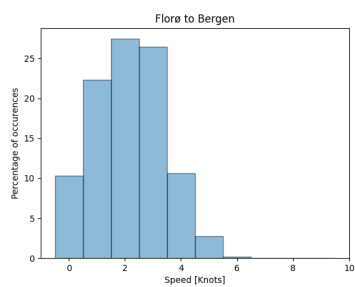
(a) Florø to Bergen
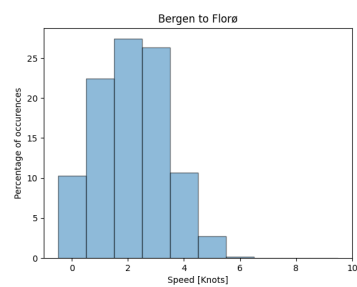
(b) Bergen to Florø

Figure A.12: Histogram for route between Florø and Bergen
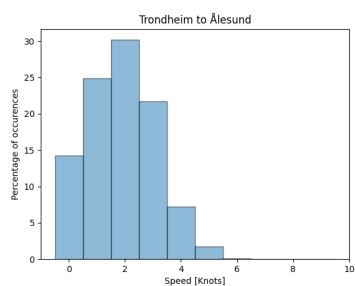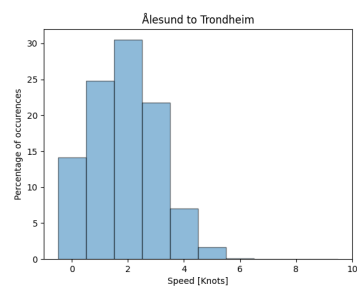

(a) Newcastle to Aberdeen

(b) Aberdeen to Newcastle

Figure A.13: Histogram for route between Newcastle and Aberdeen

(a) Trondheim to Ålesund

(b) Ålesund to Trondheim

Figure A.14: Histogram for route between Trondheim and Ålesund